

Washington University in St. Louis

Washington University Open Scholarship

McKelvey School of Engineering Theses & Dissertations

McKelvey School of Engineering

Winter 12-15-2021

Mapping neural responses onto innate and acquired behavior: from insect olfaction to realizing a bio-hybrid chemical recognition system

Rishabh Chandak

Washington University in St. Louis

Follow this and additional works at: https://openscholarship.wustl.edu/eng_etds



Part of the [Neurosciences Commons](#)

Recommended Citation

Chandak, Rishabh, "Mapping neural responses onto innate and acquired behavior: from insect olfaction to realizing a bio-hybrid chemical recognition system" (2021). *McKelvey School of Engineering Theses & Dissertations*. 718.

https://openscholarship.wustl.edu/eng_etds/718

This Dissertation is brought to you for free and open access by the McKelvey School of Engineering at Washington University Open Scholarship. It has been accepted for inclusion in McKelvey School of Engineering Theses & Dissertations by an authorized administrator of Washington University Open Scholarship. For more information, please contact digital@wumail.wustl.edu.

WASHINGTON UNIVERSITY IN ST. LOUIS

McKelvey School of Engineering
Department of Biomedical Engineering

Dissertation Examination Committee:

Baranidharan Raman, Chair

Dennis Barbour

Shantanu Chakrabartty

Daniel Kerschensteiner

Srikanth Singamaneni

Mapping Neural Responses Onto Innate And Acquired Behavior:

From Insect Olfaction To Realizing A Bio-hybrid Chemical Recognition System

by

Rishabh Chandak

A dissertation presented to
The Graduate School
of Washington University in
partial fulfillment of the
requirements for the degree
of Doctor of Philosophy

May 2022
St. Louis, Missouri

© 2022, Rishabh Chandak

Table of Contents

List of Figures	v
Acknowledgments.....	viii
Abstract	x
Chapter 1: Introduction	1
1.1 The olfactory system	2
1.1.1 Structural organization.....	2
1.2 Olfactory coding principles.....	4
1.3 Olfaction and behavior	8
1.3.1 Innate and acquired behaviors.....	8
1.3.2 Quantifying behavior	11
1.4 Simultaneous neural and behavioral monitoring.....	13
1.5 Insect-based chemical sensing	14
1.6 Thesis outline	16
Chapter 2: Methods.....	17
2.1 Odor stimulation.....	17
2.2 Behavior experiments to characterize innate palp-opening responses.....	17
2.3 Preference index	18
2.4 Vapor pressure analysis.....	18
2.5 Monte Carlo simulations for behavior	19
2.6 Electrophysiology experiments – PN recordings	19
2.7 PID experiment	20
2.8 Projection neuron response classification	20
2.9 Dimensionality reduction analysis (fully invasive experiments)	21
2.10 Hierarchical clustering analysis	21
2.11 Linear regression to predict valence from PN activity.....	21
2.12 Monte Carlo simulations for electrophysiology.....	22
2.13 Angle between odors.....	22
2.14 Electrophysiology experiments – ORN recordings.....	23
2.15 Behavior experiments – classical conditioning.....	23

2.16 Palp-tracking algorithm.....	24
2.17 Responsive locusts	25
2.18 Individual locust responses	25
2.19 Mapping neural responses onto palp-opening response dynamics	25
2.20 Behavior experiments – operant conditioning	26
2.21 Minimally-invasive electrophysiology experiments	27
2.22 Monitoring neural responses in behaving locusts	27
2.23 Custom tetrode fabrication.....	28
2.24 Signal processing for RMS	30
2.25 Response stability and correlation.....	31
2.26 Dimensionality reduction analysis (minimally invasive experiments)	31
2.27 Classification analysis.....	32
2.28 Walking locust recordings.....	32
2.29 Freely moving recordings.....	33
2.30 Processing data from freely moving recordings.....	33
Chapter 3: Encoding of innate appetitive preferences in the early olfactory pathway	35
3.1: Introduction	35
3.2 Results	37
3.2.1 Innate appetitive preferences of locusts to an odor panel	37
3.2.2 Individual projection neuron responses to appetitive and non-appetitive odorants	42
3.2.3 Ensemble projection neuron responses to appetitive and non-appetitive odorants.....	46
3.2.4 Predicting behavioral preferences from odor-evoked neural responses.....	49
3.3 Discussion and conclusions.....	53
3.3.1 Chemical (input) vs. neural vs. behavioral (output) spaces	54
3.3.2 Individual PN responses vs. ensemble responses	55
3.3.3 Valence encoding at the level of sensory neurons	56
3.4 Acknowledgments and contributions	57
Chapter 4: Neural constraints on acquired appetitive preferences.....	58
4.1 Introduction	58
4.2 Results	61
4.2.1 Stimulus history and ambient conditions induce variations in PN responses	61

4.2.2 Robust odor recognition despite varying history and ambient conditions	63
4.2.3 A flexible neural decoder produces accurate behavioral predictions.....	67
4.2.4 Effectiveness of the classical conditioning approach.....	68
4.2.5 Innate versus acquired preferences for odorants	70
4.2.6 A linear model predicts behavioral response dynamics and cross-learning.....	74
4.2.7 A neural coding logic for encoding appetitive odor preferences	80
4.3 Discussion and conclusions.....	83
4.3.1 Invariant odor recognition.....	83
4.3.2 Acquired appetitive preferences.....	84
4.3.3 Neural manifolds for generating and patterning behavioral outcomes	85
4.3.4 Operant conditioning.....	87
4.4 Acknowledgements and author contributions	88
Chapter 5: Neural recordings in moving and behaving insects: from neuroscience to engineering applications	90
5.1 Introduction	90
5.2 Results	92
5.2.1. Minimally invasive neural recording technique.....	92
5.2.2 Effect of appetitive conditioning on odor representation.....	95
5.2.3 Neural activity in fully moving locusts	101
5.2.4 Explosive detection using minimally invasive recordings.....	106
5.3 Discussion	114
5.4 Acknowledgments and author contributions.....	117
Chapter 6: Conclusion.....	118
6.1 Summary of findings.....	118
6.2 Future work	125
6.2.1 Mechanisms in the antennal lobe	125
6.2.2 The functional role of opponent PN ensembles	126
6.2.3 Understanding behavioral readout of olfactory inputs.....	132
6.2.4 Real-world chemical detection using locusts	133
References.....	136

List of Figures

Figure 1.1: A schematic showing the insect olfactory anatomy	3
Figure 1.2: Labeled-line coding scheme	6
Figure 1.3: Spatiotemporal coding scheme using ON and OFF responses.....	7
Figure 1.4: Different behavioral assays in insects.	11
Figure 1.5: Approaches for quantifying insect behavior	12
Figure 1.6: A schematic showing how insects can be used to detect chemicals of interest in a field setting.....	15
Figure 3.1: Innate appetitive preferences of locusts to a diverse odor panel.....	38
Figure 3.2: Additional controls for assaying innate appetitive preference	41
Figure 3.3: Extracellular PN responses to the odor panel.....	43
Figure 3.4: Characterizing individual PN responses.....	45
Figure 3.5: Ensemble PN responses for appetitive and non-appetitive odorants	47
Figure 3.6: ON and OFF responses to odorants are encoded by distinct subsets of PNs	48
Figure 3.7: Neural response patterns robustly predict innate behavioral preferences for odorants	50
Figure 3.8: Monte Carlo simulations	52
Figure 3.9: Additional controls for regressor specificity	53
Figure 3.10: Mapping chemical features/properties onto behavioral valence	54
Figure 3.11: Mapping odorant responses in olfactory receptor neurons to innate valence	57
Figure 4.1: Projection neuron responses vary in a stimulus-history dependent manner	61
Figure 4.2: Projection neuron responses vary under altered humidity conditions.....	62
Figure 4.3: An appetitive conditioning assay to train locusts.....	63
Figure 4.4: Locusts can robustly respond to an odorant with varying stimulus history	65

Figure 4.5: Locusts can robustly respond to an odorant with varying ambient humidity conditions	66
Figure 4.6: A flexible classifier can accurately predict behavior from PN responses	68
Figure 4.7: Locust responses to hexanol are consistent across multiple unrewarded trials.....	70
Figure 4.8: Diverse odorants used for Pavlovian conditioning assays	71
Figure 4.9: Only innately appetitive odorants can be reinforced using classical conditioning	72
Figure 4.10: ON- and OFF- conditioning produce temporally distinct responses.....	73
Figure 4.11: Predictable behavioral response dynamics, cross-learning, and generalization between trained odors	75
Figure 4.12: Quantifying locust learned responses and model performances	77
Figure 4.13: Linear regression models to map neural responses to behavior.....	79
Figure 4.14: Neural manifolds can explain innate and acquired behaviors	81
Figure 4.15: Operant conditioning to reinforce locusts using appetitive and non-appetitive odorants.....	88
Figure 5.1: Minimally invasive surgical technique.....	93
Figure 5.2: Custom tetrodes for minimally invasive recordings.....	94
Figure 5.3: Long-term acquisition of odor-evoked signals.....	95
Figure 5.4: Using glucose as a food reward for appetitive conditioning.....	96
Figure 5.5: Simultaneous neural recordings and appetitive conditioning assay	98
Figure 5.6: Neural response manifolds in behaving locusts	100
Figure 5.7: Setup for freely moving locust experiments.....	101
Figure 5.8: Neural recordings from freely moving locusts.....	103
Figure 5.9: Controls for walking locust experiments.....	105
Figure 5.10: Minimally invasive procedure to record PN responses to different explosive chemicals.....	108
Figure 5.11: Neural responses can be used to decode chemical identity.....	111
Figure 5.12: Freely moving locust responses to an explosive precursor	114

Figure 5.13: Long-term recording from walking locusts.....	117
Figure 6.1: Opponent PN ensembles for behaviorally distinct odorants	127
Figure 6.2: Concentration coding in PNs.....	129
Figure 6.3: Concentration coding in humid ambient conditions.....	131
Figure 6.4: Markerless tracking for pose estimation in locusts	134

Acknowledgments

Just like the neurons that I studied, this dissertation may be my output, but it would be nothing without the collaborative inputs I have received from my advisors, lab mates, and friends during this time. First and foremost, I would like to thank my advisor, Dr. Barani Raman, for giving me the freedom to ask questions and support as I searched for answers. My time in the Raman Lab has been immensely pleasurable thanks to all the wonderful friends whom I have had the chance to interact with and grow professionally and personally.

I would like to thank Michael Traner for his invaluable friendship and support - collaborating with you has been the most memorable part of this journey. A big thank you to Suyash Harlalka – I hope our discussions on science, sports, and (most importantly) food never end! Doris Ling, Dr. Darshit Mehta, and Avishek Debnath – thank you for enduring my humor and the discussions we had on our walks and over countless cups of tea and coffee.

I sincerely thank the members of my dissertation committee Dr. Dennis Barbour, Dr. Shantanu Chakrabarty, Dr. Daniel Kerschensteiner, and Dr. Srikanth Singamaneni for their time, advice, and feedback through the course of my PhD.

Lastly, I would like to thank my parents for their unwavering love and support throughout the last ten years that I have spent away from them. Thank you for always letting me pursue my dreams.

Rishabh Chandak

Washington University in St. Louis

May 2022

Dedicated to my parents.

ABSTRACT OF THE DISSERTATION

Mapping neural responses onto innate and acquired behavior:

from insect olfaction to realizing a bio-hybrid chemical recognition system

by

Rishabh Chandak

Doctor of Philosophy in Biomedical Engineering

Washington University in St. Louis, 2022

Professor Baranidharan Raman, Chair

In many organisms, the sense of smell, driven by the olfactory system, serves as the primary sensory modality that guides a plethora of behaviors such as foraging for food, finding mates, and evading predators. Using an array of biological sensors, the olfactory system converts volatile chemical inputs from an organism's environment into well-patterned neural responses that inform downstream motor neurons to drive appropriate behaviors (e.g., moving towards food or away from danger). For many external cues, the elicited neural responses are often determined by the genetic makeup of the organism, which assigns an innate preference, or valence, for these different stimuli. However, our environment is constantly in flux, and the same stimulus can be encountered in a variety of different contexts, such as following other cues or under different ambient conditions (e.g., humidity). This can modify the neural activation pattern ascribed to the stimulus and potentially alter the corresponding behavioral output. The objective of this dissertation is to understand how neural responses in the early olfactory system of locusts (*Schistocerca americana*) are spatiotemporally structured to robustly represent innate valence in different scenarios to drive appropriate behaviors and how they can be altered through learning.

To achieve this goal, we used a large panel of chemically diverse odorants and characterized the neural responses they elicited in the antennal lobe (at the level of ensembles of principal or projection neurons) as well as the innate appetitive behavioral response they produced. We found that neural responses generated both during (ON response) and after (OFF response) termination of the odorant contained information regarding its identity and could be used to predict the innate behavioral outcomes. Notably, predictions made using the ON and the OFF responses differed in the sets of neurons they used to generate the predictions, indicating that neural-behavioral transformations could be achieved in multiple ways. Furthermore, both these ON and OFF neural response classifiers outperformed attempts to predict behavior using chemical features of the stimuli (detected by NMR or IR spectra), indicating that the antennal lobe was transforming and encoding olfactory inputs to map them onto the innate valence associated with the sensory cue.

We found that the organization of odor-evoked neural responses that readily map onto innate preferences may also constrain learned odor-reward associations. While odorants with an innate positive behavioral preference alone could support learning odor-reward associations, the conditioned responses were not odor-specific but appeared to generalize to other odorants that evoked similar neural responses. The timing of the behavioral responses could be varied by delivering rewards during epochs when the odorant would generate either the ON or the OFF neural responses. Overall, we found that the organization of ON and OFF neural responses in the antennal lobe clustered into manifolds or subspaces that could be explained using innate behavioral preferences and suitability for reinforcement learning.

To understand the robustness of these results, we developed novel minimally invasive experimental methods to record locust neural responses while they actively sampled their

surroundings. We found neural responses in this more naturalistic scenario to maintain their manifold organization, and classical conditioning enhanced the separation between neural responses evoked by innately appetitive and non-appetitive odorants. Our results also indicate that neural and behavioral responses in freely moving locusts were consistent with those observed earlier in highly compromised preparations. Finally, we exploited our newly-developed recording techniques to engineer an insect-based chemical sensor that could be used for a real-world application.

Chapter 1: Introduction

All organisms, ranging from humans to bacteria, have evolved sensory systems to help perceive and internalize information about their environment. Chemosensation, or the detection of both volatile and non-volatile chemicals, is one of the oldest and most prevalent sensory modalities available to an organism. The sense of smell is a form of chemosensation that involves the detection of volatile compounds (odorants) in an organism's immediate surroundings. The process of smelling odorants, or olfaction, drives a plethora of human behaviors and emotions ranging from pleasurable experiences such as baking a chocolate cake to detecting a dangerous gas leak. Odor-evoked memories such as smelling a perfume that reminds you of a relative have been shown to activate regions of the brain linked with vividness and emotion^{1,2}. Conversely, a loss in the sense of smell (anosmia) has been associated with hazardous events such as food poisoning³ and is an early symptom of neurological disorders such as Alzheimer's⁴ and Parkinson's⁵ disease. Thus, from a human perspective, gaining a thorough understanding of our olfactory system is highly desirable. However, for many organisms, the olfactory system plays an even larger role in survival and propagation.

In invertebrate organisms such as insects, the olfactory system serves as the primary sensory modality. It guides basic behaviors such as foraging for food, finding mates through the detection of conspecific cues (e.g., pheromones⁶), and evading predators⁷. Colonies of ants, which can number in the hundreds of millions, communicate through the detection of pheromones via their antennae to signal the presence of food or to alert other members of the group to imminent danger⁸⁻¹⁰. Similar approaches have also been demonstrated in honeybees¹¹,

fruit flies (*Drosophila*)¹², and locusts¹³, making them ideal model systems to study olfaction. In this work, I will investigate how the locust (*Schistocerca americana*) olfactory system encodes for different stimuli to drive fast and robust behavioral responses and how we can leverage this efficient biological neural network to solve real-world chemical recognition problems.

1.1 The olfactory system

1.1.1 Structural organization

The detection of a chemical begins when its molecules bind to one of the many olfactory receptors (ORs) expressed in olfactory receptor neurons (ORNs) located at the periphery of the olfactory system (nose in humans, antennae in insects). Each ORN expresses one type of OR, which typically detects a limited set of molecular features. The 2004 Nobel Prize in Physiology was awarded to Buck and Axel for their groundbreaking work demonstrating the existence of approximately one thousand genes that encode for different ORs in the rat DNA¹⁴. The exact number of these genes varies vastly across species – for example, evolutionary differences¹⁵ have resulted in humans possessing about four hundred of these genes^{16,17}.

In insects, ORNs similarly detect and transduce chemical cues to electrical signals and relay them to a region of the brain known as the antennal lobe (AL). In locusts, each antenna houses ~50,000 ORNs which project onto a network of ~1,000 glomeruli in the AL. In each glomerulus, ORNs make synaptic connections with cholinergic projection neurons (PNs). The network of ~830 PNs also forms reciprocal dendro-dendritic connections with GABAergic local neurons (LNs). The funneling of information from a large number of ORNs onto fewer PNs as well as the feed-forward and recurrent inhibition via LNs serves to minimize single-neuron response fluctuations observed at the level of individual ORNs and sharpens the signal-to-noise

ratio¹⁸⁻²⁵. Studies have also found that PNs respond to a wider/more diverse set of odorants than their upstream counterparts and in more temporally diverse patterns²⁶.

From the AL, axons of PNs project to the mushroom body (MB) and the lateral horn (LH). In the mushroom body, PNs form excitatory synapses with intrinsic Kenyon cells (KC), with each KC receiving input from a random subset of approximately half the PNs²⁷. The ~50,000 KCs also receive inhibitory input from a giant GABAergic neuron (GGN), which further sparsens odor responses²⁸. The MB integrates olfactory information with signals it receives from other regions such as the optic lobe (visual system) and is believed to be the seat of memory and learning²⁹.

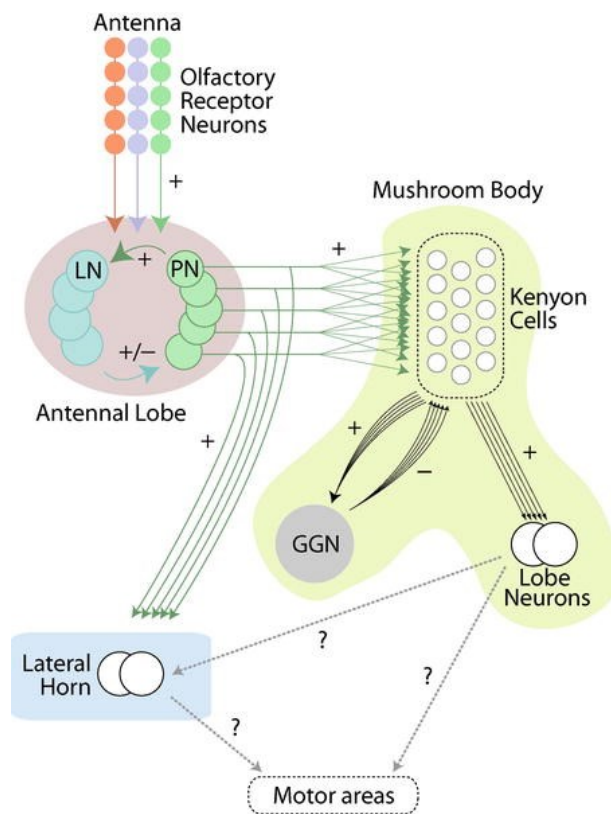


Figure 1.1: A schematic showing the insect olfactory anatomy

ORNs detect chemicals in the immediate surroundings and relay this information to PNs and LNs in the AL where it is transformed via combinations of excitatory and inhibitory interactions. PNs then relay this

to the MB and LH via excitatory outputs, where this information is further sparsened through inhibition provided by the GGN. (Figure reproduced as is from Gupta et al.³⁰)

The role of the lateral horn in locusts is much less understood. Similar to the MB, this region receives excitatory input from PNs and inhibition from the GGN, and has also been implicated in integrating multi-modal stimuli^{28,31}. However, the exact role of this region is yet to be fully understood, with some studies associating it with encoding innate preferences³² and others proffering bilateral integration of information and intensity encoding as the primary functions²⁸. Lastly, the mapping from olfactory information from the mushroom body and lateral horn to downstream motor areas also remains an open area of research.

1.2 Olfactory coding principles

Along the locust antenna, ORNs are distributed among conical protruding structures known as sensilla. There are four major types of sensilla in locusts – basiconica, trichodea, coeloconica, and chaetica, and each sensillum houses between 5-50 ORNs within it³³. The distribution of these sensilla along the length of the antenna varies by type and has also been shown to vary as a function of age³³. Each sensillum is thought to house ORNs that detect chemical stimuli with similar features (e.g., alcohols, ketones), while some function as mechano- and hygro- receptors. Typically, ORNs within a sensillum function independently of one another and relay their information to glomeruli in the antennal lobe using temporally structured ‘spike trains’ (bursts of action potentials). However, an exception to this rule can arise when ORNs within the same sensillum compete for limited resources in the extra-sensillar lymph. In such cases, the strong activation of one ORN can often transiently silence its neighbors through a phenomenon known as ephaptic coupling^{34,35}. While this approach can allow the selective detection of biologically important cues in a complex environment and has been shown to modulate innate preferences of *Drosophila*³⁶, it remains to be observed in locusts.

Another popular motif of stimulus encoding is the ‘labeled-line’ approach (**Fig. 1.2a**), where dedicated ORNs respond to ‘private’ odors and ultimately drive behavior by evoking neural responses in similarly dedicated downstream channels³⁷⁻⁴¹. A confounding factor for this coding approach is the observation that an increase in the intensity (concentration) of a stimulus often recruits more and more ORNs to be activated, which can then trigger undesirable/non-labeled line downstream responses^{42,43}. This form of encoding is primarily ascribed to *Drosophila* and is rarely observed at the level of second-order neurons (PNs) in other model systems (note an exception in moths shown in **Fig. 1.2b**). For instance, in locusts, individual PN responses to a chemical are easily perturbed when variations in stimulus history (non-overlapping cues), stimulus background (overlapping cues), ambient conditions (humidity), and stimulus durations were introduced^{23,44-46}. In a recent study⁴⁶, it was shown that hexanol (a commonly studied odorant) elicited strong responses in 42% of recorded PNs when it was presented solitarily with no additional confounds. However, the introduction of just five distractor cues preceding hexanol (presented as 5 different sequences of distractor-hexanol) resulted in no single PN retaining a strong and unique response to hexanol across all perturbations (**Fig. 1.2c**).

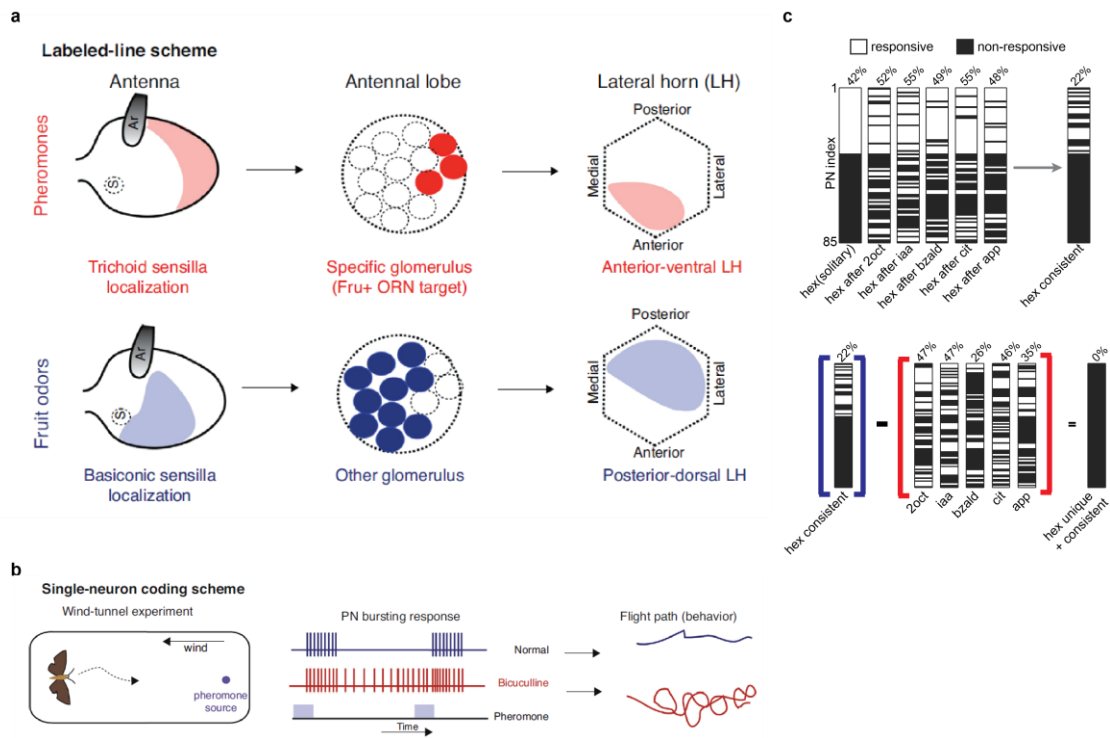


Figure 1.2: Labeled-line coding scheme

a) In *Drosophila*, pheromones and fruity odors are detected by distinct classes of sensilla, which relay information to distinct regions of the second- and third-order centers.

b) Altering the firing properties of a subset of specialized PNs in the moth antennal lobe interfered with successful odor detection.

c) Locust PNs cannot encode for odorants robustly using labeled-line coding schemes. The introduction of just five distractor cues resulted in no single PN that could retain unique responses to hexanol. (panels a, b reproduced as is from Saha et al.⁴⁷; panel c reproduced as is from Nizampatnam et al.⁴⁶)

Instead, locust PNs encode for stimuli using a ‘combinatorial coding’ approach, where the same stimulus evokes excitatory and inhibitory responses across subsets of these PNs (i.e., ON-responses). These responses are unique for different chemicals and can vary both in the distribution of PNs that produce a response, as well as in the temporal structure of the responses (response latency, firing patterns, and duration) (‘spatiotemporal’ coding; **Fig 1.3a**)²².

Interestingly, subsets of PNs are also similarly activated when a stimulus is terminated (i.e., OFF-responses)⁴⁴. However, it has been shown that the subsets of PNs that are ON- and OFF-

b) A model combining spatiotemporally diverse ON and OFF PN responses produces robust behavioral predictions. (Figure reproduced as is from Traner et al.⁴⁸)

Beyond the antennal lobe, the MB responds to olfactory stimuli with relative sparsity, with KCs often firing a single action potential in response to a stimulus lasting on the order of seconds²³. Neurons in the lateral horn (LHNs) have been shown to exhibit great morphological and functional diversity, with at least ten different classes identified – each with different stimulus-response dynamics²⁸. Given the multi-modal integration behavior of LHNs, the precise role of these different classes in the context of olfaction remains to be elucidated.

1.3 Olfaction and behavior

1.3.1 Innate and acquired behaviors

One of the fundamental goals of neuroscience is to understand how the nervous system encodes different sensory cues to generate appropriate behavioral responses⁴⁹. In the context of olfaction, behavioral responses can be broadly characterized by how much an organism likes (attraction) or dislikes (aversion) a particular smell. We are likely to venture into the kitchen if we smell our favorite meal cooking, whereas the smell of rotten eggs would keep us away. These preferences for different smells can either be genetically pre-programmed (innate) within an organism or can be acquired/learned/altered over its lifetime.

Innate preferences arise as organisms evolve to successfully interact with their environment – for example, mice are innately aversive to the smell of chemicals commonly released by their predators such as those found in the excreta of foxes and cats^{50,51}, whereas the smell of cheese is more likely to attract them. Most insects are innately attracted to the pheromones released by their mates^{6,9} and are repelled by odorants that signal the presence of toxic microbes⁵². However, the environment around us is constantly in flux, and we can often

encounter novel stimuli that do not directly map to any innate preferences. In such cases, we develop or acquire preferences for these stimuli based on our experiences. Additionally, our innate preferences for a stimulus can also be altered through experience. Getting food poisoning after consuming your favorite meal can make you less likely to consume it the next time!

In the 19th and early 20th centuries, two approaches to induce alterations in or allow the acquisition of behavioral responses in response to a stimulus were demonstrated. Ivan Pavlov was awarded the Nobel Prize in 1904 for his pioneering work in developing classical conditioning, where he famously induced salivation in a dog in response to the ringing of a bell⁵³. Pavlov achieved this by pairing the ringing of the bell with the presentation of food, a phenomenon that innately triggers salivation in dogs. Through repeated trials, the dog associated the bell with the expectation of food and acquired the salivation response even when no food was presented. The second approach demonstrated by Thorndike⁵⁴, and more famously by B.F. Skinner⁵⁵, is known as operant conditioning. This is a more ‘voluntary’ form of learning associations compared to classical conditioning. Simple examples of operant conditioning are children learning to avoid touching a hot stove to prevent injury or learning to do their homework in anticipation of chocolate rewards.

In many invertebrate model systems, a similar association of behavioral responses to stimuli has been well-studied through various classical and operant conditioning assays⁵⁶. Avoidance behaviors have been induced in *Drosophila*⁵⁷ and honeybees⁵⁸ through the pairing of electric shocks (negative reinforcement) with otherwise neutral odorants. Similarly, the pairing of food rewards with different olfactory stimuli has been successfully demonstrated in moths^{59,60}, honeybees^{61,62}, and *Drosophila*⁶³ (positive reinforcement; **Fig. 1.4a**). After conditioning, the changes in behavior towards different stimuli are typically measured using either unrewarded

presentations of the olfactory stimulus or in assays such as T-maze (**Fig 1.4b**) or free exploration (**Fig. 1.4c**). Recently, a classical conditioning assay was shown to be effective in positively conditioning locusts with olfactory cues⁶⁴. The authors devised a protocol wherein the locusts were trained to associate a conditioned stimulus (odorant) with an unconditioned stimulus (food reward) that was known to elicit a strong unconditioned response (palp-opening response). The efficacy of training was then quantified during an unrewarded testing phase, where the locusts who were trained showed an increase in their preference for the trained odorant compared to their untrained counterparts. In this work, we will apply multiple behavioral assays to understand the robustness of innate olfactory preferences in locusts, and how conditioning assays can be applied to alter these innate behaviors.

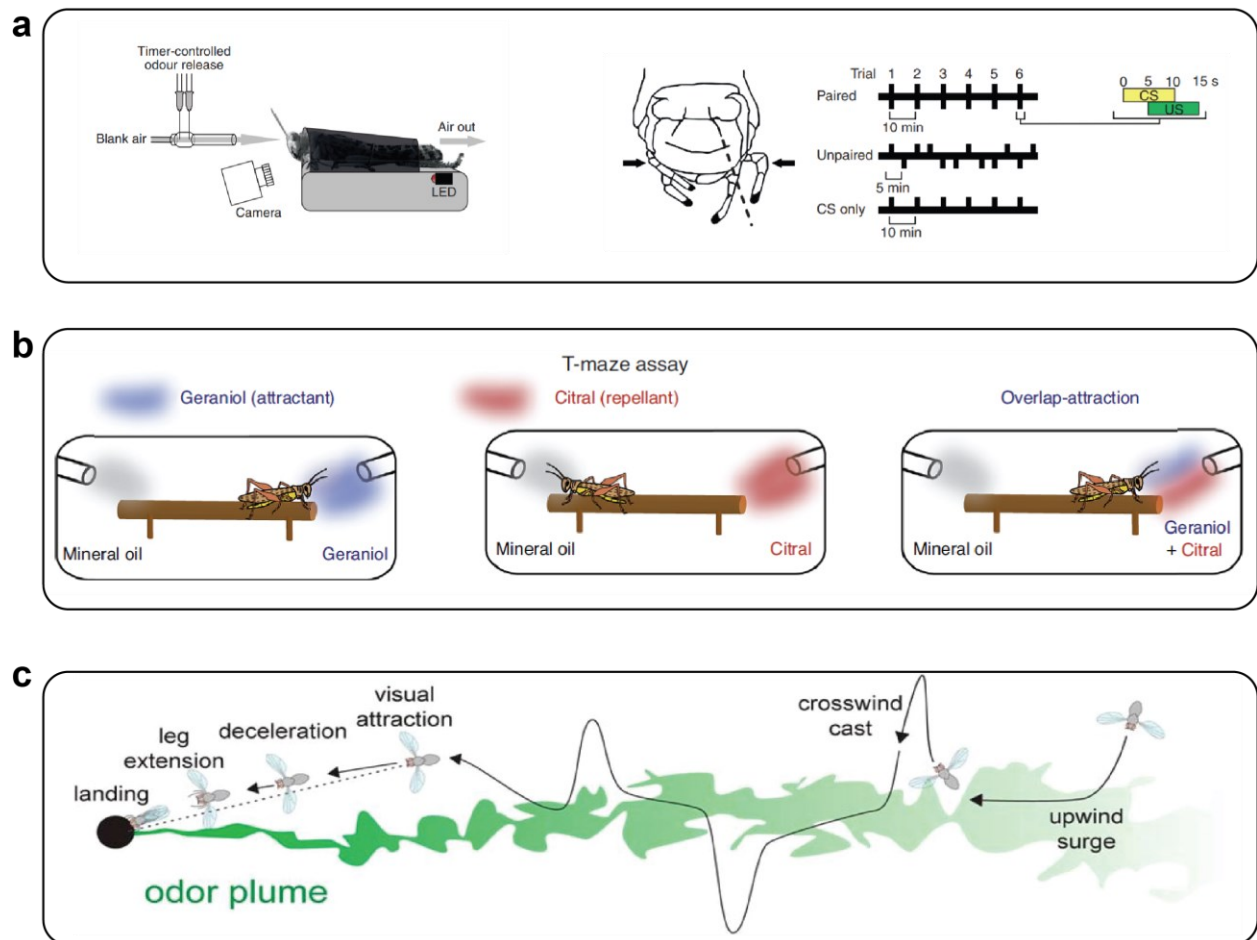


Figure 1.4: Different behavioral assays in insects.

a) Insects can be classically conditioned to alter their preferences to an odorant. Here, a food reward was paired with an olfactory stimulus to condition the palp-opening response in locusts. The protocol used to achieve this is shown on the right.

b) After conditioning, changes in behavioral preferences of insects can be measured using two-choice assays such as T-maze. Here, one side of an arena contains an olfactory cue and the other side contains a control. The preferences of locusts to different cues are measured by computing the time they spend near the odorant relative to control.

c) Behavioral preferences can also be assayed using odor-detection assays such as plume or trail following in wind tunnels or field settings. Metrics such as ease of trail-following, time spent near the trail, and time taken to localize the odor source can be used to compare relative preferences of different cues. (Figure panels reproduced as is from a⁶⁴, b⁴⁷, and c⁶⁵)

1.3.2 Quantifying behavior

Recent progress has allowed both monitoring and controlling large populations of neurons with high spatial and temporal resolution. Transgenic insects that express fluorescent markers in select groups of neurons are widely being used to characterize how these populations encode information about various sensory cues and drive different motor programs⁶⁶⁻⁶⁸. However, similar approaches for characterizing invertebrate behavior are only beginning to be adopted, given the challenges of their smaller scale and unique anatomy compared to mammals.

Modern advances in data acquisition and processing allow behavioral responses to be monitored at fine temporal and spatial resolutions. Error-prone and time-consuming manual tracking of animal position is gradually becoming obsolete as computer vision algorithms that can track the centroid/center-of-mass of an object of interest are becoming easier to deploy. The addition of markers such as tagging individuals with unique RFID⁶⁹⁻⁷³ or QR tags⁷⁴⁻⁷⁸, or applying non-inhibitive paint^{44,79} have further optimized these approaches (**Fig. 1.5**). Insects are highly social organisms, and their behaviors are often modulated by other members of the group present in their vicinity. These new behavioral tracking approaches can be easily extended to study group behaviors, such as social interactions in honeybees and ants⁸⁰⁻⁸⁵, behavioral variance

in groups of locusts⁸⁶, and social enhancement of light avoidance abilities in cockroaches⁸⁷.

More recently, applications of deep learning have allowed markerless recognition of individual organisms. Noteworthy tools include DeepPoseKit and DeepLabCut, where the authors trained deep convolutional neural networks (CNNs) to detect organisms by providing a handful of frames labeled with poses of interest⁸⁸⁻⁹⁰.

In this work, I will train and apply deep learning frameworks to track and quantify different locust behaviors. In particular, the accurate measurement of behavior at fine spatial and temporal resolutions will be necessary as we look to understand the nuances of conditioning-induced alterations in the locusts' behavioral responses.

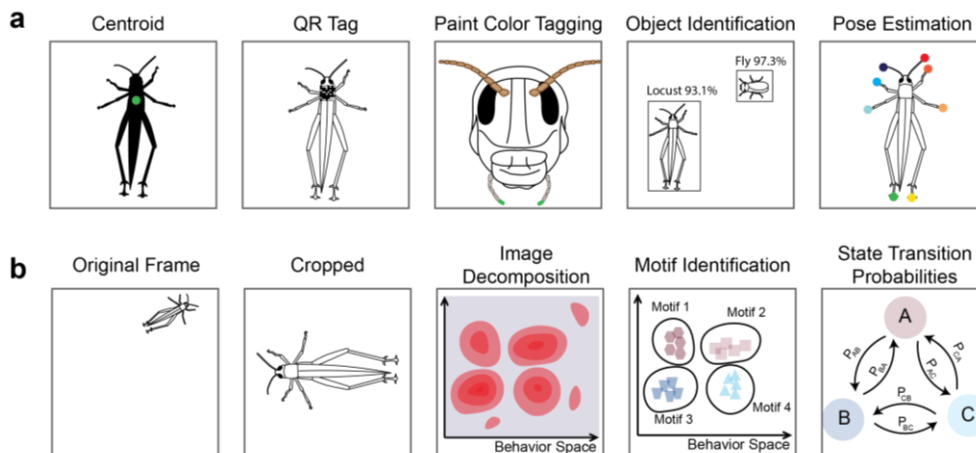


Figure 1.5: Approaches for quantifying insect behavior

a) A wide range of tracking such as centroid tracking, addition of QR codes, and non-inhibitive paint. Novel markerless tracking approaches using deep learning allow tracking of untagged individuals.

b) A schematic of a pipeline for extracting behavioral motifs from data using object detection and dimensionality reduction. (Figure reproduced as is from Traner et al.⁴⁸)

1.4 Simultaneous neural and behavioral monitoring

A drawback of the current approaches in insect neuroscience is that the mapping from the neural space to the behavioral space remains largely correlational and not causal. With the established techniques to monitor large populations of neurons within an individual organism and the ability to quantify the complex behaviors of individuals, the final piece of the puzzle remains the simultaneous achievement of these feats in the same organism.

One approach to achieve this has been through the use of virtual reality (VR) setups, which can be used to study tethered flight or head-fixed walking in most insect models while visual, olfactory, or mechanosensory inputs are varied. VR was recently applied to study how different insects successfully navigate complex environments and perform long-range search behaviors using their visual and olfactory systems while simulating flight⁹¹. Going beyond the VR environments to more realistic settings has been hindered due to the scale of insects, which pose a significant engineering challenge to design and fabricate electrodes. While miniature electrode arrays have been developed for use in insect models, their commercial availability remains limited, and preparing custom in-house electrodes is often an easier solution⁹². Traditionally, mobile preparations have required balancing the increase in noise with electrode length against the mobility offered to the animal. While relatively long electrodes that do not hinder the insect's movement have been used successfully^{93,94}, they still limit experiments to laboratory settings. Innovations in technology are now beginning to allow the placement of miniaturized amplifiers and digitizers directly on the animal⁹⁵⁻⁹⁷. These systems can additionally be combined with onboard data-logging or wireless transmission capabilities to provide unrestricted movement to the animal – and increase the physical range of the experiment.

However, these developments are still in early stages and require research in optimizing battery technology, conserving signal fidelity, and reducing the overall bulkiness of the system.

In this work, we will develop methods to achieve simultaneous neural and behavioral monitoring in freely moving locusts. This will not only enhance our experimental repertoire for neuroscientific studies but also have practical use cases, such as those discussed in the next section.

1.5 Insect-based chemical sensing

Insect models have been successfully used to not only understand the neural basis of olfactory processing but also in many practical applications – such as using *Drosophila* ORNs to detect breast cancer⁹⁸ or training wasps to detect fungal toxins in healthy crops⁹⁹. More recently, advances in engineering have led to the development of hybrid biosensors. These part biological – part engineered systems allow us to tap into the rich repertoire of the insect olfactory system, which can robustly detect a wide variety of chemicals at concentrations that are challenging for current state-of-the-art silicon-based sensors^{100–103}. Proof-of-concept studies deploying insects mounted on manually controlled drones^{104–107} or through direct control of their flight and movement¹⁰⁸ have been proposed to perform chemical exploration assays in settings where human intervention is infeasible (tightly enclosed spaces) or undesirable (harmful chemicals). Recent work in locusts has demonstrated the potential of tapping into their antennal lobe to perform chemical localization⁹⁴ (**Fig. 1.6**). In this work, we will develop novel experimental approaches to demonstrate how the locust antennal lobe can be used as a sensor for fast and accurate detection of explosive chemicals.

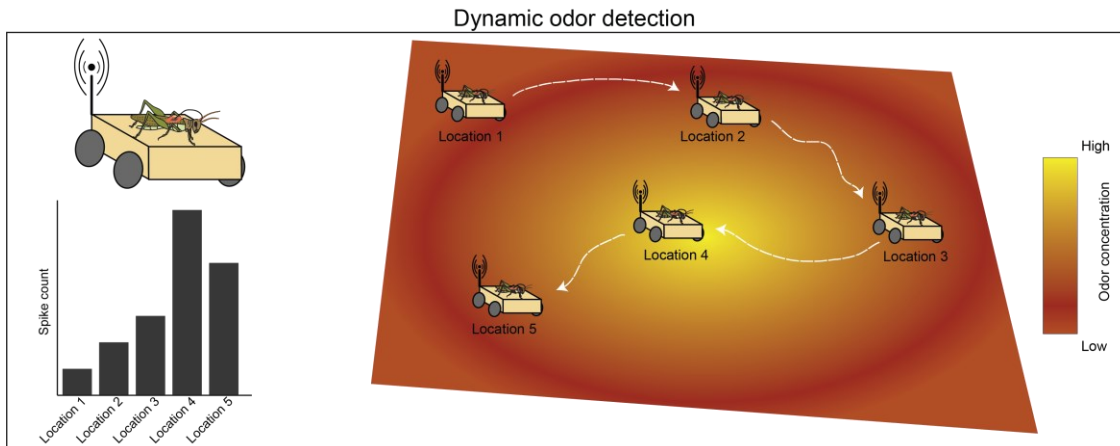


Figure 1.6: A schematic showing how insects can be used to detect chemicals of interest in a field setting

In this experiment, the neural responses of locusts would be monitored as the locust is systematically moved on a guided robot in an arena containing a chemical of interest. The concentration of the chemical varies in different regions of the arena, which can be mapped by monitoring the locusts' spiking activity – the higher the concentration of the chemical, the higher the spike count. (Figure reproduced as is from Saha et al.⁹⁴)

1.6 Thesis outline

In this thesis, I will investigate how neural responses to a variety of stimuli in the early locust olfactory system are organized to efficiently map onto different innate and acquired behavioral outcomes. To achieve this goal, in Chapter 3, I will demonstrate how locusts display a broad range of innate appetitive preferences to a large panel of chemicals and how we can use information from temporally diverse neural responses in the antennal lobe to predict a chemical's innate preference. In Chapter 4, I demonstrate that locusts can achieve behavioral invariance despite neural variability and how this potential confound can be resolved using simple algorithms. I will also show how locusts can be conditioned to alter their behavioral responses to a stimulus using classical conditioning and explore the limits of this approach. In Chapter 5, I show novel recording techniques that allow the simultaneous monitoring of behavior and neural activity in the same locust, and how we can use these methods to validate observations made from more traditional experimental approaches.

Additionally, in Chapter 5, I will also explore how our enhanced understanding of the biological olfactory coding principles can be exploited to solve real-world chemical detection problems. I will demonstrate how the novel preparations generated in our basic neuroscience investigation can be applied to solve the problem of detecting explosive chemicals with high accuracy and low latency.

Chapter 2: Methods

2.1 Odor stimulation

All odorants were delivered at a 1% v/v dilution in mineral oil and placed in dark 60-ml bottles. A constant background air stream (desiccated and filtered) at 0.75 L/min was used as the carrier stream for 0.1 L/min pulses of odorants. A large vacuum funnel placed directly behind the antenna allowed for the constant clearing of the odorants delivered.

For behavioral experiments to quantify innate and acquired appetitive preferences, each odorant in the panel was presented for one trial in a pseudorandomized order. Odorants were delivered by displacing a 0.1L/min of headspace in the odor bottles using a pneumatic picopump (WPI Inc., PV-820). Each odor pulse was 4 s, except for distractor-hexanol sequences where odors were delivered as 4 s – 0.5 s gap – 4 s. The inter-trial interval was 60 s for innate preference experiments and at least 20 minutes for acquired preference assays.

For electrophysiology experiments (Chapter 3-4), each odorant was presented for ten trials in a pseudorandomized order. To minimize interference during the experiment, we designed and built a custom olfactometer (SMC valves, NI-DAQ controller) that was automated and triggered using MATLAB. Each odor pulse was 4 s in duration, and the inter-pulse interval was 60 s. For minimally invasive electrophysiology experiments (Chapter 5), each odorant was presented for five trials.

2.2 Behavior experiments to characterize innate palp-opening responses

Young adult locusts of either sex were starved for 24 hours before the experiment. Locusts were immobilized within a plastic tube and their compound eyes were covered using black tape. All twenty odorants were diluted to 1% v/v as previously described. Hexanol alone

was additionally diluted to 0.1% and 10% dilutions (i.e., a total of 22 odorants in the panel). Each locust was presented with all 22 odorants in a pseudorandomized order for 4 s pulses separated by 56 s inter-pulse intervals (60 s between the starts of two consecutive pulses). The experiments were recorded using a video camera (Microsoft). An LED was used to track stimulus onset/offset. The POR responses were scored offline in a blind fashion with no odorant information to remove any experimenter biases. Responses to each odorant were scored a 0 or 1 depending on if the palps remain closed or opened. A successful POR was defined as an opening of the maxillary palps beyond the facial ridges as shown on the locust schematic (**Fig. 3.1a**).

2.3 Preference index

As noted above, locust responses to each odorant were binarized. The responses of all locusts to an odor were then summed to obtain a Total Score. A normalized score for each odorant was then calculated as follows:

$$Norm_score_{odor} = \frac{Total\ Score_{odor}}{Total\ \# \ locusts} \quad (2.1)$$

The preference index (**Fig. 3.1c**) was then calculated for each odorant by performing a median subtraction from the Norm_score as follows –

$$Preference\ index_{odor} = Norm_score_{odor} - Norm_score_{median} \quad (2.2)$$

$Norm_score_{median}$ was obtained by calculating the median across all odorants.

2.4 Vapor pressure analysis

Vapor pressure data for 18 odorants were obtained from an online database (The Good Scents Company)¹⁰⁹. Data for neem and garlic could not be obtained and these odors were omitted from our analyses in **Fig. 3.1d**. Regression analysis was performed between vapor pressure values and the POR Total Scores. An R^2 value was obtained using the ‘fitlm’ function

in MATLAB (**Fig. 3.1d**). One of the odorants in the panel (ethyl acetate) had a vapor pressure much higher than all other chemicals, and hence the weak correlations in **Fig. 3.1d** could be driven by this potential outlier. To control for this, a similar analysis was performed in **Fig. 3.2b**, but using only seventeen odorants (i.e., excluding ethyl acetate).

2.5 Monte Carlo simulations for behavior

We performed Monte Carlo simulations on the data shown in **Fig. 3.1b**. We randomly sampled locusts (n ranging from 1 to 26) and calculated preference indices for all odors using POR scores using the selected subsets of locusts. For each n , we performed 100 such simulations and computed an average preference index, which was then compared with the preferences obtained using all twenty-two locusts. The mean correlation for each n is shown in **Fig. 3.1f**. Error bars indicate the standard error of the mean (s.e.m.).

2.6 Electrophysiology experiments – PN recordings

Young adult locusts of either sex were used for these experiments¹¹⁰. The legs and wings were removed, and they were immobilized on a custom platform. The head was fixed into place by a wax cup and the antennae were held in place inside a thin tube using epoxy glue. The cuticle above the brain was cut open, the air sacs covering the brain were removed, and the locusts were degutted to minimize any internal movements. A metal wire platform was then inserted underneath the brain to lift and stabilize it. Finally, the transparent sheath covering the brain was removed after applying protease enzyme.

Locust brains prepared this way were super-fused with artificial saline buffer and a reference electrode (Ag/Ag-Cl) was inserted into the saline. Multi-unit recordings were made from the antennal lobe projection neurons (PNs) using a 4x4 silicon probe (NeuroNexus) with impedance in the 200-300 k Ω range (**Fig. 3.3a**). Data were acquired at a 15 kHz sampling rate

using a custom MATLAB program and filtered between 0.3-6 kHz using an amplifier system (Caltech) that provided a 10,000 gain.

Offline spike-sorting (IgorPro) was performed using the best 4 channels recorded¹¹¹. To identify single units (PNs), the following previously published criteria were used: unit cluster separation >5 noise s.d., the number of spikes within 20 ms $<6.5\%$, and spike waveform variance <6.5 noise s.d. To account for baseline drift and loss of neurons during an experiment, we only included PNs with consistent baseline spiking activity in all 220 trials (22 odors, 10 trials each). We defined a PN as being consistent if its baseline firing rate (during a 4 s period before odor presentation) in all trials was no less than 15% of the maximum baseline firing rate for that PN. A total of 89 PNs were identified using these criteria (originally acquired 131 PNs from 26 locusts).

2.7 PID experiment

We used a fast-photoionization diode (miniPID, Aurora Scientific) to characterize the stimulus delivery dynamics of all odors used in the electrophysiology experiments. Each odor was presented for 5 trials and PID signals were acquired at 15 kHz using a custom MATLAB program. The mean signals for all odors are shown in **Fig. 3.3b**.

2.8 Projection neuron response classification

We defined 4 s of odor presentation as an ON period, and the 4 s immediately following odor termination as an OFF period. PNs were classified as ON-responsive if the firing activity was 6.5 s.d. above mean baseline (2 s preceding the stimulus) firing activity in at least 5 of the 10 trials during the ON period. Similarly, PNs were classified as being OFF-responsive using a similar metric applied to the OFF period. PNs were classified as 'Inhibited' if their firing activity did not exceed 2 s.d. of baseline in any time bin during odor presentation and the mean firing rate

during the entire stimulus duration (4 s) was lower than mean baseline activity (in at least 5 out of 10 trials). These classifications are summarized for all odors in **Fig. 3.4**.

2.9 Dimensionality reduction analysis (fully invasive experiments)

We used Principal Component Analysis (PCA) to visualize ensemble PN activity (**Fig. 3.5a; Fig. 4.14a**). The spiking activity for each PN during 4 s of odor presentation was averaged across all 10 trials and binned in 50 ms non-overlapping time bins. In this manner, we obtained an 89 PN x 80 time-bin matrix for each odorant. We concatenated these data matrices obtained for each odor to obtain an 89x1760 data matrix (80 bins * 22 odors). We then computed a covariance matrix (89x89) for this data matrix.

Each 89-dimensional response vector was then projected onto the top three eigenvectors (that captured the highest variance). For visualization, the first time-bin was subtracted from each odor to obtain a similar pre-stimulus baseline for all odors. The odor trajectories were smoothed using a three-point moving average low-pass filter.

2.10 Hierarchical clustering analysis

The spiking activity of each PN during 4 s of odor presentation was summed to obtain an 89x1 (89 PNs) vector per odorant. Agglomerative hierarchical clustering was performed on vectors for all 22 odors using the ‘linkage’ function in MATLAB. The odors were clustered based on a correlation distance metric, and the farthest pairwise distance between clusters was minimized. The clustering was visualized using the ‘dendrogram’ function (**Fig. 3.5b**) after obtaining a leaf ordering using the ‘optimalleaforder’ function.

2.11 Linear regression to predict valence from PN activity

Mean odor-evoked activity for each PN (n_i) was used as the input for the linear regressor and the behavioral Norm_score for each odor was used as the output. A softmax layer was added

to ensure that the final prediction was always between 0 and 1. A leave-one-out-cross-validation (LOOCV) approach was used, where the model weights were trained using data for 21 odors using gradient descent, and then the neural response for the test odorant was used to predict the behavioral POR preference index. The mean squared error cost function was minimized.

$$\text{Predicted POR} = \text{softmax} \left(\sum_{i=1}^{89} w_i * n_i + \text{bias} \right) \quad (2.3)$$

Where n_i is the number of spikes evoked during odor exposure in PN_i , and w_i is the weight assigned by the linear regressor for PN_i .

As controls for the regressors, the POR preference indices of different odorants were shuffled randomly before training. We used the entire 4 s of PN activities during odor presentation for the ON-regressor, and 4 s of OFF activity immediately following odor termination for the OFF-regressor (**Fig. 3.7**).

2.12 Monte Carlo simulations for electrophysiology

We performed Monte Carlo simulations to gauge the performance of the linear regressors as a function of the number of PNs used for the analysis was varied. To achieve this, we randomly sub-sampled n (where n ranged from 1 to 89) PNs and quantified the predictive performance using mean squared error (MSE). For each n , we performed 1000 simulations and reported the average MSE (**Fig. 3.8**). We performed these simulations for both the ON- and OFF-regressors.

2.13 Angle between odors

To calculate the angular distance between two conditions, we used the high-dimensional vectors obtained from the activity of all 89 recorded PNs during 4 s of ON activity and 4 s of OFF activity (**Fig 3.6**). We averaged the response over the duration of the entire periods (4 s) to

generate mean ON (m_{ON}) and OFF (m_{OFF}) templates. The angle between these vectors was then computed as:

$$\text{Angular distance } (^{\circ}) = \cos^{-1} \left(\frac{m_{ON} \cdot m_{OFF}}{|m_{ON}| |m_{OFF}|} \right)$$

The angular distance was computed for each odor combination within a group (attractive or aversive as defined above) and across groups (**Fig 4.14c, d**).

2.14 Electrophysiology experiments – ORN recordings

Young adult locusts of either sex were immobilized by placing within a plastic tube with their antennae left accessible. The antennae were stabilized using wax, and a reference electrode (Ag/AgCl wire) was inserted into the contralateral eye. Glass micropipettes (5–10 M Ω) filled with locust saline were inserted into the base of sensilla and odorant stimuli were prepared and delivered similar to PN recording experiments. Signals were acquired using a differential amplifier (Grass P55) at 15 kHz sampling rate and filtered between 0.3 and 7.5 kHz. Recordings across all locusts were pooled and clustering analysis was performed similar to the approach described in section 2.10 (results in **Fig 3.11**)

2.15 Behavior experiments – classical conditioning

Appetitive classical conditioning experiments were performed on young adult locusts of either sex starved for 24 hours before the experiment. Locusts were immobilized within a plastic tube, their eyes were closed using black tape, and their maxillary palps were painted using a zero-volatile-organic-chemical green paint (Valspar ultra). A brief 20-minute buffer period was allowed for paint to dry and the locust to acclimatize back to baseline activity levels.

For data shown **Fig 4.8** onwards, prior to conditioning, each locust was presented with a 4 s pulse of all four odorants used in the experiment (hexanol, isoamyl acetate, benzaldehyde,

and citral). If a locust had a palp-opening response to any of these odorants, it was deemed ‘pre-conditioned’ and was discarded from the experiment. A 15-minute buffer was allowed between this pre-test and the training phase.

During the training phase, locusts were presented the training odorant diluted at 1% v/v at a rate of 0.1 L/min diluted in a constant background air stream (desiccated and filtered) of 0.75 L/min. A vacuum funnel placed behind the locust allowed for odor clearance. The odor was presented for 10 s and a food reward (wheat grass or glucose solution 1g/10 mL in water) was presented at 5 s post-odor onset for ON-conditioning. The odor was presented for 10 s and a food reward was presented at 0.5 s, 2 s, or 4 s post-odor termination for OFF-conditioning. Six such training trials were performed with an inter-trial interval of 10 minutes. Locusts that met the training criteria (>3 food reward acceptances out of 6) were then evaluated in the testing phase.

During the testing phase, locusts were presented with 4 s pulses of various odorants (at 1% dilution) in a pseudorandomized manner with a minimum interval of 20 minutes between successive tests. The palp-opening responses of the locusts were recorded using a video camera (Microsoft) at 30 fps. The odor delivery and video acquisition were synced using a custom LabView program.

Locusts were kept on a 12 h day – 12 h night cycle (7 am – 7 pm day). All behavioral experiments were performed between 10 am – 3 pm to ensure that the training phase coincided with the daily feeding time for the locusts.

2.16 Palp-tracking algorithm

To accurately track maxillary palp separation, we trained a UNet convolutional neural network using randomized initialization of weights in Keras and Tensorflow¹¹². During the

training phase, the input into this network was a single channel (green) 128x128 image cropped around the palps. The outputs were manually labeled palps (as binarized 128x128 matrices with 1's indicating palps and 0's indicating no palps). We trained the network using the Adam optimizer and binary cross-entropy loss function. We performed image augmentation using the 'imgaug' Python library and trained the network on approximately 2000 labeled frames.

Videos were input into the trained network frame-by-frame and the output was thresholded and binarized using a combination of Otsu, mean, and triangle filters from the 'skimage' library. Palp distance for each frame was calculated as the distance between the centroids of the two predicted palps using the 'regionprops' function.

2.17 Responsive locusts

Locusts were considered 'responsive' to a particular odor if they had a palp-opening response that was >6.5 s.d. above pre-stimulus baseline (2 s) for at least 30 frames (1 s) with palp separation > 1.5 a.u. (which was the noise threshold of the tracking algorithm) (**Fig. 4.9; Fig. 4.11**).

2.18 Individual locust responses

For the normalized POR traces shown in **Fig. 4.9**, we scaled each locust's response such that 0 corresponded to the minimum palp separation and 1 corresponded to the maximum palp separation the locust had across all test odors. Note that after each training paradigm, we tested locusts on four odors – hexanol, isoamyl acetate, benzaldehyde, and citral.

2.19 Mapping neural responses onto palp-opening response dynamics

PN activity and POR responses (distance between palps) for hexanol, isoamyl acetate, benzaldehyde, and citral were averaged across trials and down-sampled to 10 Hz. For each odor, we used 2 s baseline, 4 s of odor presentation, and 4 s after odor termination to obtain a 10 s

vector (100 elements at 10 Hz). We then concatenated responses from all 4 odors to obtain 400-dimensional vectors. The input data was hence 89x400 (89 PNs; spiking activity at each time point) and the output was 400x1 (palp-separation at each time point). A regularized model was fitted using ‘lasso’ (sklearn in Python) with an ‘alpha’ value of 0.01. The learned 89x1 weights were then used with the input data to generate predicted POR responses shown in red in **Fig. 4.11**.

We trained 6 such models for each training condition shown in **Fig. 4.11**. The weights obtained for all 6 models were sorted using the weights from the hexanol-ON model and are shown in **Fig. 13a**. **Fig. 4.13b** shows pair-wise correlations between each weight vector pair. The weights across all six models were averaged for each PN. 21/89 PNs had a weight > 0 and 19 PNs had a weight < 0 , with the remainder of PNs assigned a weight of 0 due to regularization. The PSTH’s of the PNs assigned positive and negative weights are shown for all 4 odors in **Fig. 4.13c**.

2.20 Behavior experiments – operant conditioning

Young adult locusts of either sex were chosen and starved for 24 hours prior to these set of experiments. All odorants used were diluted to 1% (v/v) concentration in mineral oil and the food reward was sugar water (glucose 1g/10 mL distilled water). Each locust was trained on only one of the four odorants (hexanol, isoamyl acetate, benzaldehyde, or citral). Each experiment comprised 100 trials where the odorant was presented as 4 second pulses and the inter-trial interval was set to 30 seconds. Food reward was presented to the locust if it performed a palp-opening response (POR) in a trial (no food was presented in control experiments). The number of POR responses were tabulated for each locust and each odorant to obtain final curves as a function of trial number (**Fig. 4.15**).

2.21 Minimally-invasive electrophysiology experiments

We developed a minimally invasive surgical procedure to record PN activity in tethered-but-intact locusts as well as fully moving locusts (**Fig. 5.1**). We immobilized locusts by attaching them to a custom 3D-printed manifold after removing their two hind legs to prevent jumping. A small incision in the cuticle was made to expose the brain, which was stabilized using a twisted-wire platform, and then de-sheathed to allow electrode implantation. For stationary preparations, tetrode design A (see 2.23) was implanted into one of the antennal lobes and odorants were presented. Neural signals were amplified and acquired using a miniaturized amplifier (Intan Recording System, RHD2132 16-Ch headstage) and a custom MATLAB script. Each odorant was delivered for 5 trials with each trial comprising a 4 second odor pulse. The inter-stimulus-interval was set to 56 seconds (**Fig. 5.6, 5.10**). A constant background air stream at 0.75 L/min was presented to the locust antenna and the odorant pulses were delivered at 0.2L/min atop this carrier stream. A vacuum suction was placed behind the locust to constantly clear the air stream.

2.22 Monitoring neural responses in behaving locusts

The neural recordings were performed similarly to the previous set of electrophysiology experiments. Before conditioning, we recorded 5 trials of responses to each of the 6 odors used (appetitive – hexanol, isoamyl acetate, 2-octanol; non-appetitive – cyclohexanone, benzaldehyde, citral). After a 15-minute gap, we performed the conditioning as follows - locusts were presented with 6 trials of trained odor (hexanol or benzaldehyde) with overlapping presentations of a food reward (sucrose in water 1g/10ml concentration) similar to conditioning methods described above. To minimize movement of the locust and conserve neural stability, we switched from solid food reward (grass) to liquid food reward (sucrose in water) and presented it in an automated manner using a pneumatic pump (WPI Inc., PV-820). The inter-trial interval was set to 3 minutes for the training phase. Post-training, we waited for 15 minutes and then repeated the

presentations of all 6 odors for 5 trials each. In all blocks of neural recordings, we pseudorandomized the order of odor presentation.

The neural data acquired in these experiments could not be reliably spike sorted using the approach mentioned above. As a result, we used an alternative approach for processing this dataset¹¹³. The raw data signals (acquired at 15 kHz) were de-noised using a band-pass between 300 Hz and 6000 Hz followed by clipping of signals 5 s.d. above or below the baseline level. These were then passed through a continuous moving root-mean-squared (RMS) filter with a 20 ms window (DSP toolbox on MATLAB), down-sampled by a factor of 150, smoothed by a 10-point moving average filter, and finally down-sampled by a factor of 5 to produce a temporal resolution of 20 Hz (50 ms, similar to spike sorted PN responses). The samples were finally baseline subtracted using the mean of 1 s baseline prior to odor presentation (two sample recordings shown in **Fig. 5.6a**) to obtain the Δ RMS signal. For the PCA analysis shown in **Fig. 5.6b**, we followed a similar approach as mentioned above. We used the mean of 4 s of odor presentation and 4 s of responses immediately after odor termination to obtain a 160-dimension vector for each odor (8 seconds x 20 samples per second) for each locust. We recorded from 10 locusts each for hexanol and benzaldehyde training experiments and concatenated these neural responses to obtain a final 20 locust x 160 bin response matrix for each odor during both the pre- and post-training periods.

2.23 Custom tetrode fabrication

Tetrode Design A (PDMS-Embedded Electrodes)

PDMS (Polydimethylsiloxane) microchannels-based electrode assembly fabrication were produced in three major steps, namely, patterning microchannels on a thin PDMS substrate using photolithography techniques, securing the fibers in the microchannels, and forming fiber-dip

socket connections (**Fig 5.2a**). Firstly, a chrome mask was made using a Heidelberg DWL66+ Laser writer system using a 10 mm lens. Once the laser writing of the pre-defined design was completed on the chrome disk, the pattern was finally developed using the Microposit MF -319 developer for 100 sec. Then the chrome mask was loaded to a UV-LED mask aligner (KLOE UV-KUB3) to pattern SU-8 photoresist on a 4-inch Si substrate. Before that, an appropriate amount of SU-8 2025 photoresist was spin-coated on the clean Si substrate at 3000 rpm for 30 sec using a Brewer Science CEE 200X Spin Coater to create a 30 μm photoresist layer. The pattern was then developed using a SU-8 developer. All the parameters for photoresist patterning were optimized according to the SU-8 2025 photoresist datasheet. Approximately 10 gm of bubble-less PDMS mixture (10:1) was poured on the Si master mold and cured at 60° C for 5 hours to create a 500 μm thick PDMS substrate with microchannels.

Then the cured PDMS was peeled off from the Si mold, cut into small parts at desired dimensions for housing the fibers for electrodes, secured on the appropriate position in a custom-designed 3D printed structure, and the whole assembly was glued on a dip-socket connector. Here, the final electrode housing consisted of four 50 μm channels with 30 μm walls in between to assemble the fibers with approximately 80 μm pitch on the PDMS substrate. Then four 12.8 μm diameter Nickel Chromium (NiCr) fibers were cut into the desired length and placed in the microchannels under a stereomicroscope. The PDMS housing with the fibers was then plasma etched for 90 s and UV epoxy was applied to the channels to firmly secure the fibers inside the channels. Next, the other side of the fibers were burnt using a lighter and connected to a dip-socket connector using conductive silver paste. Finally, the tips of the fibers at the recording side were cut using a serrated/surgical scissor to the desired length (approx. 0.5 -1 mm).

Tetrode Design B (Flexible Tetrodes)

Flexible tetrodes (**Fig 5.7a**) were produced from nickel-chromium tetrode wires (Sandvik RO800, 0.0005" NiCr). The ends of four uniform 1m lengths of nichrome wire were taped together, and hung from a clamp above a tetrode twister¹¹⁴. A weight bar was clipped onto the dangling end of the wires and rested in the slot of the tetrode twister. The upper clamp was adjusted to raise the weight bar approximately 1 cm above the bottom of the slot. The tetrode was then twisted to achieve a ratio of 180 turns/meter. A heat gun was used to fuse the filaments, and then the upper end of the tetrode was raised to allow the tetrode to uncoil after it had cooled for at least one minute. The tetrode was removed from the clamps and cut in half. A 50 cm length of coated silver wire (A-M Systems) was inserted along with the tetrode into a flexible polyethylene tube. The insulation on the end of the silver wire was removed using a lighter, and the cleaned silver wire and the unfused ends of the tetrode were soldered into machine-pin DIP sockets. A 32-gauge aluminum wire was soldered to the same pin as the silver wire for use as a ground, and a removed dip socket pin was soldered to the end to ensure a consistent ground connection. The upper part of the dip socket was then encased in UV-cure epoxy to mechanically stabilize and protect the assembled electrode. (**Fig 5.7b**)

2.24 Signal processing for RMS

The raw data were acquired at 15 kHz and processed using previously published techniques¹¹³. The signal from each recorded electrode was processed independently. Briefly, the signals were filtered using a bandpass filter between 0.3 and 7.5 kHz and passed through a continuous moving RMS (root-mean-squared) filter (MATLAB DSP toolbox) with a 20 ms window size. They were then down-sampled by a factor of 150, smoothed by a ten-point moving average filter, and further down-sampled by a factor of 5. This brought the final resolution of the

data to 50 ms. Data were then baseline subtracted using 2 s pre-stimulus window to obtain Δ RMS. This resulted in an 80-point vector for 4 seconds of odor presentation per electrode/trial.

2.25 Response stability and correlation

To measure the stability of responses to an odorant over repeated presentations, the pairwise correlation between all five trials for that odor was computed (5-choose-2 or 10 comparisons) and the mean of all ten resulting comparisons was taken to obtain the average correlation or stability of the responses to that odorant [7 per odor per channel, 7×12 channels = 84 data points]. (**Fig. 5.11**)

To measure similarity/distinctness of responses across odorants, cross-odor correlations was computed by computing the mean RMS response for each odor and then the pair-wise correlation of these mean responses for different odor pairs [7-choose-2 comparison for 1 locust = 21, for 4 locusts = 84 comparisons; the same number was used for comparison between distributions].

2.26 Dimensionality reduction analysis (minimally invasive experiments)

Principal Component Analysis (PCA) was used to visualize the responses to odors across all recorded electrodes ($n = 12$ electrodes from 4 locusts). For each electrode, a response matrix was computed as follows. The binned responses (50 ms bin size; 80×1 vector) to 4 s of odor presentation for each stimulus were taken and concatenated to obtain 1 large 560-dimensional vector for an electrode. This was computed for all 12 electrodes to obtain a 12×560 matrix of stimulus responses. PCA dimensionality reduction was then performed, and the data projected on to the top three eigenvectors that captured the highest variance (3×560 dimensional matrix). For each odor in the reduced PCA-space, a Gaussian distribution was fitted, and the corresponding Gaussian ellipse plotted in 3-dimensions as shown in (**Fig. 5.11**).

2.27 Classification analysis

To predict the identity of an odor from its neural responses, the data after transformation in the PCA-space (as described above) was used. For **Fig. 5.11c**, all data from all 12 electrodes was used to make predictions. The ‘fitcdiscr’ function in MATLAB was used to fit a quadratic discriminating function for each class (odor) and predict the class labels using this set of learned classifiers. The results were visualized using a confusion matrix showing the target labels on the y-axis and the predicted labels along the x-axis. For predictions in **Fig. 5.11e, f**, only the data from the corresponding 4 electrodes was used, and a similar analysis was performed. Note that in each case, the chance level of accuracy was 1-in-7, or approximately 14%.

For the analysis in **Fig. 5.11d**, data from all 12 electrodes was used, but the duration (number of bins) of responses used as input to train the classifiers was varied. After training, predictions were made on all 80 time-bins for each odorant. The classification analysis was repeated as described above and the average accuracy of the models across all 7 classes for each number of bins n obtained (n going from 4 to 80 bins; 4 being the minimum requirement for the model). The average accuracy as a function of time is shown, with a chance level of 14% indicated in red.

2.28 Walking locust recordings

To record from freely moving locusts, the locust brain was prepared for electrode implantation similar to the method described above. For this set of experiments, custom tetrodes B (as described above) were used due to their increased flexibility and robustness to movement. After de-sheathing the locust brains, the electrodes were implanted and fortified in place using a combination of dental wax and epoxy glue. The electrodes were then secured to the back of the locusts using a 3D-printed brace attached to the back of the locust, and the locusts allowed to

recover for a few minutes. They were then released into the behavioral arena and their behavioral and neural responses to different odorants recorded.

2.29 Freely moving recordings

A custom two chamber behavioral arena was designed to assay locust preferences in a freely moving setting. In the design air was passed through a small 3D printed chamber that would hold the KimWipe, into a mixing chamber, and from there the two streams passed through the behavioral chamber and out the far side. The two-chamber assay was placed within a wooden cabinet into which a faraday cage had been installed, and a red backlight installed beneath the chamber provided the only source of illumination to minimize visual stimuli. To ensure light isolation, the wooden cabinet was further covered with a black cloth during experiments. A 4" fan was used to apply negative pressure to the wooden cabinet and to exhaust the air.

For these experiments, an odorant was introduced into the arena by pipetting a 100 uL onto a KimWipe and background air (2L/min) allowed to flow over it as it entered the box. The locust was placed in the center of the box at the start of each trial and was allowed to explore the box for a period of 5 minutes and its neural and behavioral responses were recorded. For each trial, the side on which the odorant was placed was pseudorandomized. Neural data was acquired using Intan (similar as above) and behavioral data was recorded using a webcam (Microsoft LifeCam). The neural and behavioral data were synchronized offline using a red LED flash to signal the start of the experiment.

2.30 Processing data from freely moving recordings

The acquired neural signals were first bandpass filtered to between 0.3 and 7.5 kHz. It was found that significant movements of the locusts produced mechanical noise that became superimposed atop the neural signals of interest and could not be fully filtered out. Hence, data

from segments where the locust produced large movements was discarded. To achieve this, an object detection algorithm where we computed the number of pixels showing significant changes in their intensities (>30 on a 0-256 grayscale) between successive frames was used. If the number of pixels with significant changes crossed 1000 (a threshold found to work well for this approach), the corresponding neural data acquired for that particular frame was discarded. After discarding frames with significant movement artifacts, the neural signals were also limited to within 5 standard deviations of the average baseline signal to remove any remaining noise artifacts. Finally, a list of putative spiking events was found using the ‘findpeaks’ function in MATLAB and the results confirmed after a manual inspection.

A pre-trained YOLOv4^{115,116} model was fine-tuned to accurately track the position of the locust in the behavioral arena. The behavioral data was acquired at 30 fps and hence 9000 frames per 5-minute trial (300 s * 30 frames/s) was obtained. To allow for comparison with neural signals acquired at 15 kHz, the final spiking data was binned to have the same sampling rate as the behavioral data. To generate the results shown in **Fig. 5.8, 9, 12**, the time spent by each locust was computed by simply adding up the number of frames in which the locust was on the side of the odor and compared to the number of frames/time spent on the control side. To compute the mean spiking activity for each side, the corresponding number of spikes in each frame was used, and an average across all frames on that side for a particular trial was taken. A two-sampled t-test was used to perform the significance analyses shown, with a p-value < 0.05 indicating significant difference.

Chapter 3: Encoding of innate appetitive preferences in the early olfactory pathway

3.1: Introduction

In many organisms, the olfactory system serves as the primary sensory modality that guides a plethora of behaviors such as foraging for food, finding mates, communicating with conspecifics, and evading predators. Using an array of biological sensors, the olfactory system converts volatile chemical inputs from an organism's environment into patterned neural responses that inform downstream motor neurons to perform appropriate behaviors (e.g., moving towards food or away from danger). For many external cues, the elicited neural responses are often determined by the genetic makeup of the organism, which assigns an innate preference, or valence, for these different stimuli¹¹⁷⁻¹²². Given the importance of rapid and robust decision-making for survival and propagation¹²³⁻¹²⁶, how is the information regarding the valence of a stimulus encoded in the olfactory system? In this Chapter, I will present a study that examined whether and how neural responses in the early olfactory system of locusts are spatiotemporally structured to represent odor valence.

In insects (including locusts), odor stimuli are detected by a family of olfactory receptor neurons (ORNs) distributed along the antenna that transduces chemical cues to electrical signals and relays them to the antennal lobe. In locusts, the antennal lobe is comprised of a network of ~830 cholinergic projection neurons (PNs, excitatory) and ~300 GABAergic local neurons (inhibitory). In particular, the responses of PNs are patterned over space and time to rapidly encode for the identity and intensity of different odorants¹⁸⁻²⁴ and they relay this information to higher centers responsible for learning and memory (mushroom body, MB), and overall

behavioral preferences (lateral horn, LH)¹²⁷⁻¹²⁹. Until recently, it was believed that information pertaining to the encoding of innate preferences for different stimuli was encoded exclusively in the LH. However, given that the LH receives direct feed-forward input from the network of PNs¹²⁹, is information regarding the valence of an odorant already organized at the level of neural responses in the antennal lobe?

Recent work in *Drosophila*, another well-established system for invertebrate olfaction, suggests that spatiotemporally patterned neural activity in the antennal lobe appears to encode for stimulus valence^{119,130,131}. Using a panel of 12 odorants (6 attractive and 6 aversive), the authors found that innately attractive chemicals elicited responses in the medial antennal lobe, whereas innately aversive cues activated more lateral regions¹¹⁹. A second study found that the selective silencing of particular glomeruli (functional units in the *Drosophila* antennal lobe) could significantly alter the perceived valence to a stimulus¹¹⁸. Finally, work from Yamakazi et al. found that neurons in the mushroom body (directly receiving input from antennal lobe PNs) of *Drosophila* also appeared to encode valence information¹³². This result implies that PNs outputs to the MB should be organized in a manner that also encodes for valence. Taken together, these findings indicate that in *Drosophila*, the neural responses in the antennal lobe network are also organized to encode valence information. Given that the general principles of olfactory organization are similar between *Drosophila* and locusts¹³³, do we see similar evidence for valence encoding in the locust antennal lobe?

In this study, we explored the innate behavioral preferences (valence) of locusts (*Schistocerca americana*) to a large panel of biologically relevant chemicals. We began by assaying the appetitive valence of locusts using the palp-opening response (POR) as a behavioral indicator and obtained a broad range of preferences to a set of 22 chemically diverse odorants.

Next, we performed extracellular recordings to measure the responses of PNs in the antennal lobe to the same panel of odorants. We found that while individual neurons responded selectively to different subsets of neurons, the ensemble neural responses were spatiotemporally patterned to be highly predictive of odorant valence. A simple linear classifier could accurately predict the valence of all chemical cues in the panel using the PN responses as input. Taken together, these results indicate that PNs not only encode the identity and intensity of different stimuli but do so in a biologically relevant manner that re-formats chemically diverse input information to behaviorally relevant patterns.

3.2 Results

3.2.1 Innate appetitive preferences of locusts to an odor panel

Do locusts exhibit distinct innate preferences for different chemicals? Locusts use a pair of appendages, known as palps, to guide food into their mouth. They achieve this by extending the palps (palp-opening response) in a stereotyped fashion when near a source of food. We leveraged this behavior and assayed the innate appetitive preferences of starved young-adult locusts (of either sex) to a diverse panel of twenty-two odorants (diluted to 1% v/v unless stated otherwise). Each odor in the panel was presented to every locust once using a pseudorandomized order and the corresponding palp-opening responses (POR) evoked were recorded (**Fig. 3.1a**). We used a binary metric to quantify each locust's response to an odor stimulus – a score of 1 to indicate a successful POR, and a score of 0 to indicate no response. The performance of all locusts ($n = 26$) used in the assay is summarized in **Fig. 3.1b**. Note that each locust was presented a different sequence of the odors, but for visualization purposes the odors are sorted based on the number of PORs they elicited across all locusts.

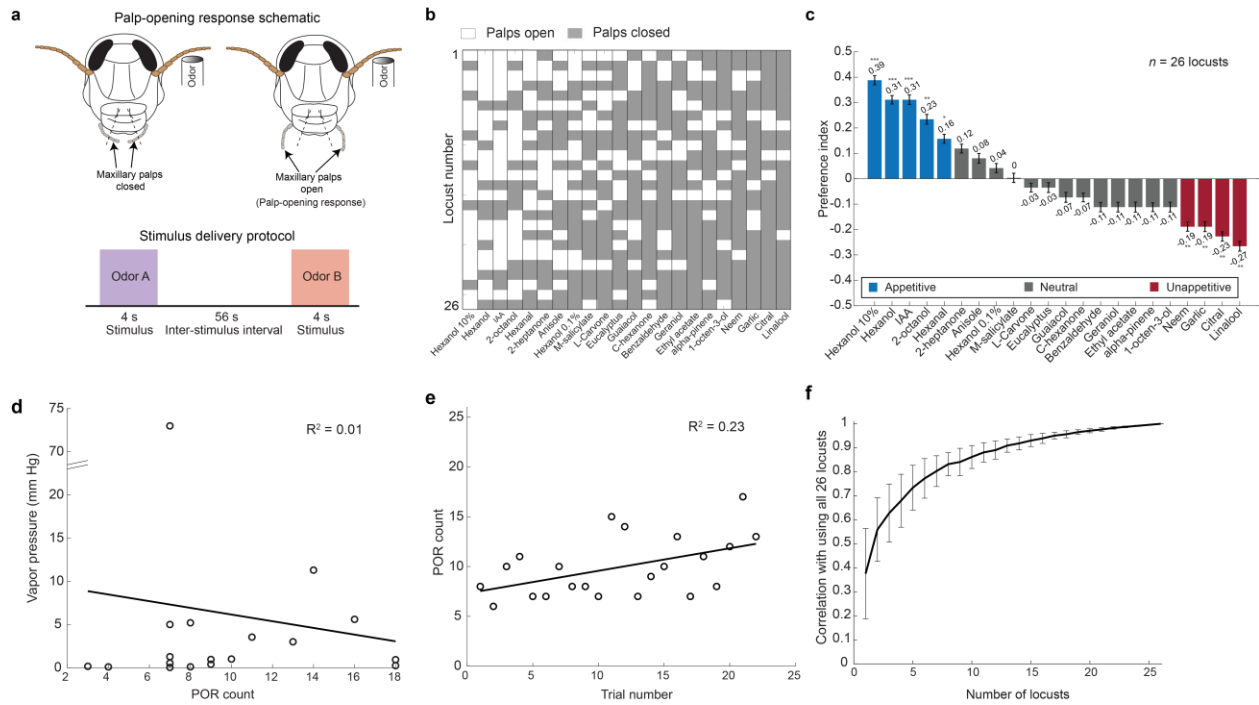


Figure 3.1: Innate appetitive preferences of locusts to a diverse odor panel

a) A schematic showing a palp-opening response (POR) and experimental protocol. A successful POR was defined as an opening of the maxillary palps beyond the facial ridges shown on the locust. Odors were delivered in a pseudorandomized order onto the locust antenna. The stimulus delivery was 4 s in duration, and the inter-stimulus interval was set to 56 s.

b) Innate preferences of twenty-six locusts for the twenty-two odorants tested are shown. Each row shows the POR responses of a locust to the odor panel. White boxes indicate a successful POR to an odor and gray boxes indicate no POR. Note that odors are sorted from those that elicited the highest number of PORs across locusts (leftmost) to the lowest (rightmost). The sorted ordering is just to facilitate the readability of data and does not represent the actual order in which each locust was tested.

c) Preference indices were calculated for all odors tested and are shown as a bar plot ($n = 26$ locusts). Blue bars indicate odors classified as appetitive, gray bars indicate neutral odors, and red bars indicate unappetitive odors. Odorants with a significant deviation from the median response (one-sided binomial test, $p < 0.1$), were classified as either being appetitive or unappetitive; * indicates $p < 0.1$, ** indicates $p < 0.05$, *** indicates $p < 0.01$). Error bars indicate s.e.m.

d) Regression analysis of odor vapor pressure versus number of PORs generated (across 26 locusts) is shown for all odorants in the panel. Each open circle indicates values (vapor pressure vs POR count) for one odorant. Only odorants with available vapor pressure data were considered for this analysis (18 out of 22 odors at 1% v/v concentration). Best fit line using a linear regression model is shown in black. The calculated R^2 value for this model is 0.01.

e) Regression analysis of POR counts versus trial number in the experiment is shown. Each circle indicates the number of locusts with successful PORs in that particular trial. Best fit line using a linear regression model is shown in black. The R^2 value calculated for this model is 0.23.

f) Results from Monte Carlo simulations are shown (see Methods). Valence predictions were obtained by using a random subset of locusts of a particular size (i.e., any n -locusts-out-of-26) and were compared with overall valence obtained using all 26 locusts using a correlation metric. For each number of locusts, 100 such simulations were performed with random subsets of locusts chosen in each simulation. The mean correlation and s.e.m. across the simulations are shown. An R^2 value above 0.95 was obtained for simulations with $n > 18$ locusts.

We aggregated the responses from individual locusts (see Methods) to obtain a preference index for all odors – higher scores on the index indicating stronger innate preferences (**Fig 3.1c**). Locusts displayed a broad range of preferences to the odor panel. Hexanol (at 10% v/v; leftmost odorant), a green-leaf volatile, had the highest preference, whereas linalool (rightmost odorant), an active ingredient in insecticides, had the lowest preference. Based on their deviation from the median preference score, we categorized odorants as being appetitive (significantly above the median), neutral, or un-appetitive (significantly below the median; one-sided binomial test comparison). In later sections, we will jointly refer to neutral and un-appetitive odors as ‘non-appetitive’.

Prior studies have found that even within a species, the preferences for certain odorants can vary between males and females^{117,134,135}. To account for this possibility, we noted the sex of each locust during our experiments and ensured that the overall dataset was comprised of an equal number of male and female locusts ($n=13$ each). We looked at the cumulative behavioral responses of locusts grouped by gender (**Fig 3.2a**) and found that while appetitive preferences for certain odorants did vary between the groups (e.g., hexanal and garlic), these differences were not significant (t-test, $p>0.1$ for all odors).

Is there a simple stimulus feature that could explain the observed trends? Since the odorants were diluted to the same concentration in solution (1% v/v in mineral oil; except two additional concentrations of hexanol at 10% and 0.1%) and delivered identically, the vapor pressure of the chemicals directly determined how much of each stimulus was delivered

(stimulus intensity). Could locusts simply be performing PORs more frequently for more volatile odors? To test this, we performed a regression analysis between the vapor pressure of odors and the number of PORs each odor elicited. As can be seen in **Fig. 3.1d** (and **Fig. 3.2b**), the variations in vapor pressure poorly explained the variations we observed in the behavioral responses.

Each locust was exposed to a panel of 22 chemicals, with a new stimulus being presented every minute. Despite the sequence of odors being pseudorandomized (**Fig. 3.2d, e**) for each locust, fatigue or loss of motivation to maintain robust behavioral responses for the later trials could potentially confound the observed preferences. To eliminate this possibility, we plotted the observed number of PORs as a function of the trial number (**Fig. 3.1e**). Our results indicate that locust performance remains robust and even slightly increased as the experiment progressed (marginally higher number of PORs in later trials compared to earlier trials; $R^2 = 0.23$; **Fig. 3.2c**).

Finally, we performed Monte Carlo simulations (see Methods) to verify that population-level responses were not biased by a handful of individuals. The simulations showed (**Fig. 3.1f**) that this is indeed the case and the results converged ($R^2 > 0.95$ with overall results) when any random subset of eighteen or more locusts was used to calculate the behavioral preference indices for different odorants. Taken together, this set of control analyses rule out many simpler explanations and potential biases in our results. Hence, we can conclude that the behavioral preferences obtained here are a strong indicator of the innate appetitive preference of the locusts.

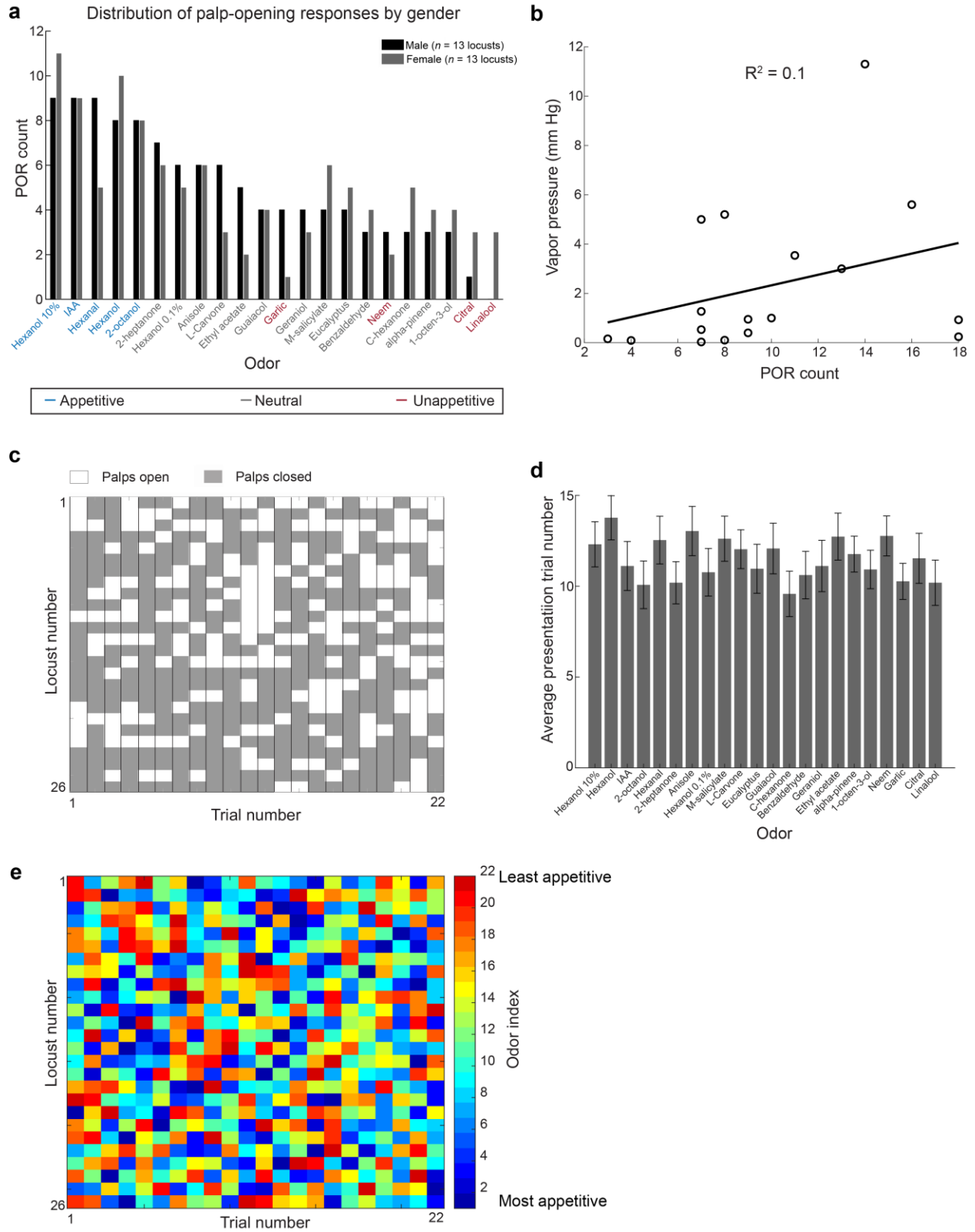


Figure 3.2: Additional controls for assaying innate appetitive preference

a) Palp-opening responses (PORs) to the odor panel do not show any significant gender-based differences (t-test, $p > 0.1$ for all pairwise comparisons). We recorded PORs from 13 male and 13 female locusts to measure innate valence. PORs were sorted from highest to lowest based on the male group responses (black bars), and corresponding female locust PORs (dark gray bars) are shown next to them. The odors are colored using the same convention used in **Fig. 3.1c**.

b) Similar plot as in **Fig. 3.1d** but without ethyl acetate. Ethyl acetate has a reported vapor pressure that is much higher than all other odors used, and hence we repeated the analysis in **Fig. 3.1d** without the outlier. The R^2 for this analysis is 0.1, which still indicates a very poor correlation between vapor pressures and the observed palp-opening responses.

c) The PORs recorded for every locust are shown as a function of trial number. Similar convention as **Fig. 3.1b**, where each row corresponds to a single locust and there are twenty-two trials one for each odorant in the panel. White boxes indicate a palp-opening response, gray boxes indicate no PORs. A summary of this data is presented in **Fig. 3.1d**.

d) The average trial number in which each odor was presented across all locusts is shown. Error bars indicate s.e.m.

e) The sequence of odor presentation for each locust is shown. Each row is the sequence of odorants presented to one locust. Colors map to preference index with more bluish odorants being appetitive and more reddish odorants being aversive.

3.2.2 Individual projection neuron responses to appetitive and non-appetitive odorants

Next, we sought to understand the neural basis for this behavioral readout. To examine this, we recorded extracellular odor-evoked responses from projection neurons (PNs) in the locust antennal lobe (**Fig. 3.3a**). We stimulated the antenna with the same odor panel used in the behavioral experiments. The stimulus dynamics of each odorant were quantified using a photo-ionization detector (PID) and the mean voltage responses for all odors are shown in **Fig. 3.3b** (left panel; see Methods). The right panel shows the peak PID response for each odorant arranged in order of innate appetitive preferences (cues that evoked the highest behavioral responses are on the left and lowest on the right).

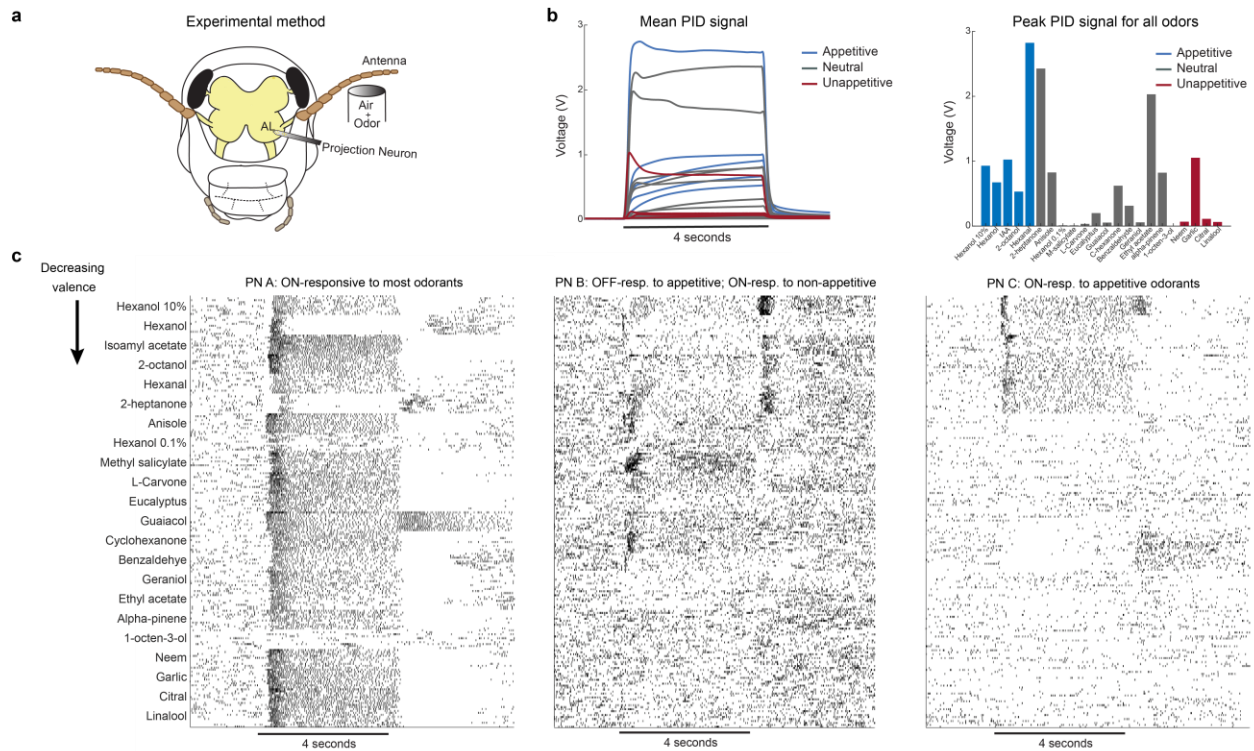


Figure 3.3: Extracellular PN responses to the odor panel

a) A schematic of the experimental setup is shown. Extracellular projection neuron (PN) recordings were made from the locust antennal lobe. Each odorant was presented for ten repeated trials and the order of odorants was pseudorandomized in each experiment.

b) Left: Mean voltage signals acquired from a photoionization detector (PID) are shown for all 22 odorants in the panel. Each odorant was presented for 4 s and repeated for 5 trials. Each trace is colored using preference indices obtained in **Fig. 3.1c**. Blue traces indicate appetitive odorants, gray indicates neutral odorants, and red indicates unappetitive odorants. Right: The peak voltage signal obtained from the PID is shown for all twenty-two odorants. Odorants are sorted from highest (leftmost) to lowest (rightmost) appetitive preference or valence. Same color convention as in the left panel.

c) Representative PN responses to all 22 odorants in the panel are shown. Each tick indicates an action potential, each row corresponds to one trial, and ten trial blocks are shown for each odorant. Odors are sorted based on their behavioral preferences, with the highest appetitive preferences shown as the top block of ten trials, and the lowest shown at the bottom (**Fig. 3.1**). A black bar along the x-axis indicates the four seconds odor presentation window.

We presented each odorant for ten repetitions in a pseudorandomized order. A total of 89 PNs (~10% of the total number of PNs in a single antennal lobe) were recorded using this approach and used for all subsequent analyses. Consistent with prior data, we found that odor-evoked responses had two prominent epochs: an ON response that occurred during the 4 s when

the stimulus was presented, and an OFF response that occurred during a 4 s window immediately following stimulus termination. We found a PN that had an ON response for most of the odorants (**Fig. 3.3c**, PN A), whereas many PNs responded to a subset of odorants either with an ON response or an OFF response. A small fraction of neurons were OFF-responders to a few appetitive odors but switched to ON-responses for some of the non-appetitive odorants (**Fig. 3.3c**; PN B; 8/89 PNs with similar tuning). Complementing these responses, we also found a small fraction of PNs that was ON-responsive to all five appetitive odorants but was OFF responsive to one or more non-appetitive odorants (**Fig. 3.3c**, PN C; 11/89 PNs with similar tuning). On average, odorants with higher positive valence elicited stronger ON and OFF responses across more PNs than those with lower valence, while inhibition increased as the odorants became less appetitive (**Fig. 3.4a**; see Methods).

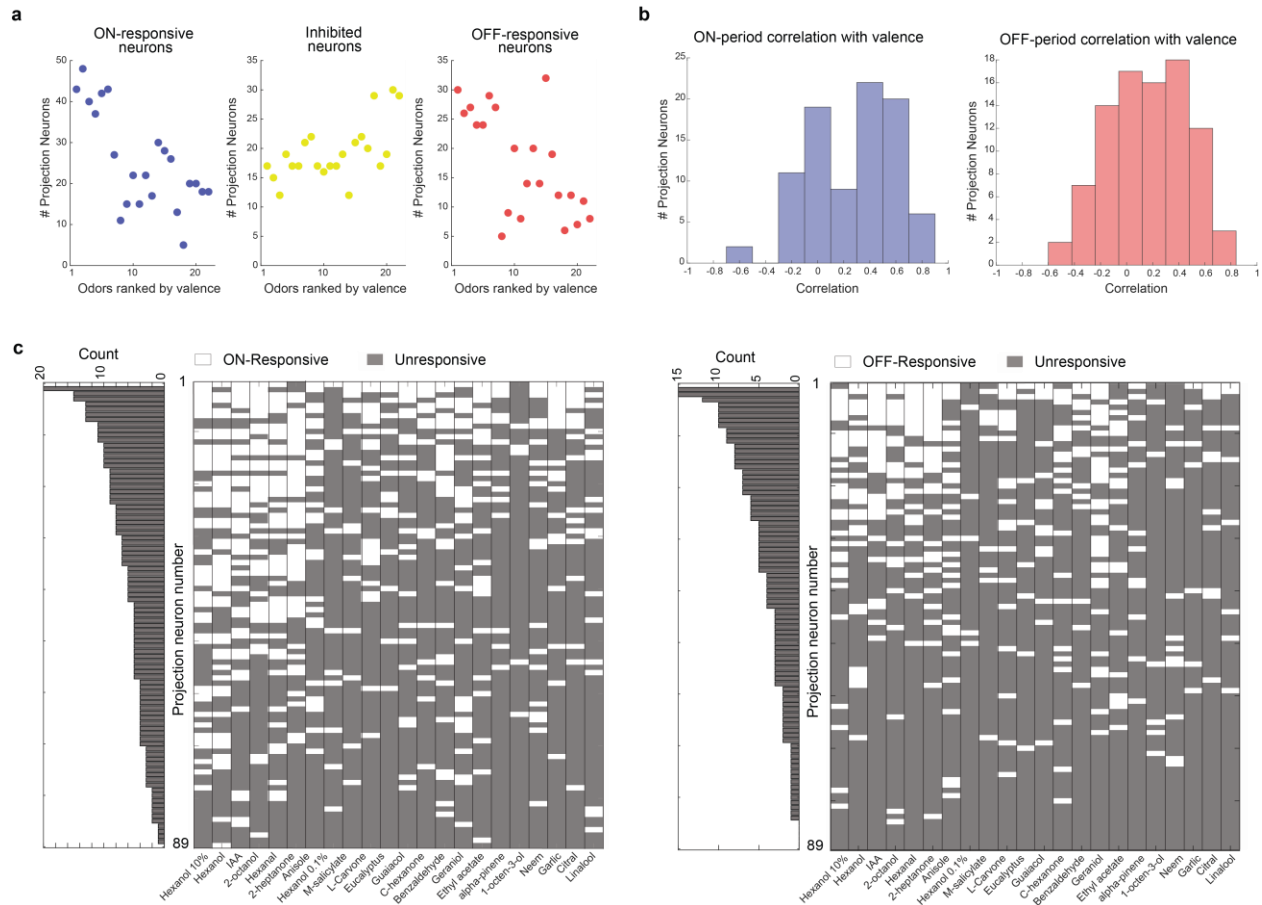


Figure 3.4: Characterizing individual PN responses

a) Left panel: Number of PNs that were activated during the odor presentation window (ON-responsive) is plotted for twenty-two different odorants in the panel. Odorants are again sorted based on their appetitive valence (highest – leftmost to lowest – rightmost). *Middle and right panels:* Similar plots but showing the number of PNs that were inhibited during odor presentation, and that number of PNs activated after odor termination (OFF-responsive) are shown for different odorants on the panel. The odorants are again arranged based on appetitive valence (same as left panel).

b) Left panel: For each PN, we took the mean of the spiking activity across 4 s of odor presentation and across all 10 trials for each odor to obtain a 22-dimensional vector. We computed the correlation between this vector and the appetitive preferences obtained for each odor (also a 22-dimensional vector; **Fig. 3.1**). The distribution of correlations obtained using this approach is shown for all 89 PNs. *Right panel:* Similar plot as the left panel, but the OFF-period PN activity (4 s immediately following odor termination) was now correlated with the overall odor valences.

c) Left: Responses of individual PNs to all twenty-two odors during the ON-period are shown. Each row corresponds to a single PN, and the odorants (columns) were organized from highest valence to lowest (from left to right). PNs were classified as ON responsive (white box) or unresponsive (gray box). Bar plot on the left indicates the number of odorants (‘Count’) that activated each PN. PNs are sorted such

that those that responded to most odorants are at the top (i.e., least selective). *Right*: Similar plot as the left panel, but characterizing OFF-responses across all eighty-nine PNs to all odorants in the panel.

We computed the correlation between the individual PN responses to different odorants with the overall behavioral preferences to the same panel (**Fig. 3.4b**). Notably, we found a small subset of neurons that had either a strong positive or negative correlation with the POR responses observed (correlations > 0.75 for 4/89 PNs for ON responses and 2/89 PNs for OFF responses). Furthermore, our results indicate that such correlations could be found when either the ON or OFF responses were used. Although, it would be worth noting that different subsets of PNs had a high correlation with appetitive preference during the ON and the OFF periods.

How selective are individual PN responses? To answer this, we computed a tuning curve for each PN during both the odor ON and OFF periods (**Fig. 3.4c**). We found that most PNs responded to at least two odorants or more during the ON period (84/89 PNs) and a small fraction of neurons (11/89 PNs) responded to ten or more odorants (**Fig. 3.4c**, bar plots along the y-axis). The odor-evoked responses were more selective during the OFF period, with 70/89 PNs responding to two or more odors and only three PNs responding to more than ten odorants. In sum, these results indicate that individual PNs responded to the odor panel with great diversity.

3.2.3 Ensemble projection neuron responses to appetitive and non-appetitive odorants

Next, we examined how the odor-evoked responses vary at an ensemble level. To visualize the ensemble neural responses and how they change as a function of time, we used a linear dimensionality reduction technique (Principal Component Analysis, PCA; see Methods). PCA neural response trajectories for the ON period are shown for all odorants (**Fig. 3.5a**). Consistent with prior findings^{22,136–138}, our data also reveal that each odorant produced a distinct looped response trajectory. Interestingly, we observed that neural response trajectories evoked by

odorants that were labeled as innately appetitive in the behavioral assay evolved in a similar direction (blue trajectories). This indicates that the combination of PNs excited by these odors had overlap and hence the PN ensemble vectors were near one another in the state space. Similarly, the trajectories for odors labeled as unappetitive also evolved in a similar direction (red trajectories) and occupied a different region of the state space. Note that the sets of red and blue trajectories did not overlap, indicating that odors within different groups (appetitive and unappetitive) were being encoded by distinct subsets of PNs.



Figure 3.5: Ensemble PN responses for appetitive and non-appetitive odorants

a) Visualization of the ensemble ($n = 89$) PN responses to the odor panel after Principal Component Analysis (PCA) dimensionality reduction are shown (see Methods). 4 s of ON-responses for all twenty-two odorants were used for this analysis, and the data were projected on to the first 3 principal components that captured the highest variance ($\sim 30\%$ captured along the three axes shown). Neural response trajectories evoked by innately appetitive odors are colored in blue, neutral odors response trajectories are indicated in gray, and unappetitive odors responses are shown as red trajectories. Note that the ensemble neural response trajectories cluster based on overall appetitive valence.

b) Dendrogram showing the overall hierarchical organization of 89-dimensional PN ON-responses. Odorants are again colored based on the corresponding behavioral preferences (blue indicates appetitive odors, gray indicates neutral odors, red indicates unappetitive odors). Appetitive odors cluster along the left branch, while unappetitive odors cluster on the right branch. It is worth noting that these results are similar to the overall arrangement of responses shown after dimensionality reduction in **panel a**.

Given the limited variance captured by the visualized dimensions (~33%), we confirmed these PCA results with a high-dimensional clustering analysis (**Fig. 3.5b**). We found that the spiking profiles for odors that belonged to the same group (appetitive or unappetitive) were similar, and hence clustered within the same branch when visualized using a dendrogram. These results support our interpretation that unique subsets of PNs in the antennal lobe are activated in a manner that is representative of the innate appetitiveness of the stimulus.

Consistent with our previous findings¹³⁹, we found that ensembles of PNs encoding for the onset and offset of odors were highly non-overlapping. Therefore, ensemble responses during these epochs were nearly orthogonal to each other (**Fig. 3.6a**). PCA visualization of odor-evoked response trajectories revealed that ON and OFF responses evolved in non-overlapping subspaces (**Fig 3.6b**). Notably, we found that odorants with the highest positive POR preferences evoked neural responses that were highly pattern matched during both ON (blue trajectories) and OFF (red trajectories) epochs.

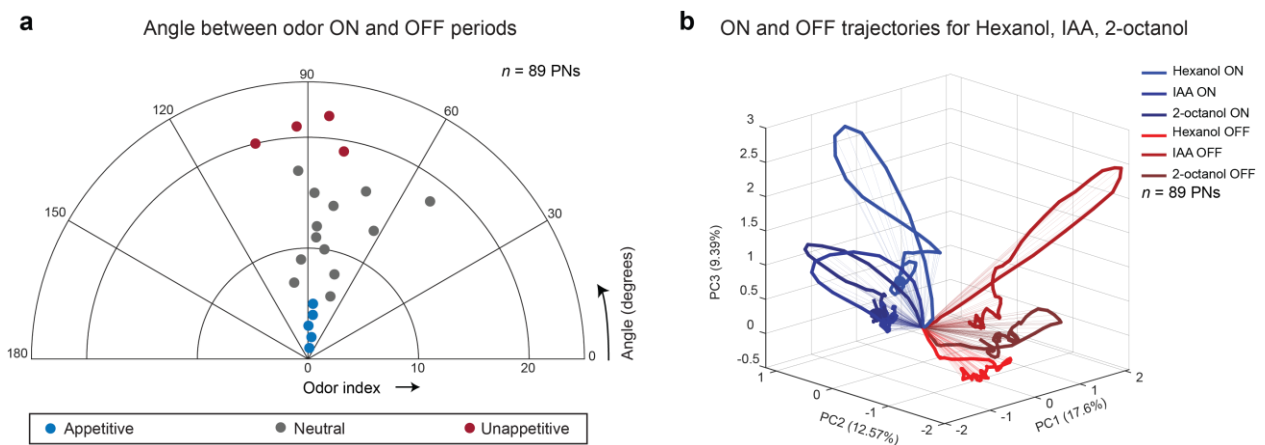


Figure 3.6: ON and OFF responses to odorants are encoded by distinct subsets of PNs

a) Angle between ON- and OFF- periods are shown for each odor. The mean activity across the respective odor period (and all 10 trials) was computed for each PN to obtain 89-dimensional vectors (89 PNs) for the ON- and OFF- periods. The angle between these vectors was computed for each odor and is shown as a polar scatter plot using a similar color convention as **Fig. 3.5**. Each dot corresponds to a single

odorant – the odor index shown along the horizontal axis ranks odors from 1 to 22 based on innate appetitiveness (same color scheme as previous plots). The distance along this dimension is arbitrary. The angles are close to 90° for almost all odors, indicating that the ON- and OFF- vectors are almost orthogonal in this high-dimensional space.

b) Similar analysis as **Fig. 3.5a**, but using the odor ON- and OFF-periods for 3 odors – hexanol, isoamyl acetate, and 2-octanol are shown. The blue ON-trajectories evolve in a different direction than the red OFF-trajectories. Note that the blue and red trajectories have minimal overlap, indicating different subsets of PNs are activated during the ON and OFF periods.

3.2.4 Predicting behavioral preferences from odor-evoked neural responses

How well do the neural responses map onto the behavioral preferences for different odorants? To examine this, we used linear regression to predict the probability of generating a POR given the ensemble PN activity elicited by that odorant. (**Fig. 3.7a**). Note that for these predictions, we used the normalized behavioral responses for each odor (see Methods), which could also be interpreted as the probability of a palp-opening response to a given odorant (across locusts). The regression weights were trained using all but one odorant and used to predict the probability of POR for the left-out odorant (i.e., a leave-one-out-cross-validation approach; 22 different linear regression models were used). We found that this simple approach yielded robust predictions for all odorants (**Fig. 3.7b, c**).

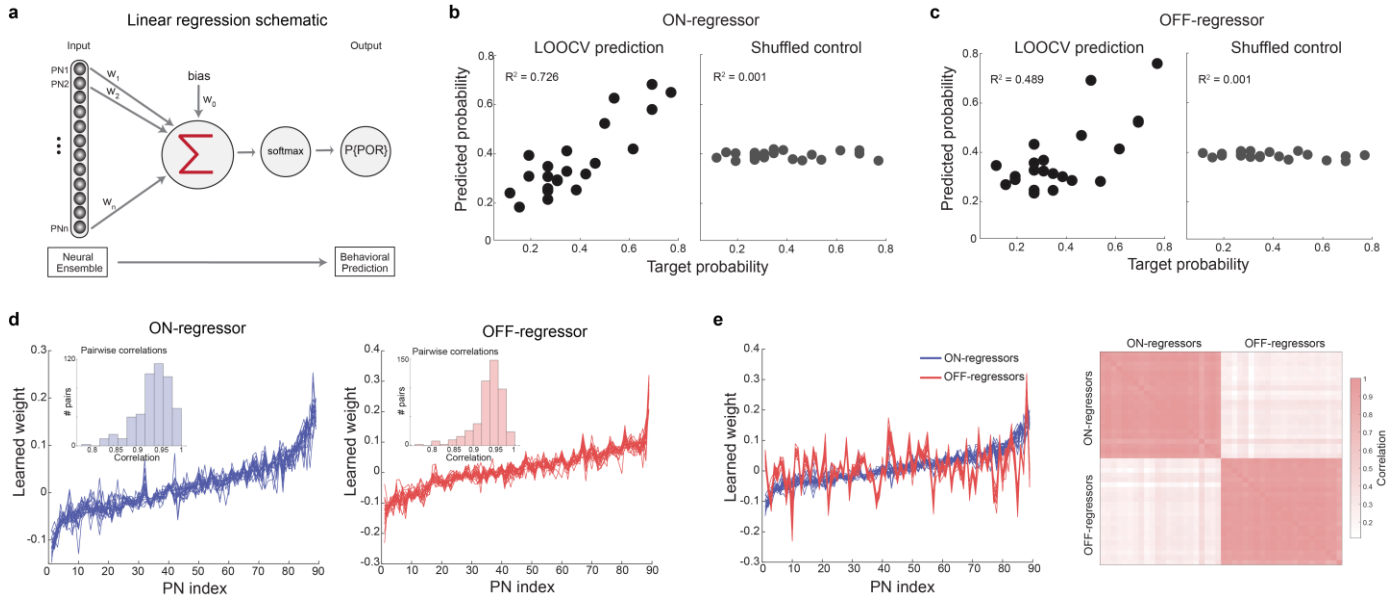


Figure 3.7: Neural response patterns robustly predict innate behavioral preferences for odors

a) Schematic of the linear regression approach is shown. The input data was the mean PN spiking activity during odor onset for the ON-regressor, or the mean PN responses in a 4 s window post odor termination for the OFF-regressor (i.e., 89 dimensional ON or OFF response vectors). The output to be predicted was the normalized preference score (interpreted as a probability of POR; see Methods) for each odorant. The regressors were trained using a gradient descent approach and validated using a leave-one-out-cross-validation (LOOCV) approach. Therefore, the POR probability for each odorant (that was left out of the training), was based on a regression model learned using the data for the remaining twenty-one odorants. This resulted in twenty-two ON-regressors (one for each odorant), and twenty-two OFF-regressors (again one for each odorant).

b) Left: Predictions from the ON-regressor versus the actual probabilities obtained from the behavioral assay for all odorants in the panel are shown. Overall, the R^2 value between the predicted value and the actual behavioral response was high ($R^2 = 0.726$). **Right:** Similar plot but for the shuffled control is shown. Here, the behavioral POR probabilities were randomized, and a regression model was fit similar to learning the unshuffled case. Note that the predictions are centered around the mean valence of ~ 0.4 ($R^2 = 0.001$).

c) Similar plots as **panel b**, but using models trained on the OFF-period responses are shown. The OFF-regressors ($R^2 = 0.489$) performed poorer than the ON-regression models but were still well above shuffled control performance levels ($R^2 = 0.001$).

d) Left: The ON-period linear regression model was validated by training 22 different models, leaving 1 of the 22 odors out each time for validation. The weights obtained for each PN are shown for all 22 models trained using this LOOCV approach. The weights assigned to eighty-nine PNs were sorted (i.e., lowest to highest) based on the model used to predict POR responses to hexanol. Inset shows the distribution of pairwise correlations between each weight vector obtained for predicting POR for different odorants. **Right:** Similar plot as left panel, but for the twenty-two OFF-regressors are shown.

e) *Left*: Blue curves indicate weight vectors obtained from the ON-period regressors as shown in panel d. Red traces show weights learned by the OFF-period regressors but sorted using the same indices as the ON-period vectors. As can be seen, the blue and red curves are uncorrelated. *Right*: Correlation analysis quantifying the similarities in weights assigned to PNs by the ON- and the OFF- regressors. As can be expected from **panel d**, weights learned by the PNs are highly correlated within the ON-period and OFF-periods (darker colors along the diagonal blocks). However, as shown in the left panel, the weights assigned to each PN are different between the ON- and OFF-regressors, and hence the off-diagonal blocks have lower correlations (lighter colors).

Note that we made predictions using the mean ensemble PN activity during 4 s of odor exposure (i.e., an ‘ON-regressor’), and using 4 s of odor-evoked activity after the termination of the odorant (i.e., an ‘OFF-regressor’). Both the regressors performed relatively well with the ON-regressor performance being better than the OFF-regressor. Further, the performance of the linear regression approach with shuffled prediction probabilities for different odorants (i.e., ‘shuffled control’ for both ON and OFF cases) predicted values around the mean POR probability for all odorants (**Fig. 3.7b, c**; mean = ~ 0.4), and was significantly inferior compared to the ON- and OFF- regression approaches. The poor performance of the shuffled control approach compared to the ON- and OFF- regressors suggests that the spiking activity across PNs is indeed organized to enable mapping between neural and behavioral responses spaces.

How consistent were the different regression models? Our results indicate that the weights assigned to each PN remained stable irrespective of the odor that was left out to train the regression model (**Fig. 3.7d**). This consistency of the assigned weights across regressors indicates that no particular odorant disproportionately influenced the regression model used to transform neural responses into POR probabilities. Additionally, Monte Carlo simulations (see Methods) revealed that both the ON- and OFF- regressors’ performance improved as the number of PNs used in the analyses was increased (**Fig. 3.8**).

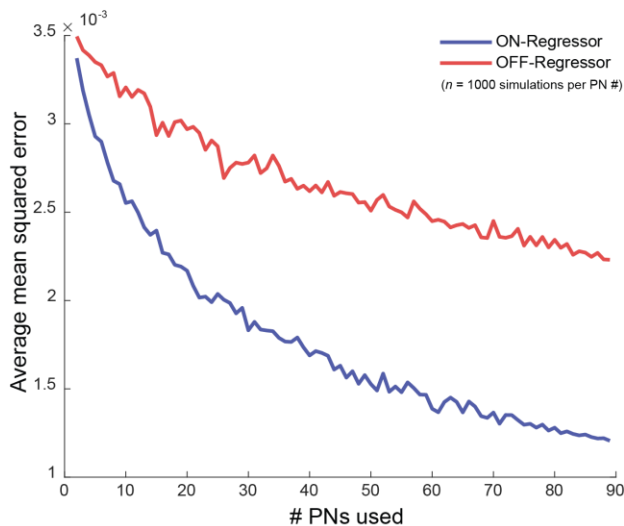


Figure 3.8: Monte Carlo simulations. We used Monte Carlo simulations to quantify the performance of the linear regression approach as a function of the number of projection neurons used to predict the behavioral preference indices. Note that the performance of both ON- (blue) and OFF- (red) regressors are plotted to allow comparison. For each n , we performed 1000 such simulations and obtained the average mean squared error for the predictions across all simulations. The average error goes down with an increase in the PN count and appears to saturate when around eighty PNs are used for the analyses.

We wondered whether the same set of PNs contributed during both ON and OFF periods to predict the preference index for different odorants. To understand this, we calculated the correlation coefficient between the weights assigned by both these regression approaches (**Fig. 3.7e**). Our results indicate that there was only a weak correlation between weights assigned by the ON- and OFF- regressors. As an additional control, we applied the weights learned by the ON-regressors to predict the preference index using the OFF-period responses of the held-out odorant, and vice versa (**Fig 3.9**). Both these classifiers had poorer performances than those shown in **Fig 3.7**, indicating that the weights assigned to PNs were indeed dependent on which odor period was used during the training phase. These results indicate that information regarding the overall appetitive preference is distributed across different sets of PNs during the ON and OFF epochs. In sum, we conclude that the ensemble neural responses during odor presentations and after their terminations are unique, and contain information about the overall innate behavioral response generated by that odorant.

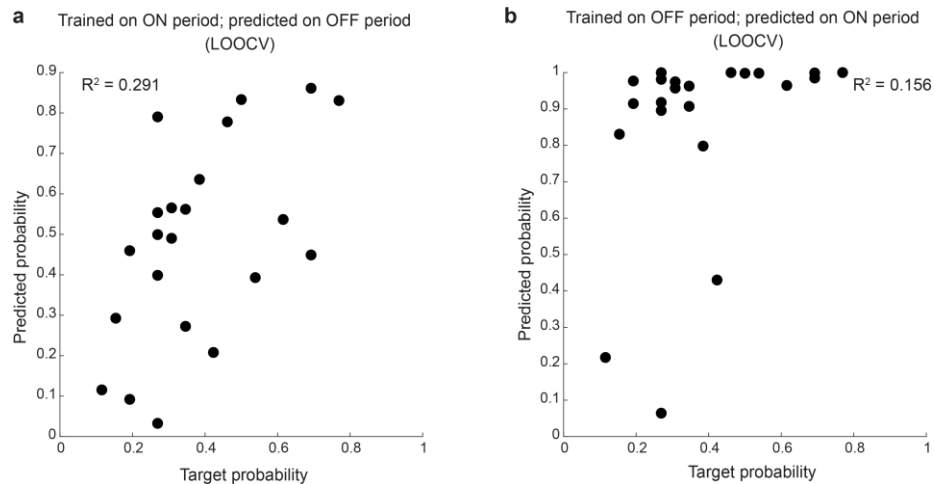


Figure 3.9: Additional controls for regressor specificity

a) We trained regressors to predict behavioral probability similar to the approach in **Fig 3.7**. Note that for this analysis, the regressor learned weights for PNs using the ON-period odor responses but made predictions using the OFF-period odor responses for the held-out odorant. These predictions had an $R^2 = 0.291$ and were poorer than those obtained in **Fig 3.7b** ($R^2 = 0.726$).

b) Similar analysis as **panel a** but weights were learned using OFF-period responses and predictions were made using the ON-period responses of the held-out odorant. These predictions had an $R^2 = 0.156$ and were poorer than those obtained in **Fig 3.7c** ($R^2 = 0.489$).

3.3 Discussion and conclusions

In this study, we examined the neural correlates of innate olfactory preferences. Our results indicate that while the neural responses evoked by an odorant were patterned over combinations of neurons activated and over time, the ensemble neural responses are still primarily constrained by the overall behavioral relevance of the chemical cue. Odorants that have a positive appetitive preference, or valence, evoked ensemble neural responses that overlapped during odor presentations (i.e., ON responses) and after their terminations (i.e., OFF responses). Similarly, odorants with a neutral or negative appetitive preference evoked spiking activities that formed similar ON and OFF response clusters that were distinct from the appetitive response clusters. As a direct consequence of this spatiotemporal organization of neural responses, the innate behavioral responses were entirely predictable from neural responses during both these epochs but using distinct subsets of neurons.

3.3.1 Chemical (input) vs. neural vs. behavioral (output) spaces

Could the observed appetitive preferences to different odorants be predicted directly from the stimulus/chemical space^{135,140,141}? We found that chemical features such as those extracted by nuclear magnetic resonance spectra (NMR) or infrared (IR) spectra did not have good correlations with the overall appetitive preferences for different chemicals on the odor panel (Fig. 3.10).

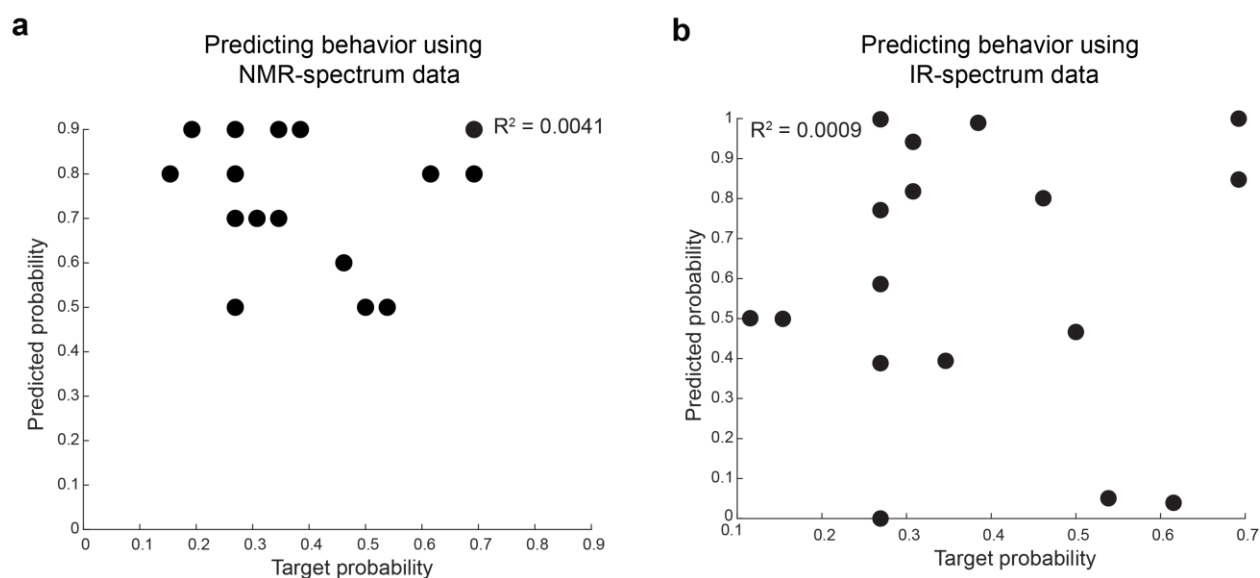


Figure 3.10: Mapping chemical features/properties onto behavioral valence

a) We obtained NMR-spectrum data¹⁴² for 16 odors (all at 1% concentration) in our panel. Using an approach similar to that in Fig. 3.7, we trained linear regressors to predict the valence of odorants in the panel based on their NMR-spectra. The plot shows the actual POR probability along the x-axis and the predictions from the regressors along the y-axis. The predictions were poor and had a calculated R² value of 0.0041.

b) Similar approach as in panel a, but using IR-spectrum data obtained for 17 odors¹⁴². The predictions were again poor and had a calculated R² value of 0.0009.

Our results indicate that chemically similar odorants evoked divergent neural responses (isoamyl acetate and ethyl acetate – both esters but opposite valences). Conversely, we found odorants that had different chemical features mapped onto similar appetitive preferences (benzaldehyde and cyclohexanone). Even features such as the vapor pressure that controls the

number of molecules reaching the antenna did not have a good correlation with the overall behavioral preference. While this is not an exhaustive list of chemical features that can be extracted, these results appear to indicate that it would be difficult to find a simple linear mapping of the chemical space onto the behavioral space. Similar results have recently been reported in the mouse olfactory bulb¹⁴³. Contrasting the non-linearity between the chemical – neural transformations, a linear mapping was indeed found between neural and behavioral spaces. These results support the idea that neural responses, even in those circuits very early in the olfactory pathway, are organized to generate appropriate behavioral outcomes rather than faithfully represent the chemical features of the odorants.

3.3.2 Individual PN responses vs. ensemble responses

Interestingly, at the individual neuron level, we found that responses in a small subset of PNs had a strong correlation with the overall innate preference for different odorants (**Fig. 3.4b**; correlations > 0.75 for 4/89 PNs for ON responses and 2/89 PNs for OFF responses). Such encoding of overall odor valence by individual neurons so early in the olfactory pathway has been reported in other invertebrate models^{118–120}. While the simplest model to predict the behavioral outcomes from the neural activity would be to just use a few of these neurons, whether such a model would be robust is unclear. Earlier studies have shown that individual projection neurons responses change unpredictably with changes in stimulus dynamics, intensity, competing cues, stimulus history, and ambient conditions^{23,139,144–146}. Notably, the behavioral recognition of odorants was found to remain invariant under a battery of these perturbations¹⁴⁷. Therefore, a more robust and fault-tolerant model to overcome such variations in neural responses that arise due to natural perturbations would involve a combinatorial read-out of the ensemble activity as proposed in our regression analyses.

3.3.3 Valence encoding at the level of sensory neurons

Do sensory neurons distributed along the locust antennae encode for valence. The primary task ascribed to these neurons is to serve as chemical feature detectors, with different ORN classes having sharp tuning curves to specific molecular groups¹⁴⁸. The responses of these neurons to repeated presentations of stimuli were also found to be inconsistent compared to their downstream counterparts (PNs) in the antennal lobe¹⁴⁹. This could be because each PN aggregates inputs from multiple ORNs, and hence can accommodate the inconsistencies of a subset of its inputs. Additionally, the antennal lobe has a network of inhibitory interneurons (local neurons; LNs), which have been implicated in transforming the neural representation of stimuli^{150,151} through the sharpening of projection neuron responses as well as through phenomena such as lateral inhibition to achieve gain control^{26,152}. Taken together, these phenomena make the antennal lobe more suited to perform non-linear computations such as assigning different valences to chemically similar odorants (refer valences of aldehydes - hexanal and benzaldehyde, esters – isoamyl acetate and ethyl acetate in **Fig. 3.1**).

In locusts, each antenna has an approximate distribution of 50,000 ORNs that serve as the primary sensory modality for the olfactory system³³. These neurons are found in cone-like structures known as sensilla, which are broadly categorized into 4 classes – *basiconica*, *trichodia*, *coeloconica*, and *chaetica*³³. Each sensillum houses a varying number of ORNs (~5-50) and the relative distribution of different sensilla can change over the locust's lifetime³³. Given the large number of receptors, any thorough investigation of the valence encoding at the level of ORNs would require monitoring of responses across thousands of experiments. Our preliminary results (**Fig. 3.11**) indicate that locust ORNs appear to do a poor job in tuning their

neural responses to encode for innate preferences compared to PNs in the antennal lobe (**Fig. 3.5b**).

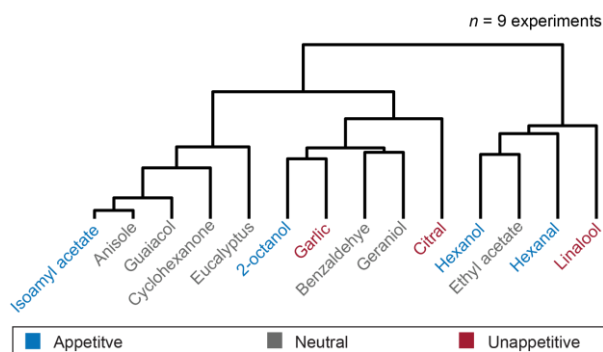


Figure 3.11: Mapping odorant responses in olfactory receptor neurons to innate valence

Dendrogram showing the overall hierarchical organization of odor responses recorded from olfactory receptor neurons (ORNs; $n = 9$ experiments). Odorants are again colored based on the corresponding behavioral preferences from **Fig. 3.1** (except geraniol, which is assigned a neutral color based on previous studies^{23,144,153}). Clustering was performed using the same approach as shown in **Fig. 3.5b** for comparison purposes.

3.4 Acknowledgments and contributions

Part of the work presented in this chapter is also included in the manuscript “*Neural manifolds for odor-driven innate and acquired appetitive preferences*” by R. Chandak and B. Raman.

We would like to thank Maida Duncan for assistance in collecting the ORN data in Fig. 3.11.

RC and BR conceived the study and designed the experiments and analyses. RC performed all the experiments and analyzed the data. RC and BR wrote the paper. BR supervised all aspects of the work. This research was supported by NSF (1453022, 2021795) and ONR (N00014-19-1-2049, N00014-21-1-2343) grants to B.R.

Chapter 4: Neural constraints on acquired appetitive preferences

4.1 Introduction

The primary goal of the nervous system is to faithfully translate external cues into meaningful behavioral responses. In Chapter 3, we discussed how innately encoded preferences that are determined by an organism's genetic makeup play an important role in achieving this feat. However, our environment is constantly in flux, and the same stimulus can be encountered in a variety of different contexts, such as following other cues or under different ambient conditions (e.g., humidity). This can modify the neural activation pattern ascribed to the stimulus and potentially alter the corresponding behavioral output. In this study, we investigate this issue using the locust olfactory system. Specifically, we look at how robustly locusts can recognize and maintain their behavioral response to an odorant when it is presented following different distractor cues as well as under different ambient conditions.

The neural representation of a stimulus can also change over an organism's lifetime, potentially altering the behavioral output produced. For example, through a phenomenon known as conditioned taste aversion¹⁵⁴, the taste of a certain food can become associated with nausea or sickness, and consequently change our preference for the food, making us less likely to consume it in the future. In many invertebrate model systems, similar alterations of behaviors to stimuli have been well-studied through various classical and operant conditioning assays. Avoidance behaviors have been induced in *Drosophila*⁵⁷ and honeybees⁵⁸ through the pairing of electric shocks (negative reinforcement) with otherwise neutral odorants. Similarly, pairing of food rewards with different olfactory stimuli has been successfully shown in moths^{59,60},

honeybees^{61,62}, and *Drosophila*⁶³ (positive reinforcement). Recently, a Pavlovian conditioning assay was shown to be effective in positively conditioning locusts with olfactory cues⁶⁴. The authors devised a protocol wherein the locusts were trained to associate a conditioned stimulus (odorant) with an unconditioned stimulus (food reward) that was known to elicit a strong unconditioned response (palp-opening response). The efficacy of training was then quantified during an unrewarded testing phase, where the locusts who were trained showed an increase in their preference for the trained odorant compared to their untrained counterparts. In this study, we will investigate if there are rules that determine which odors can be reinforced using this approach— or if all odors can be reinforced equally/similarly.

In the locust antennal lobe, odorant stimuli continue to evoke neural responses well after they are terminated (on the order of seconds). Recent studies have shown that the spatiotemporal patterns of these neural responses change most dramatically after the stimulus is terminated^{139,147}. The set of PNs activated during the stimulus presence (i.e., the ON responders) and those that get activated after stimulus termination (i.e., the OFF responders) have minimal overlap^{136,139}. Intriguingly, as our results show in Chapter 3, these OFF responses also tend to be odor-specific and appear to contain almost as much information as the ON responses (refer performances of ON and OFF regressors in **Fig 3.7**). The importance of timing between a stimulus and reward, and how it controls learning and the rate of learning is also well documented^{19,61,127,155–158}. Given that we can precisely time the delivery of rewards, can we reinforce the offset of an odorant? In this study, we will examine if the termination of a stimulus can be reinforced and whether this approach differs from reinforcing the onset of the same stimulus. Finally, we will examine how the spatiotemporal coding logic that informs the innate

neural representation for odorants (from Chapter 3) also impacts learned behavioral preferences and sensory memory.

We began by assaying the robustness of neural and behavioral responses when locusts were presented with the same stimulus under different perturbations. Our results show that PNs in the locust antennal lobe exhibited variations at the individual and ensemble level when the same stimulus (target stimulus) was encountered under perturbations such as varying stimulus histories and ambient humidity conditions. However, locusts could reliably produce behavioral responses to the target stimulus when it was encountered under the same set of perturbations. Interestingly, a simple linear classifier extracting information from flexible subsets of neurons could map PN activity to the behavioral responses with high accuracy. Next, we looked to further understand how locusts can form appetitive associations with odorants of different innate valences. We found that only innately appetitive odorants (from Chapter 3) could be used to induce PORs through appetitive conditioning, and locusts also appeared to encode a temporal component during the training phase to represent the latency between food reward and conditioned stimulus presentations. Finally, we distilled the high-dimensional PN activity to low-dimensional planes ('manifolds') that constrained odor representations to indicate whether an odorant could be successfully reinforced to induce behaviors through conditioning. These results are consistent with those we report in Chapter 3 and provide a single framework to better understand both innate and acquired olfactory preferences in locusts.

4.2 Results

4.2.1 Stimulus history and ambient conditions induce variations in PN responses

Can projection neurons (PNs) in the locust antennal lobe faithfully maintain their response to a stimulus under different perturbations? We found that PN responses to an odorant can be significantly altered when the same odor was encountered following different distractor cues, or in varying ambient (humidity) conditions. For example, in **Fig 4.1a**, two sample PNs that are ON-responsive to hexanol in solitary conditions (no distractor stimuli) are shown. However, the introduction of different distractor cues altered the subsequent response to hexanol. These variations were also seen at the population level (**Fig. 4.1b**) where we found that the hexanol-evoked PN responses created multiple, separable clusters, one for each stimulus history.

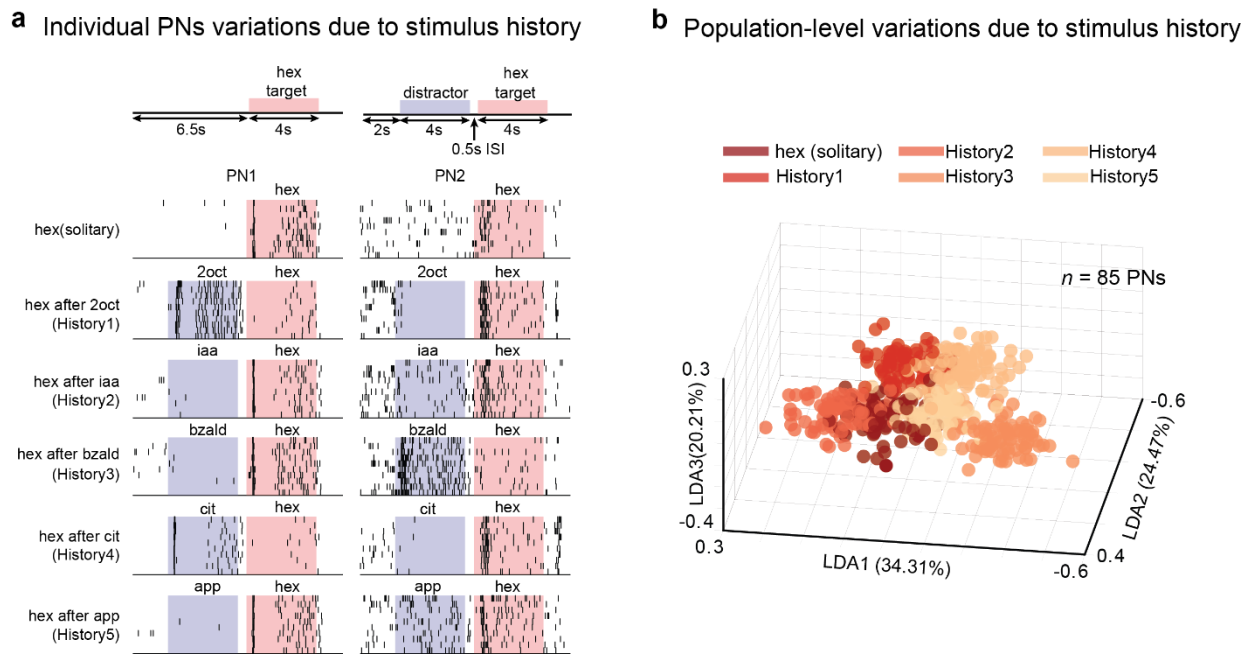


Figure 4.1: Projection neuron responses vary in a stimulus-history dependent manner

a) Raster plots showing the spiking responses of two sample PNs are shown. Hexanol (pink rectangles) was presented in solitary conditions as well as after 5 different distractor cues (blue rectangles). The distractor cues used were 2-octanol, isoamyl acetate, benzaldehyde, citral, and apple. For PN1, the

response to hexanol is limited when presented after 2-octanol and citral. For PN2, the response to hexanol is altered when presented after benzaldehyde.

b) Population-level PN responses are shown after linear discriminant analysis dimensionality reduction ($n = 85$ PNs). Each 3D-sphere represents an 85-dimensional PN activity vector in a 50 ms time bin. Eighty data points corresponding to the ensemble neural activities evoked during 4 s of hexanol presentation with a particular stimulus history are assigned the same color.

Similar results were also seen when we varied ambient humidity. In **Fig 4.2a**, we found individual PNs could modulate their firing responses to changes in humidity by both increases (PN 1) and decreases (PN 2) in their activity when conditions were more humid. When analyzing hexanol responses (taking only pink rectangles from the stimulus presentation protocol) at the population level, we found humid and dry responses across PNs also formed distinct clusters.

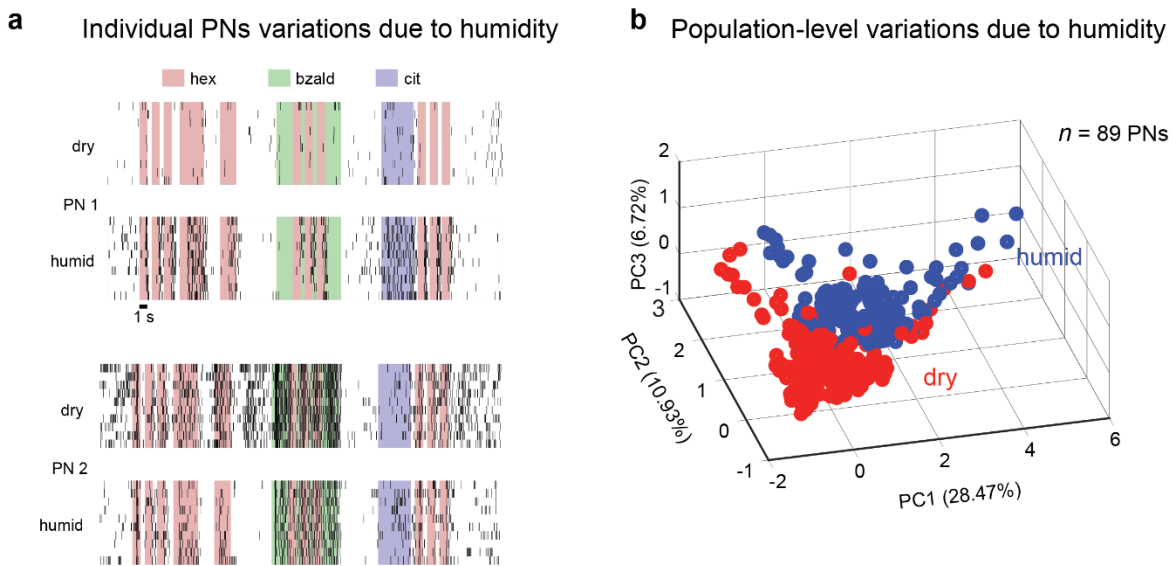


Figure 4.2: Projection neuron responses vary under altered humidity conditions

a) Raster plots showing the spiking responses of two sample PNs are shown. In each trial, hexanol (pink rectangles) was presented in short pulses, or atop benzaldehyde (green rectangles), or following citral (blue rectangles). The same sequence was presented in both dry and humid ambient conditions. Note that PN1 increased its activity in humid conditions whereas PN2 reduced its responses.

b) Population-level PN responses are shown after principal component analysis dimensionality reduction ($n = 89$ PNs). Only the periods corresponding to hexanol presentation (pink rectangles in **panel a**) in dry (red dots) and humid (blue dots) conditions were used for this analysis.

4.2.2 Robust odor recognition despite varying history and ambient conditions

Can locusts, then, reliably maintain their behavioral response to the stimulus under these perturbations? To test the recognition of an odorant across multiple different encounters, we combined the palp-opening response (POR) behavior (Chapter 3) with an appetitive conditioning assay (Fig. 4.3). In this assay, starved locusts were presented with an odorant (conditioned stimulus; CST) followed by a food reward (unconditioned stimulus; UST). The food reward alone is sufficient to evoke an innate POR response. After training with six trials, where the CST and UST were delivered in an overlapping sequence, the ability of the locusts to recognize the CST was examined in an unrewarded testing phase. To make the readout quantitative, locust palps were painted with non-odorant green paint, and the distance between the palps was tracked as a function of time (Fig. 4.3; right panel).

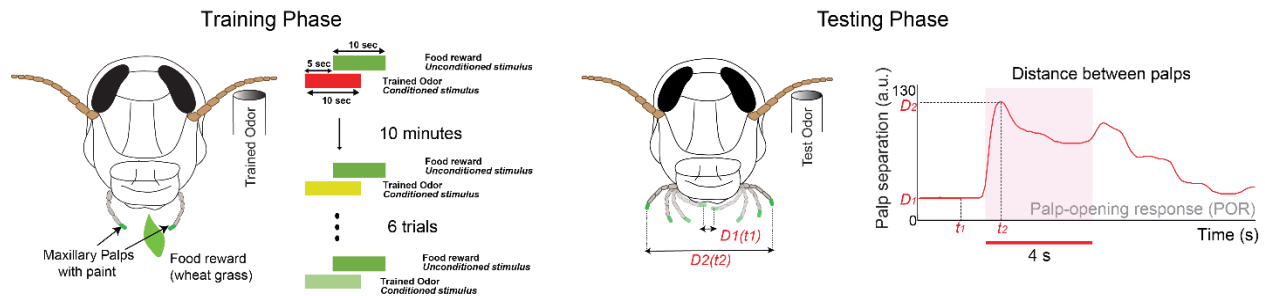


Figure 4.3: An appetitive conditioning assay to train locusts

Left: The protocol followed to train locusts to associate an odorant with a food reward is shown. *Right:* A representative test trial is shown where the palp-opening response of a locust in response to a test odorant was tracked. The response was plotted as the distance between the palps as a function of time. Red bar indicates when the test odorant was presented.

Could behavioral response to a stimulus change depending on what other cues were encountered recently? To understand this, we conditioned locusts using hexanol as the trained odorant. During the unrewarded testing phase, we presented hexanol solitarily (4 second pulse) as well as in non-overlapping sequences with ten different distractor cues. Each distractor cue

was presented for 4 seconds, followed by a 0.5 second gap, after which hexanol was presented for 4 seconds. Since prior results⁶⁴ showed that trained locust responses to conditioning stimuli remained consistent for up to six unrewarded test phase trials, we limited the testing phase to six unrewarded trials in these set of experiments. Hence, to accommodate ten distractor cues, we performed two sets of conditioning experiments with the testing phases comprising one solitary presentation of hexanol and five presentations following distractor cues. During the test phase, we presented solitary hexanol as the first trial (to establish a baseline) and pseudorandomized the presentations of the 5 distractor-hexanol sequences for each locust. The results from these experiments are summarized in **Fig. 4.4**. In panels **Fig. 4.4a** and **Fig. 4.4b**, the mean (\pm s.e.m.) responses of locusts to solitary presentations of hexanol (top-left plot in each panel) and following different cues are shown. As can be seen, locusts reliably responded to hexanol across all conditions. Note that two distractor cues (iaa and 2-octanol) also elicited PORs. To ensure that the mean responses were not dominated by a handful of locusts, we computed the fractions of locusts that had a significant response (palp separation $>$ 6.5 s.d. above baseline) for each odor presentation. Hexanol evoked significant responses in more locusts than any distractor cue (**Fig 4.4c**) and hexanol responses following distractor presentations were also reliable across locusts (**Fig. 4.4d**). These results indicate that locusts can recognize a trained odorant even when it is encountered soon after a distractor cue.

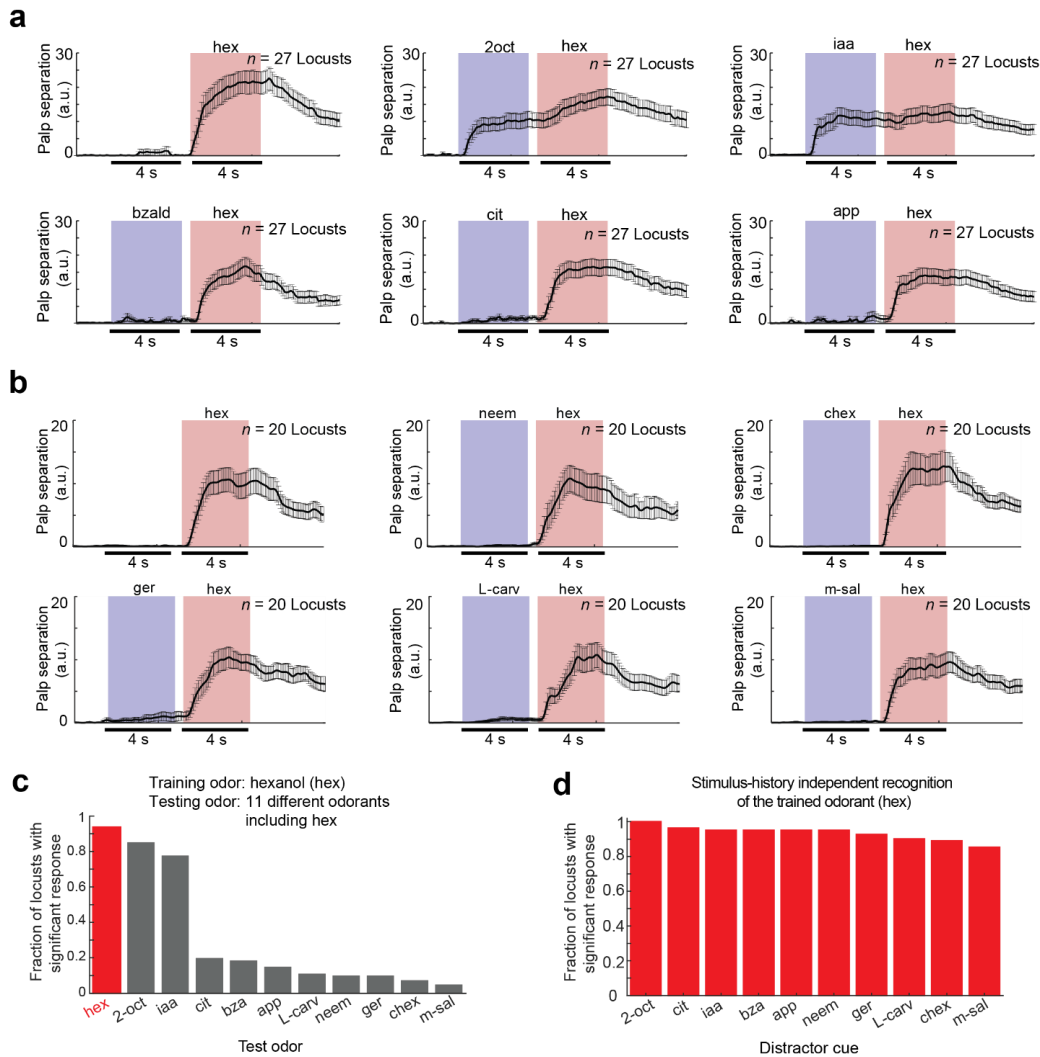


Figure 4.4: Locusts can robustly respond to an odorant with varying stimulus history

a) Mean (\pm s.e.m.) palp-opening response (POR) of locusts trained to recognize hexanol are shown. ($n = 27$). In each plot, pink rectangles indicate 4 seconds of hexanol presentation and blue rectangles indicate when different distractor cues were presented. The distractors used were 2-octanol, isoamyl acetate, benzaldehyde, citral, and apple.

b) Similar plot as **panel a** but for a different set of 20 locusts also trained to recognize hexanol. For this set of experiments, the distractors used were neem, cyclohexanone, geraniol, L-carvone, and methyl salicylate.

c) The fraction of locusts that produced significant PORs to different odors are shown. Note that only the solitary presentation of hexanol (red) across both sets (**panels a** and **b**) of experiments was combined to obtain the red bar ($n = 47$ locusts).

d) The fraction of locusts that produced significant responses to hexanol when it was presented following different distractor cues is shown.

Could changes in ambient conditions impact recognition performance? To understand this, we trained locusts in dry conditions (0% relative humidity). In the testing phase, we examined the ability of locusts to recognize the conditioned stimulus presented either in dry or humid (100% relative humidity) conditions. For these experiments, we pseudorandomized the order of testing between dry and humid conditions. Our results show that, on average, locusts opened their palps to all the introductions of the conditioned stimulus in both dry and humid conditions (**Fig. 4.5a, b**). The performance in both backgrounds was nearly identical indicating robust odor recognition that was invariant with respect to changes in ambient conditions. Similar results were also obtained when locusts were trained in humid conditions and tested in both dry and humid conditions (**Fig. 4.5c, d**). These results indicate that locusts can recognize an odorant independent of changes in ambient humidity conditions.

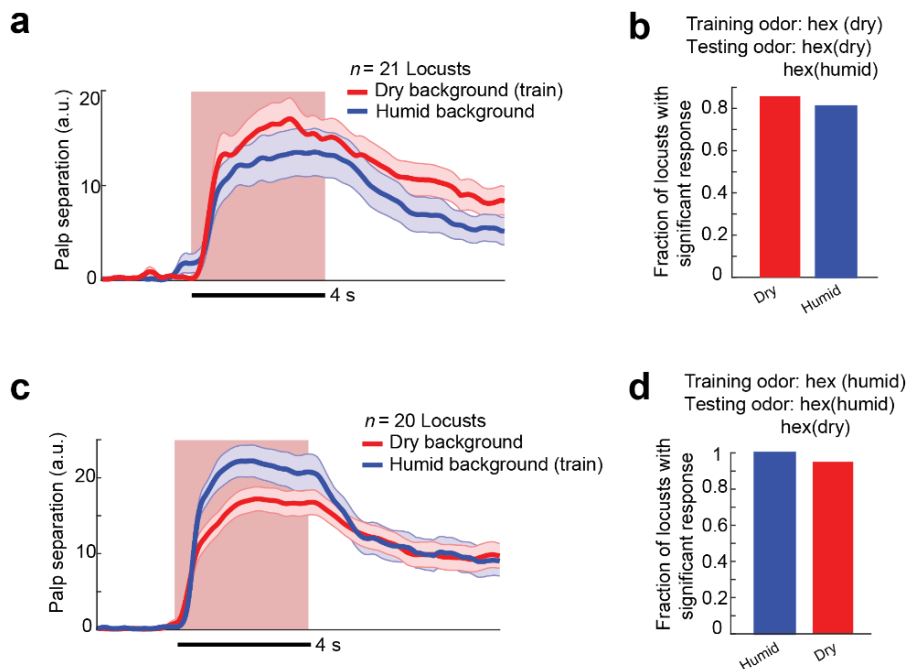


Figure 4.5: Locusts can robustly respond to an odorant with varying ambient humidity conditions

a) Locusts trained with hexanol in a dry background were tested for hexanol responses in dry (red) and humid (blue) conditions. The mean PORs of trained locusts ($n = 21$) are shown and the shaded regions indicate the s.e.m.

b) The fraction of locusts that produced significant PORs to hexanol in dry and humid conditions from **panel a** are shown.

c) Similar plot as **panel a** but for locusts ($n = 20$) trained in a humid background.

d) Similar plot as **panel b** but for locusts trained in humid conditions.

Taken together, these sets of experiments show that despite variations in PN responses, locusts could recognize and respond to a conditioned stimulus (i.e., hexanol in these experiments) when it was encountered solitarily, immediately following a distractor cue, or in varying ambient humidity conditions.

4.2.3 A flexible neural decoder produces accurate behavioral predictions

How do locusts achieve this behavioral invariance despite neural variances? We propose a flexible decoding mechanism to address this potential confound. We found that while solitary presentations of hexanol elicited strong responses in ' n ' PNs, any perturbations (such as varying history) usually resulted in only a subset ' m ' of those ' n ' neurons being activated. Additionally, which neurons comprised this subset also varied for different perturbations. Therefore, we reasoned that a classifier capable of exploiting information distributed in a flexible subset of neurons would allow robust recognition of the target odorant (hexanol). Indeed, a linear classifier that required activation of only m PNs (i.e., an activation threshold of m) could produce behavioral predictions that were highly correlated with our observed results (**Fig. 4.6**). This mechanism allows the antennal lobe to flexibly adapt its responses to different external perturbations while allowing the organism to maintain stable recognition of a target stimulus.

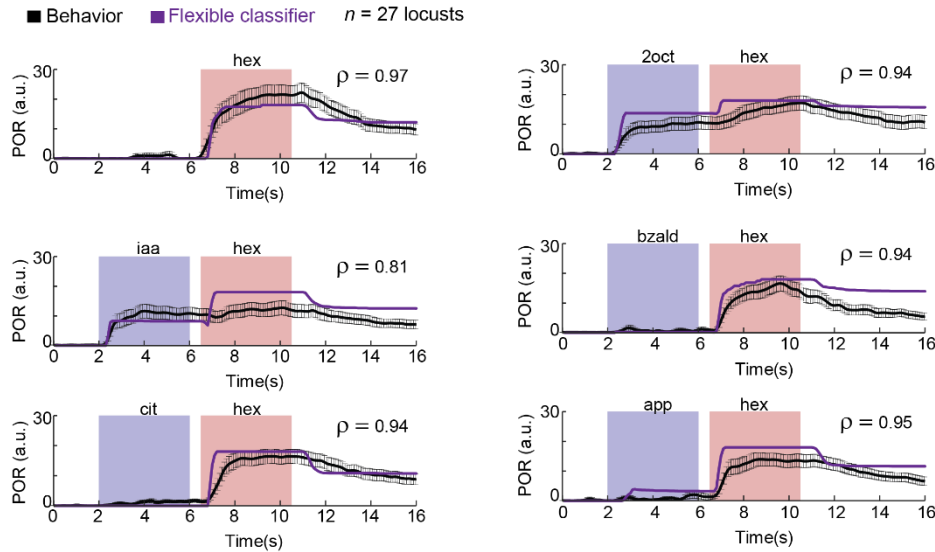


Figure 4.6: A flexible classifier can accurately predict behavior from PN responses

Observed mean (\pm s.e.m.) PORs to various presentations of hexanol (same as in **Fig. 4.4a**) are shown in black. The predicted PORs generated from the flexible classifier are shown in purple. The correlation coefficient between the actual and predicted PORs is shown on each of the six panels.

4.2.4 Effectiveness of the classical conditioning approach

Locusts can be trained to recognize hexanol under various perturbations. However, in Chapter 3, we found that hexanol (at 1% v/v) induced innate PORs in approximately 2/3rd of the test locusts (18/26 locusts or ~69%). Since we did not discard locusts that could produce innate PORs to hexanol prior to the training phase in the conditioning experiments, it can be argued that the assay did not induce any notable learning, and what we observed were simply innate responses to hexanol. However, there are two important caveats to consider. First, note that across all testing paradigms shown in **Figs. 4.4-5**, we found at least 80% of locusts produced significant responses to hexanol presentations (100% responsive locusts for humid testing shown in **Fig. 4.5d!**). Therefore, across all 16 presentations of hexanol (12 presentations in **Fig 4.4** and 4 presentations in **Fig 4.5**), we obtained above-innate levels of hexanol responses.

Adaptation or habituation to repeated unrewarded encounters of hexanol is a second caveat. Habituation is the reduction in behavior to repeated encounters of the same stimulus. It

has been reported that honeybees, another well-established model for invertebrate olfaction, habituate to repeated presentations of odorants (geraniol and isopropyl alcohol) by gradually reducing the number of proboscis extension reflex responses (a behavior analogous to the palp-opening response in locusts) over trials in the absence of food rewards¹⁵⁹. Habituation has also been demonstrated in locusts, where a reduction over time in the frequency of avoidance responses and jumps was reported in new locusts when they were introduced into a colony¹⁶⁰. Therefore, it is not unreasonable to expect that untrained locusts would display some reduction in their frequency of responses to hexanol over multiple unrewarded encounters. Do we see a similar result for trained locusts? We computed the fraction of locusts that produced significant PORs to hexanol as a function of trial number for the experiments in **Fig. 4.4**. As can be seen, the locusts are able to maintain consistent responses (significantly above baseline levels) to hexanol over trials, indicating a lack of habituation (**Fig. 4.7**). Note that this result is different from those presented above since we pseudorandomized the presentation sequence of distractor-hexanol pairs across locusts. In **Fig 4.7**, we are classifying hexanol responses by the trial number in the experiment and not by distractor identity as shown in **Fig 4.4**.

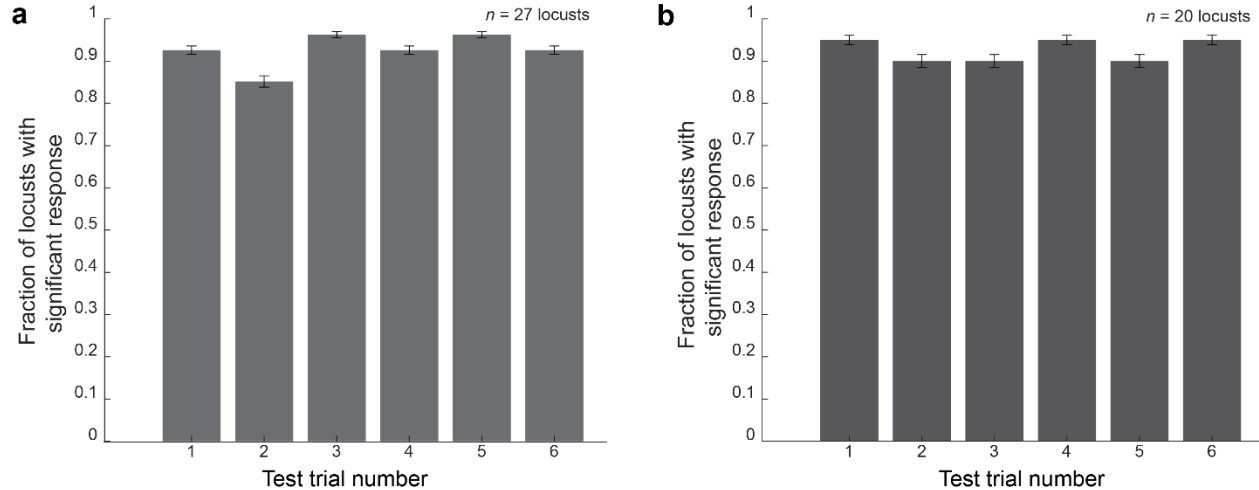


Figure 4.7: Locust responses to hexanol are consistent across multiple unrewarded trials

a) The fraction of locusts with significant responses to hexanol (from **Fig 4.4a**) are shown as a function of trial number during the testing phase. Error bars indicate the standard deviation.

b) Similar plot as **panel a** but for the results shown in **Fig 4.4b**.

Thus, while we cannot rule out the effect of innate responses to hexanol, our results indicate that conditioning locusts does appear to increase the frequency (to above innate levels) and maintains the consistency of responses (lack of habituation) to hexanol.

4.2.5 Innate versus acquired preferences for odorants

In the previous set of experiments, hexanol was the only trained odorant used. Can any odorant be similarly paired with food rewards to produce PORs? Using our results from Chapter 3, we selected 4 four chemically and behaviorally diverse odorants (**Fig 4.8**) to use as conditioned stimuli to pair with food rewards. To remove the confound of innate responses discussed above, we additionally pre-screened locusts prior to the training phase to check for innate responses to all the odorants. Only those locusts that did not have innate responses to any of the four odorants were used for the appetitive-conditioning experiments.

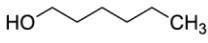
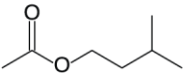
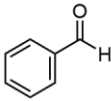
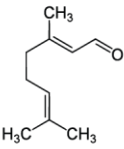
Odor	Hexanol	Isoamyl acetate	Benzaldehyde	Citral
Chemical structure				
Preference index	0.31	0.31	-0.11	-0.23

Figure 4.8: Diverse odorants used for Pavlovian conditioning assays

We used 4 odors – hexanol, isoamyl acetate, benzaldehyde, and citral for the appetitive conditioning assays. As can be seen here, these 4 odorants have very diverse chemical structures with unique functionalities, as well as diverse innate preference indices.

We trained different sets of locusts with each of the four odorants as conditioned stimuli using the same approach as described in **Fig 4.3** (referred to now as ‘ON-training paradigm’). Following training, we examined the ability of the trained locusts to respond to all four odorants in an unrewarded test phase. We found that locusts trained with hexanol or isoamyl acetate as conditioned stimulus robustly responded to the presentation of these odorants in the test trials. However, we found that locusts trained with citral and benzaldehyde showed no palp-opening response during the testing phase to these odors (**Fig. 4.9a, b**).

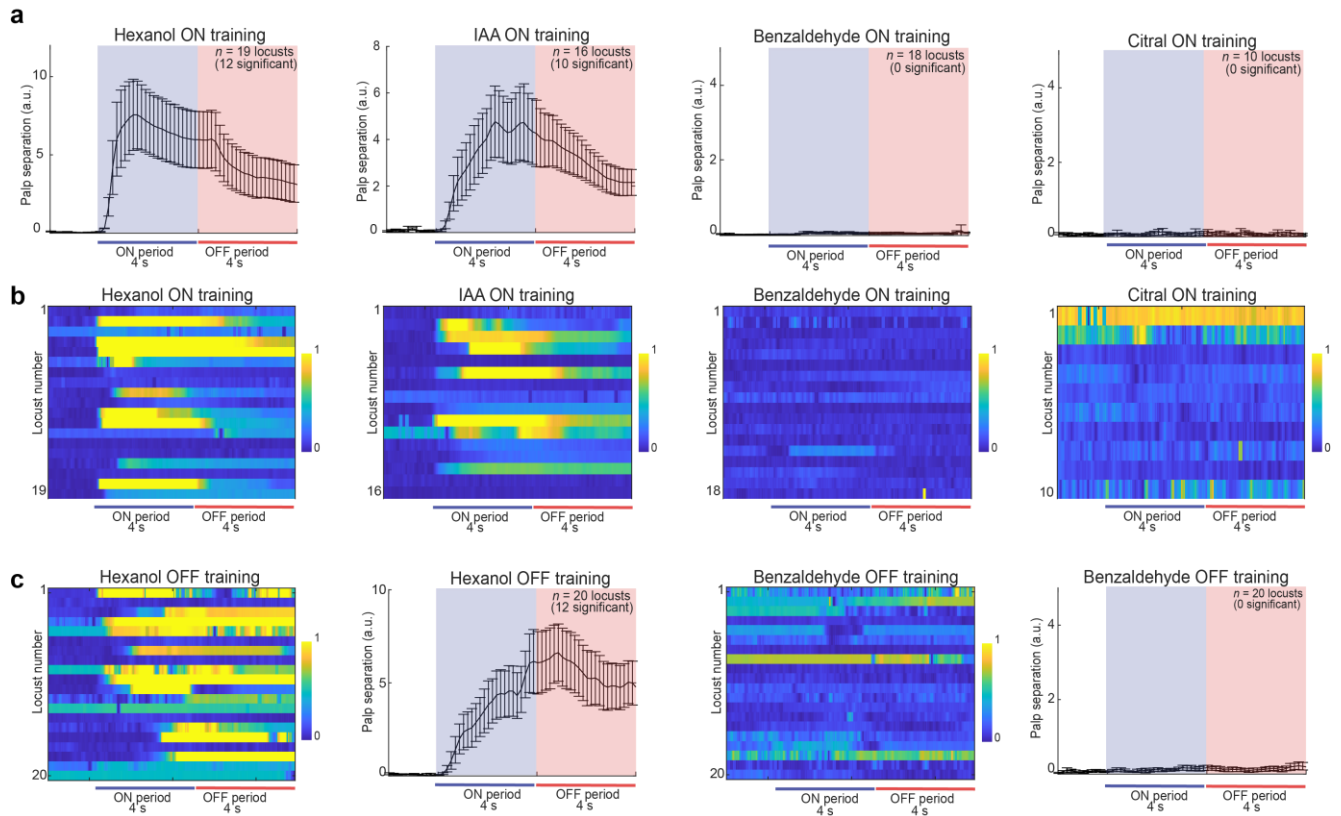


Figure 4.9: Only innately appetitive odors can be reinforced using classical conditioning

a) Results from ON-training using 4 different odors are shown. The mean POR response of locusts during the unrewarded testing phase is shown in each plot. The testing odor was the same as the training odor, as indicated on each plot. Colored bars indicate 4 s of odor presentation and 4 s immediately following odor termination. Error bars indicate s.e.m., and the number of locusts that had significant PORs for each conditioning odorant is indicated in parentheses. As can be seen, locusts trained with hexanol and isoamyl acetate were able to produce POR responses in the test phase, while benzaldehyde and citral training yielded no responses. Note that different sets of locusts were trained/tested for each odorant.

b) POR traces for the four sets of locusts trained with hexanol, isoamyl acetate, benzaldehyde or citral are shown. The PORs shown were recorded during the testing phase. Each row corresponds to the response observed in one locust. The responses were normalized to range between [0, 1] for each locust (see Methods; blue – 0 and yellow – 1). Note that for a small fraction of locusts (such as citral, first row) that only had minimal palp movement during the entire trial, the normalization protocol followed produced spurious shades of yellow, but these locusts still did not have a significant response to that odorant.

c) Similar traces as shown in **panels a and b** but for OFF-conditioning using hexanol or benzaldehyde are shown. Hexanol-OFF training produced significant PORs in 12/20 locusts, whereas benzaldehyde-OFF training yielded no significant responses. Note that the PORs for hexanol-OFF training are delayed and persisted well into the OFF period (compared to hexanol-ON trained responses shown above).

Next, we examined whether locusts could be conditioned when the reward was delayed until half a second after the termination of the conditioned stimulus (i.e., ‘OFF-training paradigm’). For this set of experiments, we only used hexanol and benzaldehyde as the conditioned stimuli (CS, **Fig. 4.9c**). Once again, our results indicated that only locusts trained with hexanol robustly responded with PORs to the trained odorant in the testing phase. However, the POR dynamics observed in OFF-paradigm trained locusts were noticeably different from those we noted in the ON-training paradigm case. In the ON-training case, we found that locust PORs began immediately after the onset of the CS, lasted the duration of the stimulus, and the palps began to close following the termination of the stimulus. The peak of the PORs always occurred during the CS presentations. In contrast, for the OFF-training case, locust PORs were significantly slower (**Fig 4.10**), and the peak of the PORs in many locusts occurred after the termination of the stimulus.

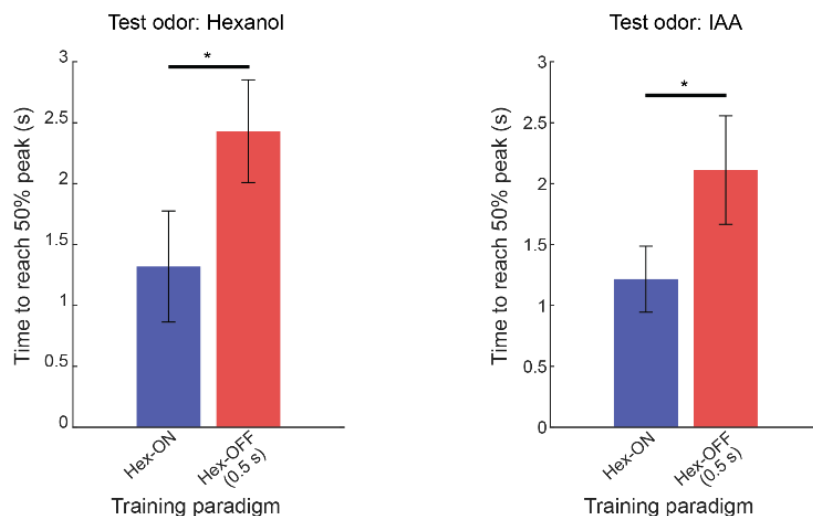


Figure 4.10: ON- and OFF- conditioning produce temporally distinct responses

Latency of locust PORs to hexanol (left) and isoamyl acetate (right) are shown. Response latency here is defined as the time taken by locusts to reach 50% of the peak palp separation (time = 0 along the y-axis indicates odor onset). Each bar plot shows the mean latency across locusts, and error bars indicate s.e.m. For each odorant tested, POR latency for two groups of locusts either trained using hexanol ON-training

paradigm (blue bars) or OFF- training paradigm (red bars) are shown for comparison. For this analysis, we used only those locusts that had significant responses to the test odorant (refer **Fig. 4.9** for fractions; see Methods). For both odors, locusts trained in the hexanol OFF-training paradigm were significantly slower in opening their palps (* indicates $p < 0.05$, one-sided t-test).

In sum, these results indicate that only innately appetitive odorants can successfully be associated with the food reward to produce PORs. Furthermore, both presentations during and after the termination of the stimulus can lead to odor-reward association but the behavioral response dynamics are significantly different between the two cases.

4.2.6 A linear model predicts behavioral response dynamics and cross-learning

Next, we wondered how locusts conditioned with a particular odorant (i.e., ‘the training odor’) respond when tested using other untrained odorants. Our results indicate that locusts trained with hexanol also responded robustly to presentations of isoamyl acetate (another odorant with a positive valence; **Fig. 4.11**). Exposures to citral and benzaldehyde evoked no responses in hexanol-trained locusts. Surprisingly, while locusts trained with citral and benzaldehyde showed little to no responses to the trained odorant, a significant fraction of them showed PORs to hexanol and isoamyl acetate (**Fig. 4.12a-c**). For the OFF-training paradigm, we found that learning/cross-learning was observed only in those locusts that received rewards within 2 s of the termination of the conditioned stimulus. The efficacy of this offset-conditioning weakened as the gap between the stimulus and food reward was extended, with almost no learning observed in locusts trained with the longest gap (4 s gap training shown in **Fig. 4.12 b, c**). This result served as an in-built control that our assay was not simply producing trivial innate responses upon sufficient encounters with an odorant (sensitization) and that pairing the conditioned stimulus sufficiently closely with food rewards was essential to produce POR responses. Indeed, the lack of any increase in responses to non-appetitive odorants (even to their innate levels) also refutes this potential pitfall.

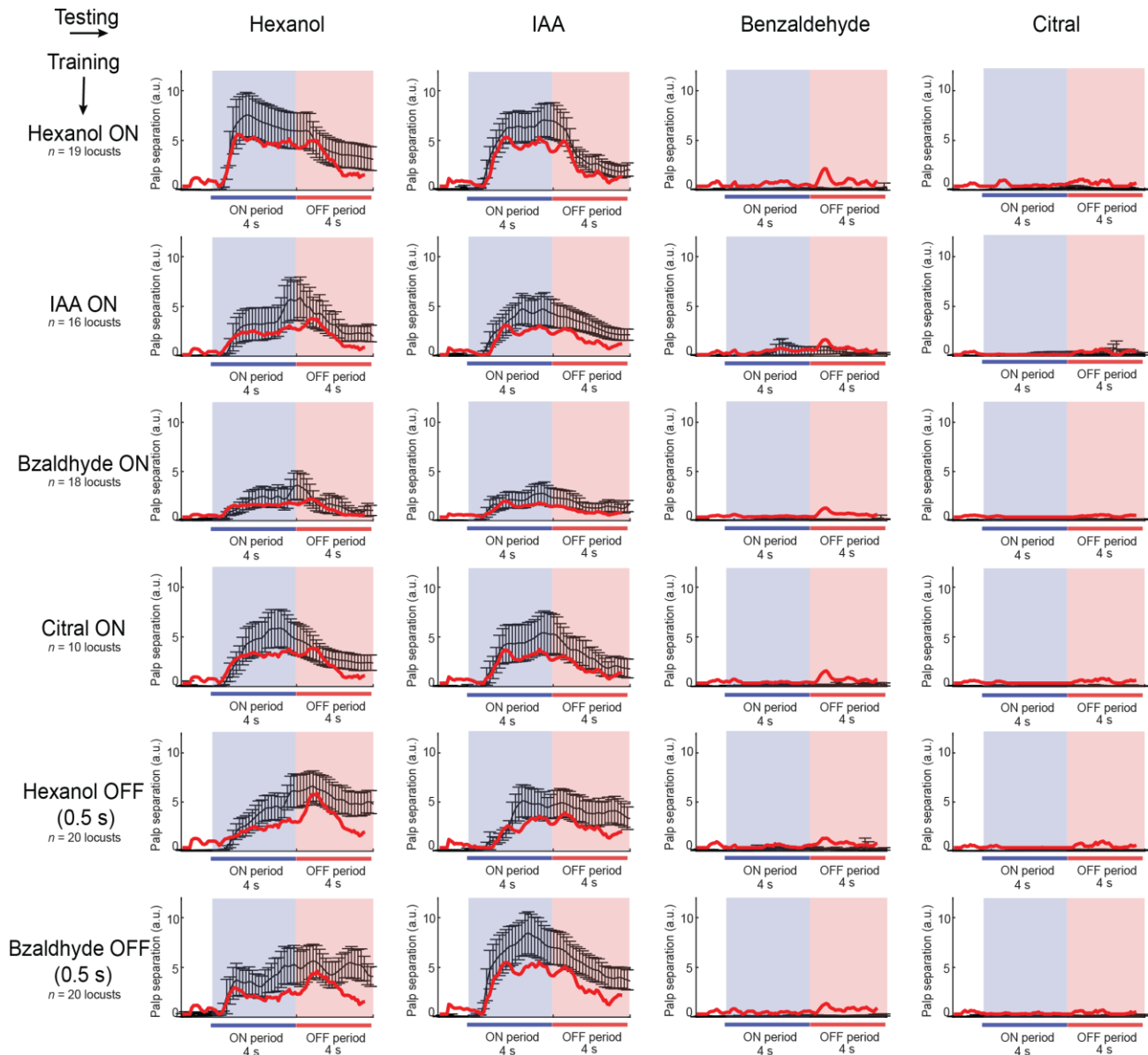


Figure 4.11: Predictable behavioral response dynamics, cross-learning, and generalization between trained odors

Summary of observed and predicted POR responses for six different training conditions are shown: row 1 – ON-trained with hexanol, row 2 – ON-trained with isoamyl acetate, row 3 – ON-trained with benzaldehyde, row 4 – ON-trained with citral, row 5 – OFF-trained (0.5 s gap) for hexanol and row 6 – OFF-trained with benzaldehyde. The number of locusts tested in each training paradigm is shown on the left. Responses of the trained locusts were examined for all four odorants during the unrewarded testing phase. The mean PORs to each odorant are shown in black and error bars indicate s.e.m. Colored bars indicate odor ON and OFF time periods. Red traces on each plot show PORs produced by linear regression model that used ensemble PN activity for the four different odorants as inputs (see Methods).

How predictable are these behavioral response dynamics and memory cross-talks given the neural responses evoked by these four odorants? To understand this, we set up determining

the neural-behavioral transformation as a regression problem with sparsity constraints. For each training paradigm, the goal was to predict the POR responses to all four odorants examined given the time-varying ensemble neural responses evoked by each odorant. Six such regression problems were set up, one for each training paradigm used in our study. We found that POR responses to all four odorants could be predicted reliably for all cases (red curves, **Fig. 4.11**). We found that a linear mapping could indeed be found where the POR dynamics predicted from the neural responses were in good agreement with those observed in behavioral experiments (**Fig. 4.11**; black (actual) vs. red (predicted); **Fig. 4.12d**). Notably, the regression weights assigned to different PNs to predict the POR for each training paradigm were highly similar (**Fig. 4.13a, b**). This result indicates that the mapping between neural responses and the PORs is highly consistent. However, this is not surprising since the main trend observed in all cases were PORs to positive valence odorants (hex and iaa) and a lack of response to those with negative valence (citral and bzald).

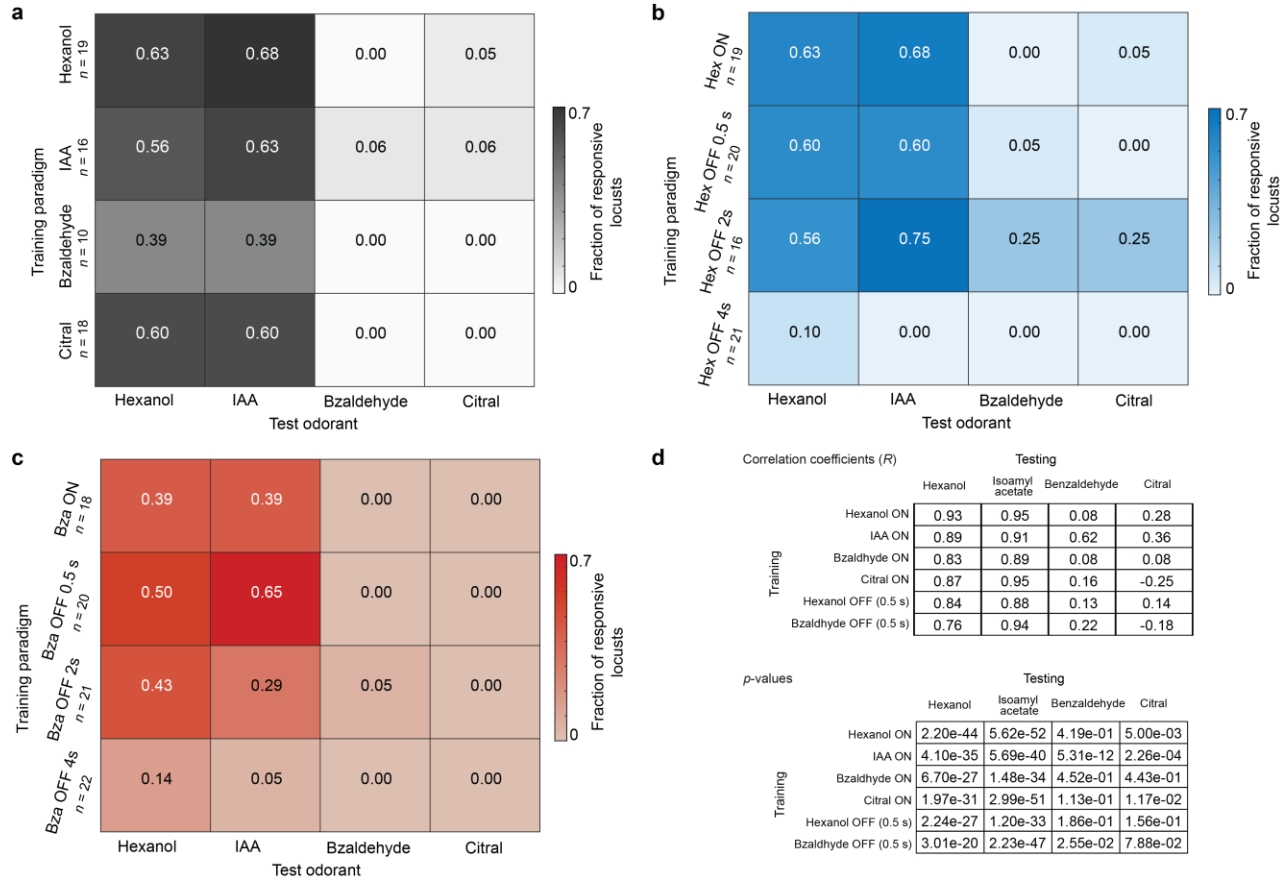


Figure 4.12: Quantifying locust learned responses and model performances

a) Heatmap showing the fraction of locusts that produced significant PORs to the test odorant (x-axis) for ON-training with four different odorants (y-axis).

b) Similar plot as **panel a** but for locusts trained with hexanol using ON- and OFF-training (0.5 s, 2 s, 4 s gaps) paradigms.

c) Similar plot as **panel a** but for locusts trained with benzaldehyde using ON- and OFF-training (0.5 s, 2 s, 4 s gaps) paradigms.

d) The two tables show the correlation between the predicted POR versus the observed behavioral response dynamics (R, top table) and significance (p-value, bottom table) (red traces in **Fig. 4.11**). Similar to the convention in **Fig. 4.11**, each row corresponds to one training paradigm and each column shows one test odor.

Next, we visualized the neural responses to PNs that received a non-zero weight. Given the sparsity constraints used to learn the weights, 21 PNs were assigned a positive weight, 19 were assigned a negative weight, and the remaining 40 PNs were assigned a weight of 0. We

found that those PNs that received positive weights responded strongly to both positive valence odorants and had relatively weaker responses to exposures of benzaldehyde and citral (**Fig. 4.13c**). On the other hand, the negatively weighted PNs had strong spiking activities to the non-appetitive odorants, which would allow the suppression of POR responses (**Fig. 4.13c**; gray traces taller than black traces for benzaldehyde and citral). This was further quantified by looking at the correlation between the magnitude of response of a PN and the weight assigned to it (**Fig 4.13d, e**). Hexanol and isoamyl acetate had positive correlations for these comparisons for both positively and negatively weighted neurons, with a slightly stronger trend in the positively weighted subset (r-values in top panels). More interestingly, for non-appetitive odorants, we found the model weights to be negatively correlated with neural activity for positively weighted PNs ($r < 0$ in bottom panels **Fig 4.13d**), and this trend reversed for negatively weighted PNs ($r > 0$ in bottom panels **Fig 4.13e**), indicating how the model suppressed POR predictions for these odorants.

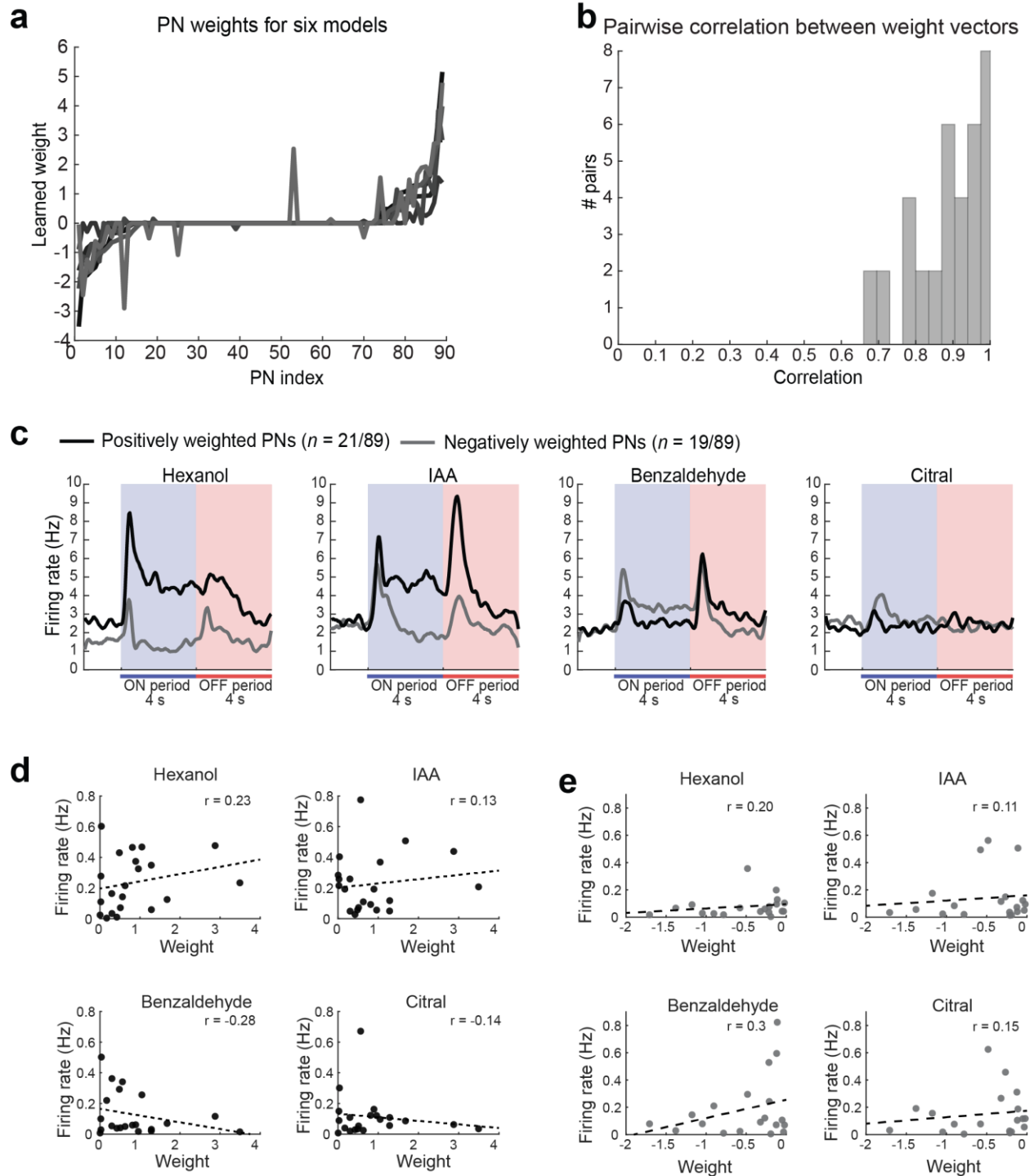


Figure 4.13: Linear regression models to map neural responses to behavior

a) We trained 6 linear regression models with sparsity constraints to map PN responses to PORs from 6 training paradigms (Fig 4.11). The weights learned by these models are shown here. PN indices are sorted by the weights assigned for the hexanol-ON model.

- b)** The distribution of pairwise correlations between different pairs of weight vectors from **panel a** are shown. As can be seen, the weights assigned to PNs are highly similar, given the high correlation for all pairwise comparisons.
- c)** Summed spiking activities of all PNs that were assigned positive (black) or negative (gray) weights are shown. 21 PNs were assigned positive weights, 19 PNs received negative weights < 0 , and the remaining 49 PNs were assigned a weight of 0.
- d)** Relationship between the mean firing rate and model weight for PNs assigned positive weights are shown for all four odorants. The correlation coefficient for each distribution is indicated.
- e)** Similar plot as **panel d** but for PNs assigned negative weights.

In sum, these results indicate that the behavioral responses' strength and dynamics evoked by different odorants could be predicted from time-varying ensemble neural responses observed in the antennal lobe, and that a robust linear mapping involving ~50% of the total neurons (40/89 PNs assigned non-zero weights) was sufficient to transform neural activity into POR output.

4.2.7 A neural coding logic for encoding appetitive odor preferences

Are the neural responses to appetitive and non-appetitive odorants organized in an interpretable fashion to explain the diverse set of neural and behavioral observations? To understand this, we visualized the ensemble neural activities of different odorants during both the ON and OFF periods. As can be observed, the odor-evoked ensemble responses were organized into four well-defined subspaces/clusters: appetitive ON, appetitive OFF, non-appetitive ON, and non-appetitive OFF (**Fig. 4.14a, b**). Note that the different directions in this coding space indicate different combinations of PN responses, and nearby regions indicate pattern-matched neural responses. Therefore, these results indicate that while the neural activities during appetitive odorant exposures varied from one odorant to another (**Fig. 4.14a, b** – cluster 1), they were still constrained to exploit only a limited combination of PN responses and therefore restricted to a particular subspace/region in this coding space. Extending this logic, these results also indicate that activities after the termination of appetitive odorants (**Fig. 4.14a, b** – cluster 2),

during exposures to non-appetitive odorants (**Fig. 4.14a, b** – cluster 3), and after cessation of the non-appetitive stimuli (**Fig. 4.14a, b** – cluster 4) all employed restricted combinations of ensemble neural responses that were different from each other.

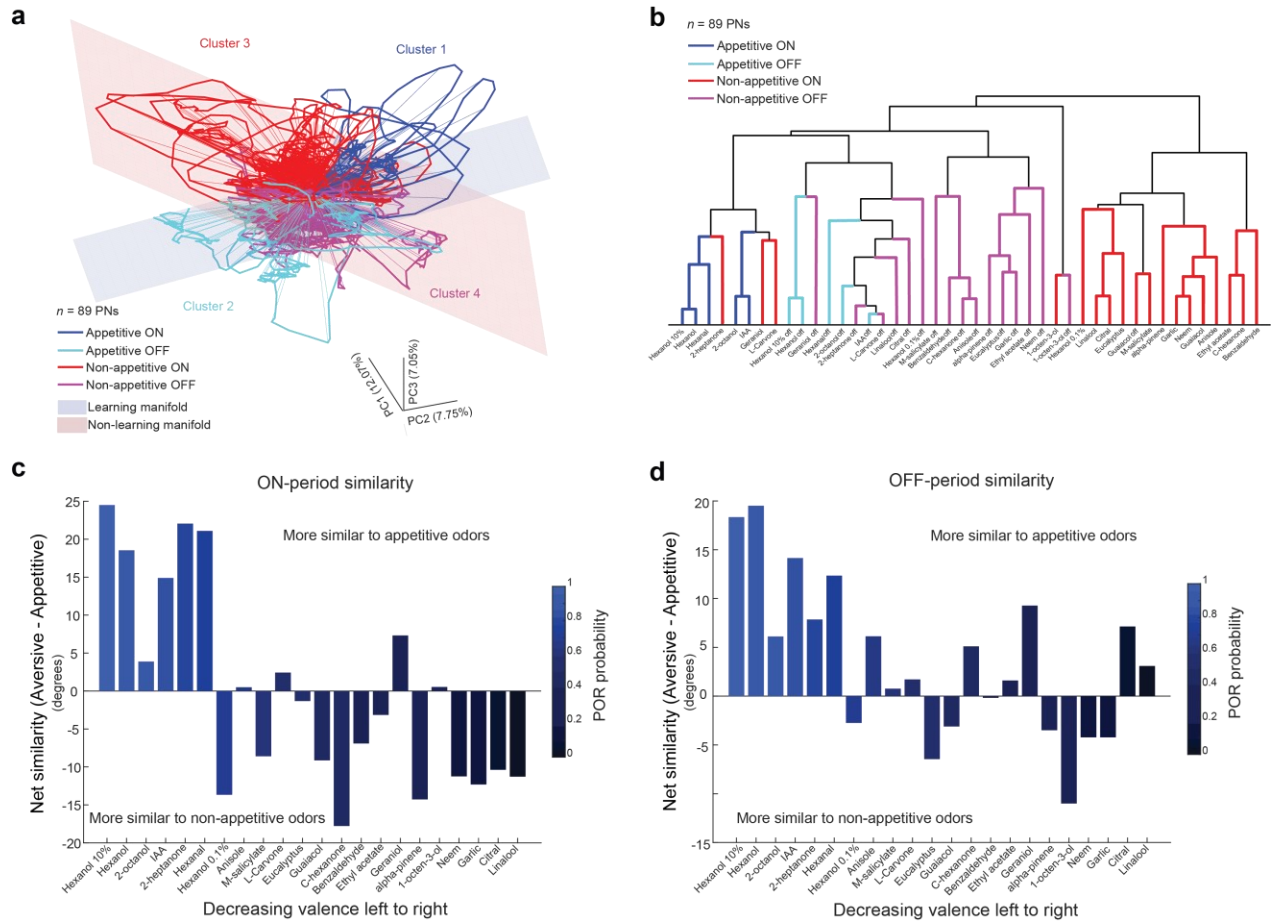


Figure 4.14: Neural manifolds can explain innate and acquired behaviors

a) PCA trajectories showing ensemble neural responses during both the ON- and the OFF- periods for all 22 odors are shown along the top 3 principal components ($n = 89$ PNs; see Methods). The trajectories were colored as follows: blue – appetitive odorants ON responses, cyan – appetitive odorants OFF responses, red – non-appetitive odorants ON responses, and magenta – non-appetitive odorants OFF responses. Variances in odor-evoked responses of appetitive odorants were not uniformly distributed but confined a subspace and are shown as using a linear plane (see Methods; plane colored in blue that encompasses appetitive ON and appetitive OFF neural ensembles). Similarly, non-appetitive odorants ensemble responses are confined to a distinct neural manifold schematically shown in red.

b) Dendrogram showing the categorization of odor-evoked ON and OFF responses of all twenty-two odors in the panel are shown. A correlation distance metric was used to assess the similarity between

89-dimensional PN response vectors. Coloring convention similar to **panel a**. Note that the appetitive and non-appetitive odorants form supra-clusters, each containing ON and OFF responses sub-clusters.

c) Plot showing the average similarity of an odorant to other appetitive and non-appetitive odorants. For each odor, we took the ON-response across 89 PNs (i.e., 89-d vector) and computed its cosine similarity with the ON-responses for all other odorants. Twenty-one such angles were obtained for each odorant (22 odors, ignoring self-comparison). The angles obtained from comparison with appetitive and non-appetitive odorants were grouped, and the average for each group was taken. The difference between the average angles for each group (non-appetitive minus appetitive) is shown here as a bar plot (smaller cosine angle denotes higher similarity between vectors). The odorants along the x-axis are shown in order of decreasing innate valence going from left to right, and the bars are colored to indicate the probability of innate PORs (**Fig. 3.1**). Note that a positive similarity score indicates the odor responses were more similar to appetitive odors while a negative score indicates better pattern-match with non-appetitive odorants. On average, the probability of PORs appears to reduce as the neural similarity with appetitive odorants diminishes.

d) Similar plot as **panel c** but using the OFF-responses across all 89 PNs.

Notably, the variance in neural responses evoked by appetitive odorants primarily spanned a low-dimensional space (i.e., a ‘neural manifold’) that contained clusters 1 and 2. Only odorants that evoked neural responses limited to this manifold could be associated with food rewards (therefore referred to as the ‘learning manifold’; **Fig. 4.14a**). Presenting the reward during activation of neurons primarily in either cluster 1 or 2 led to learning. However, the behavioral response dynamics significantly varied depending on whether the reward overlapped with cluster 1 or 2 (**Fig. 4.10**). In contrast, the variance in neural responses evoked by non-appetitive odorants spanned a different manifold that contained clusters 3 and 4. Presenting reward during the activation of either of these ensembles of PNs did not result in successful conditioned stimulus-reward associations (therefore referred to as the ‘non-learning manifold’).

We further quantified these low-dimensional patterns by computing the similarity between odor-response vectors obtained using all 89 PNs. For each odor, we obtained an 89-dimensional vector to capture the mean response during the ON period and calculated the angle between all such vectors for all odors. Note that a smaller angle (in degrees) represents greater

similarity between two vectors. For each odor, we computed 21 angles (22 odors, ignoring self-comparison) and grouped them based on comparison with either appetitive or non-appetitive odors. We then subtracted the average angle of the appetitive group from the non-appetitive group to obtain a single similarity angle for each odor. A net positive angle indicates that the odor's responses were more similar to the appetitive group while negative angles denote better pattern-match with non-appetitive odors. In Fig 4.14c, we plot this net angular similarity for each odor. The odors are sorted by valence and the bars are colored to denote the probability of innate PORs (Fig 3.1) for the odorant. Overall, these results are quite similar to those obtained from the manifold analyses (clusters 1 and 2), indicating that high-dimensional neural responses agree with the low-dimensional approximations. A similar result was also obtained when using the OFF-period responses to perform this analysis (Fig 4.14d; similar to clusters 3 and 4).

In sum, these results reveal an organizational logic for patterning ensemble neural responses to mediate not only innate (Chapter 3) but also acquired appetitive preferences.

4.3 Discussion and conclusions

4.3.1 Invariant odor recognition

We began by examining how invariant recognition of odorants can be achieved in a relatively simple locust olfactory system. Our results indicate that while individual and ensemble PN responses can vary with perturbations such as stimulus history and changes in ambient humidity conditions, locusts could maintain robust behavioral recognition of a target stimulus. Interestingly, this seeming mismatch between the lack of stability in the neural representation and behavioral robustness could be addressed through a simple linear classification scheme that decoded information from flexible subsets of neurons to produce highly accurate behavioral predictions. How generalizable is this approach? Recent work suggests that a similar decoding

approach using information from combinations of ON- and OFF-responsive PNs can also be used to accurately predict behavioral responses when a stimulus is encountered with variable durations or in an overlapping fashion with other distractor stimuli¹⁴⁷. While the exact mechanism(s) through which this invariance is achieved remains to be investigated, candidates include variable adaptation at the level of sensory neurons (ORNs)^{161,162}, interference from OFF-responses of distractor stimuli¹³⁹, and variable inputs from inhibitory local neurons¹⁶³.

4.3.2 Acquired appetitive preferences

Next, we wanted to understand the appetitive preferences of locusts to different appetitive and non-appetitive odorants (from Chapter 3) using the palp-opening response. To understand the rules that constrain learning in this paradigm, we screened and identified locusts that did not have any innate responses. We were concerned that repeated exposures to an odorant may induce PORs in these locusts. In this scenario, the PORs observed in the testing phase may not arise from conditioning but rather from sensitization due to repeated exposures to a stimulus. However, our results indicate that when the introductions of the reward were delayed to occur well after the termination of the odorant (hexanol OFF 4 s and benzaldehyde OFF 4 s paradigms), locusts did not show PORs and maintained their lack of responses to the conditioning odorants (**Fig. 4.12**). We interpreted this result as an appropriate control indicating that locusts did not become sensitized to generate PORs to the conditioned stimulus, and that PORs in these locusts were observed only in certain scenarios that suited associative learning.

Our conditioning experiments revealed that only two of the four odorants (hex and iaa) used resulted in successful associations between the odorant and the reward. As a result, locusts responded with PORs to presentations of these odorants during the testing phase. We observed generalization of the observed responses to other odorants. Locusts trained with hexanol also

showed responses to isoamyl acetate and vice versa. Intriguingly, locusts trained with citral and benzaldehyde also increased PORs to hexanol and isoamyl acetate. We again found that a linear mapping between neural and behavioral responses existed and captured all the important trends in our data (**Fig. 4.11**).

We found that delaying reward such that it was delivered either during the presentation of hexanol (ON-training paradigm) or immediately after its termination (OFF-training paradigm) both resulted in associative learning. However, we found that the POR dynamics were different between these two training paradigms. We note that locusts in the ON-training paradigm had PORs that were significantly different from those observed in locusts trained using the OFF-paradigm. This result suggests that the timing of the reward could be controlled to coincide during different phases of neural response dynamics and such manipulations result in predictable changes in behavioral responses.

4.3.3 Neural manifolds for generating and patterning behavioral outcomes

In Chapter 3, we demonstrated that linear mappings could generate robust predictions for innate preferences from PN responses. Extending those results, we found that there exists a theoretical framework that would allow us to integrate the observations from this study with those from Chapter 3 to better understand the neural underpinnings of behavior. We regarded the ensemble neural activity to each odorant as a high-dimensional neural response trajectory. Each odor-evoked response trajectory consisted of two non-overlapping segments, one during odor presentation (i.e., ON response), and the other after its terminations (i.e., OFF response). Notably, we found that ON responses and OFF responses evoked by innately appetitive odorants were on or near a low dimensional sub-space or ‘manifold’ (**Fig. 4.14a**). Similarly, we found that

ON and OFF responses evoked by odorants with non-appetitive valences were on or near a separate low-dimensional manifold in the coding space (**Fig. 4.14a**).

We note that neuronal manifolds that encode for different behavioral response motifs have been reported in other model organisms^{164,165}. In *C. elegans*, these neuronal manifolds appear to arise globally and engage several circuits throughout the entire brain. Importantly, even those neuronal circuits that are directly downstream of sensory neurons were incorporated in these brain-wide dynamics to orchestrate the innate behavioral outcomes¹⁶⁴. If this is indeed a generic phenomenon, we would expect the spiking response patterns in the early olfactory circuits such as invertebrate antennal lobe or vertebrate olfactory bulb would be organized into behaviorally relevant neural manifolds. Our results indeed reveal that this is the case at least in the locust olfactory system.

Results from our conditioning experiments indicated that delivering rewards while the odor-driven neural activities were in the ‘appetitive manifold’ resulted in successful conditioning, whereas no associative learning occurred while delivering rewards during responses excursion in the ‘non-appetitive manifold’. Interpreted differently, this result suggests that neural activity patterns on some manifolds are conducive for learning, while activity patterns outside this manifold could be harder to learn. Similar results have been reported in the context of motor control in primate motor cortex^{166,167}. While the motor cortex result arose from constraints imposed by the neural circuitry making certain neural activity patterns difficult to generate, here the antennal lobe network could generate neural response excursions in both learnable and non-learnable manifolds depending on the identity of the stimuli.

4.3.4 Operant conditioning

In this study, we looked at acquired olfactory preferences using classical or Pavlovian conditioning. An alternative method to induce and study learning is through operant conditioning. Operant conditioning has been widely demonstrated in vertebrate model systems^{168,169}, but is less commonly studied in invertebrates^{61,170}. We attempted to reinforce the POR response to different odorants using an operant paradigm. For each locust, we performed 100 trials where an odorant was presented for 4 seconds every 30 seconds and the locust was given a food reward if it performed a successful POR in the trial. We also performed a set of control experiments where the locusts were similarly presented with 100 trials of an odorant but were not rewarded in any trial. We used the same set of four odors – hexanol, iaa, benzaldehyde, and citral, as conditioned stimuli for this set of experiments.

Our results show that while operant reinforcement of all four odorants could increase the frequency of PORs (**Fig 4.15a**, solid lines vs dotted controls), the efficacy of this assay appeared to be significantly higher for innately appetitive odorants (**Fig 4.15b**, hex and iaa) vs. non-appetitive odorants (bzald and citral). While preliminary, these results agree with the neural manifolds we propose in this study, indicating a more generalized learning constraint governed by neural responses.

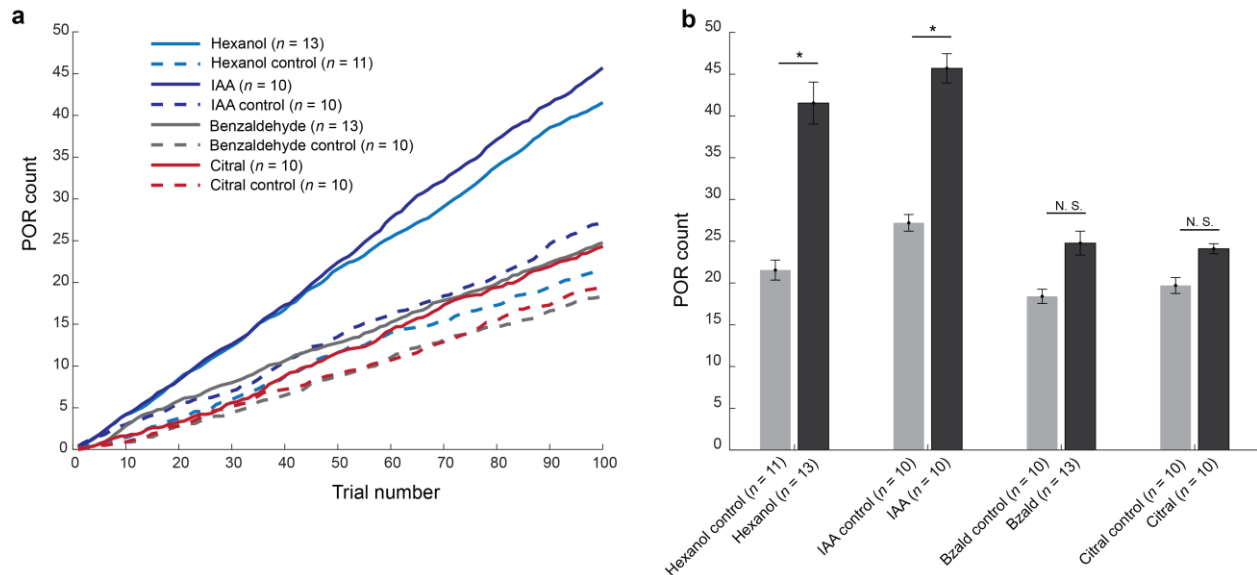


Figure 4.15: Operant conditioning to reinforce locusts using appetitive and non-appetitive odors

a) We attempted to reinforce the palp-opening response (POR) in locusts using an operant conditioning paradigm. For this set of experiments, we used hexanol, isoamyl acetate (innately appetitive odors), benzaldehyde and citral (innately non-appetitive odors) as the trained odors. In these experiments, each locust was presented 100 trials of an odorant and a food reward was provided in trials where locusts performed PORs to the trained odorant (no food reward was presented in control cases or if no POR was performed). Our results show that using this approach, the average number of palp-opening responses can be increased for all odors.

b) The average number of PORs elicited across all locusts and training conditions are shown. Error bars indicate s.e.m. PORs almost double (compared to control) for rewarding innately appetitive odors, while the change is less pronounced for non-appetitive odors (* indicates $p < 0.05$, two-sampled t-test).

4.4 Acknowledgements and author contributions

Parts of the work presented in this study are adapted from the manuscripts (* indicates co-first authors):

1. “Invariant Odor Recognition with ON-OFF Neural Ensembles” by S. Nizampatnam*, L. Zhang*, R. Chandak*, J. Li, B. Raman, PNAS, 2022
2. “Dynamic contrast enhancement and flexible odor codes” by S. Nizampatnam*, D. Saha*, R. Chandak*, B. Raman, Nature Communications, 2018
3. “Neural manifolds for odor-driven innate and acquired appetitive preferences” by R. Chandak and B. Raman, in review.

We would like to thank Ina Chen for assistance in collecting the behavior data in Fig. 4.15.

D.S. collected the data in Fig 4.1, S.N. collected the data in Fig 4.2 and trained the classifier in Fig 4.6. R.C. collected all the behavioral data and performed all the analyses. R.C. and B.R. co-wrote this study. This research was supported by NSF (1453022, 2021795) and ONR (N00014-19-1-2049, N00014-21-1-2343) grants to B.R.

Chapter 5: Neural recordings in moving and behaving insects: from neuroscience to engineering applications

5.1 Introduction

Olfactory encoding has primarily been studied in different insect systems under well-controlled laboratory settings. These setups typically involve complete immobilization of the insect, often including the removal of external (appendages) and internal (digestive system) sources of perturbations, as well as precise and well-characterized delivery of odorant stimuli (square-wave odor pulses). The strict control of variables in this approach has informed our understanding of how insects, including locusts, may perform essential tasks such as odorant identification and discrimination to guide their behaviors. However, it remains to be seen whether the principles uncovered in the laboratory are still applicable in more naturalistic settings.

In a typical laboratory experiment, the antennae are restrained to limit any movements and the stimuli are delivered directly onto them in stereotyped on-off square pulses controlled via highly precise automated systems^{23,171,172}. While it minimizes extraneous noise, this approach precludes the insect's ability to actively move its antennae using well-characterized flicking and sweeping motions that create localized turbulences in the odor stream¹⁷³. This method of active sensing is odor-specific¹⁷³ and hence, limiting this ability may obfuscate our understanding of how odor detection is performed in natural settings. Moreover, natural odor sources are rarely encountered as sharp on-off pulses, but rather as volatile plumes with varying concentration gradients¹⁷⁴. Whether the encoding principles observed in the pulsatile scenarios are also

applicable in detecting more chaotic encounters remains to be seen. In this study, we develop novel, minimally-invasive neural recording methods that allow us to study odor-coding while preserving the ability of locusts to actively sense their environment using their antennae.

In Chapters 3 and 4, we determined the nature of mappings between neural response patterns in the antennal lobe and overall olfactory preferences. However, in these experiments, different sets of locusts were used for the behavioral and neural studies. How reliable and robust are the conclusions drawn using this approach? To answer this, we develop an experimental approach that allows us to monitor neural activity in locusts as they are trained to associate odorants with food rewards (as in Chapter 4). We will assess if our proposed ‘neural manifolds’ approach of encoding for innately appetitive and non-appetitive odorants is also observed in this less invasive approach and if so, whether the neural-behavioral transformations are perturbed as we classically condition locusts. Additionally, the innate olfactory preferences reported in Chapter 3 were assayed using immobilized locusts. Whether the results obtained in such stationary preparations are also observed in more realistic, mobile assays remains to be investigated. In this study, we will assay olfactory preferences in more naturalistic settings and make advances towards recording neural activity from freely moving locusts as they are exposed to different odorants in a two-choice assay.

We began by developing a stable and robust minimally invasive recording technique to allow long-term monitoring of antennal lobe neural activity in tethered locusts with freely moving antennae. We classically conditioned locusts while acquiring PN responses to a panel of appetitive and non-appetitive (from Chapter 3) odorants. Our results indicate that the manifold-based organization of odor-responses we proposed is conserved in naïve (before conditioning) locusts and that reinforcing odorants enhances the separability of these latent structures (after

conditioning). Next, we demonstrated the feasibility of recording neural activity from freely moving locusts. We validated our approach by designing a simple two-choice behavioral arena and found that locusts show similar preferences to odorants in this assay as those reported in Chapter 3. Finally, we applied these novel recording techniques to demonstrate how the locust can be used as a biological sensor to recognize explosive chemicals. In sum, these results show the efficacy of our novel recording techniques and indicate that neural coding approaches and behavioral preferences appear to be conserved as we move towards untethered experiments.

5.2 Results

5.2.1. Minimally invasive neural recording technique

We began by developing a stable and robust minimally invasive recording technique to allow long-term monitoring of antennal lobe neural activity in tethered locusts with freely moving antennae. An overview of the procedure is illustrated in **Fig 5.1**. Locusts were tethered at the neck to allow stable access to their brain while their antennae were left free to move. A small incision was made in their cuticle and the air sacs above the brain were cleared to allow access to the antennal lobe. Next, a metal wire was inserted below their brain to minimize mechanical noise from the movements of their limbs and digestive tract. Finally, the layer of glial cells above the antennal lobe was removed (i.e., the brain was de-sheathed), recording electrodes were inserted, and a reference wire (Ag/AgCl) was placed proximal to the brain. This entire process was optimized to take approximately 15 minutes, making it significantly faster than fully invasive techniques that can require up to 2 hours.

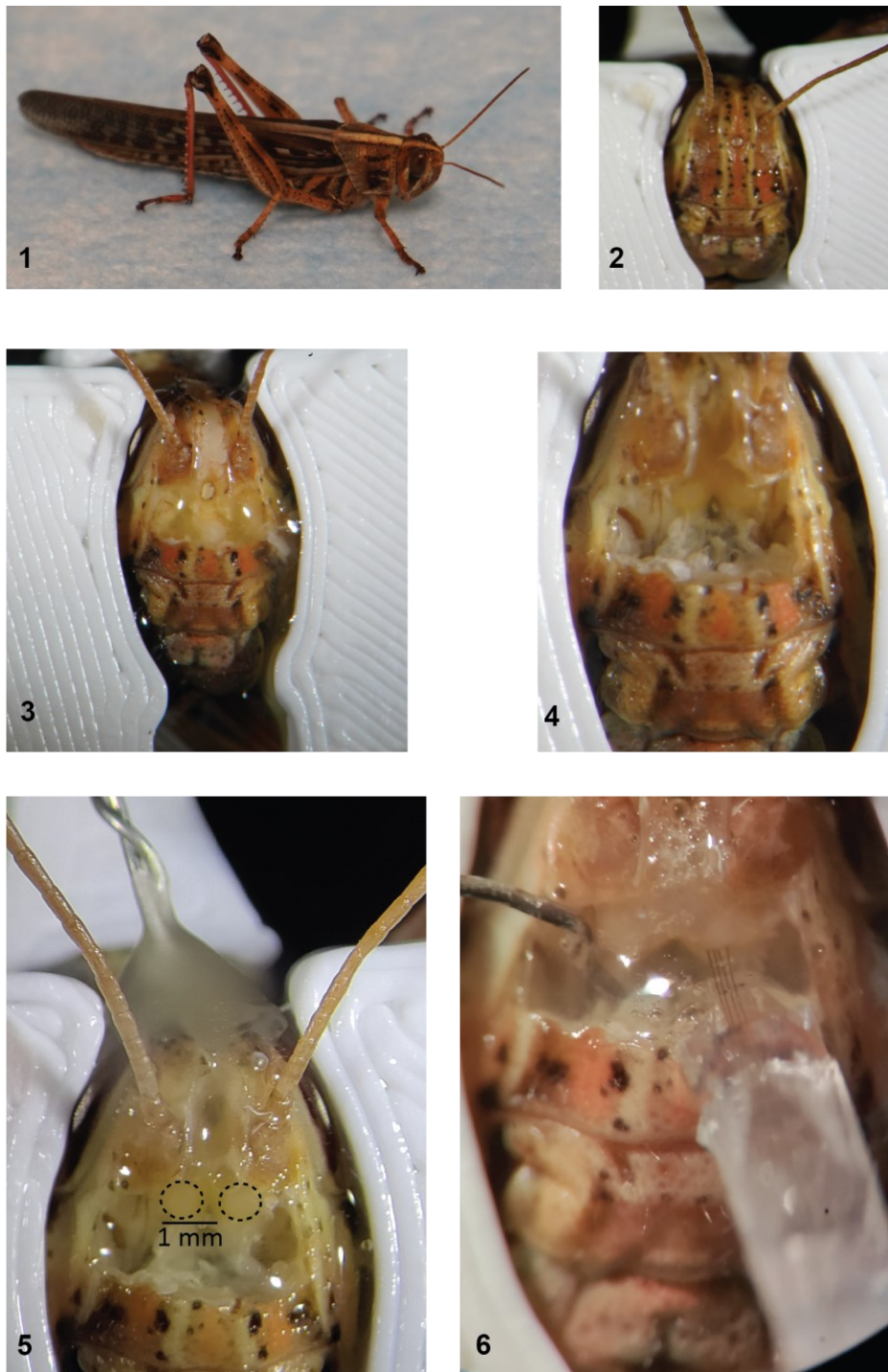


Figure 5.1: Minimally invasive surgical technique

The key steps involved in performing our minimally invasive surgery are illustrated. We begin by attaching intact locusts (1) to a custom 3D-printed manifold by tethering them at the neck region (2). A small incision is made in the cuticle (3) and the air sacs covering the brain are removed (4). To minimize noise from mechanical movements of the limbs or digestive tract, we attach a metal wire platform (5)

below the brain and secure it to the cuticle using wax. Finally, the antennal lobe is de-sheathed, recording electrodes are inserted into the brain, and a reference wire is placed proximal to the brain (6).

We designed custom tetrodes that would allow us to sample a large proportion of the antennal lobe simultaneously. Each electrode channel in the tetrode was a NiCr alloy wire with an impedance in the range of 3-4 M Ω and the spacing between wires was kept between 40-60 μm to span across most of the width of the antennal lobe (average diameter of $\sim 400\mu\text{m}$) (Fig 5.2a).

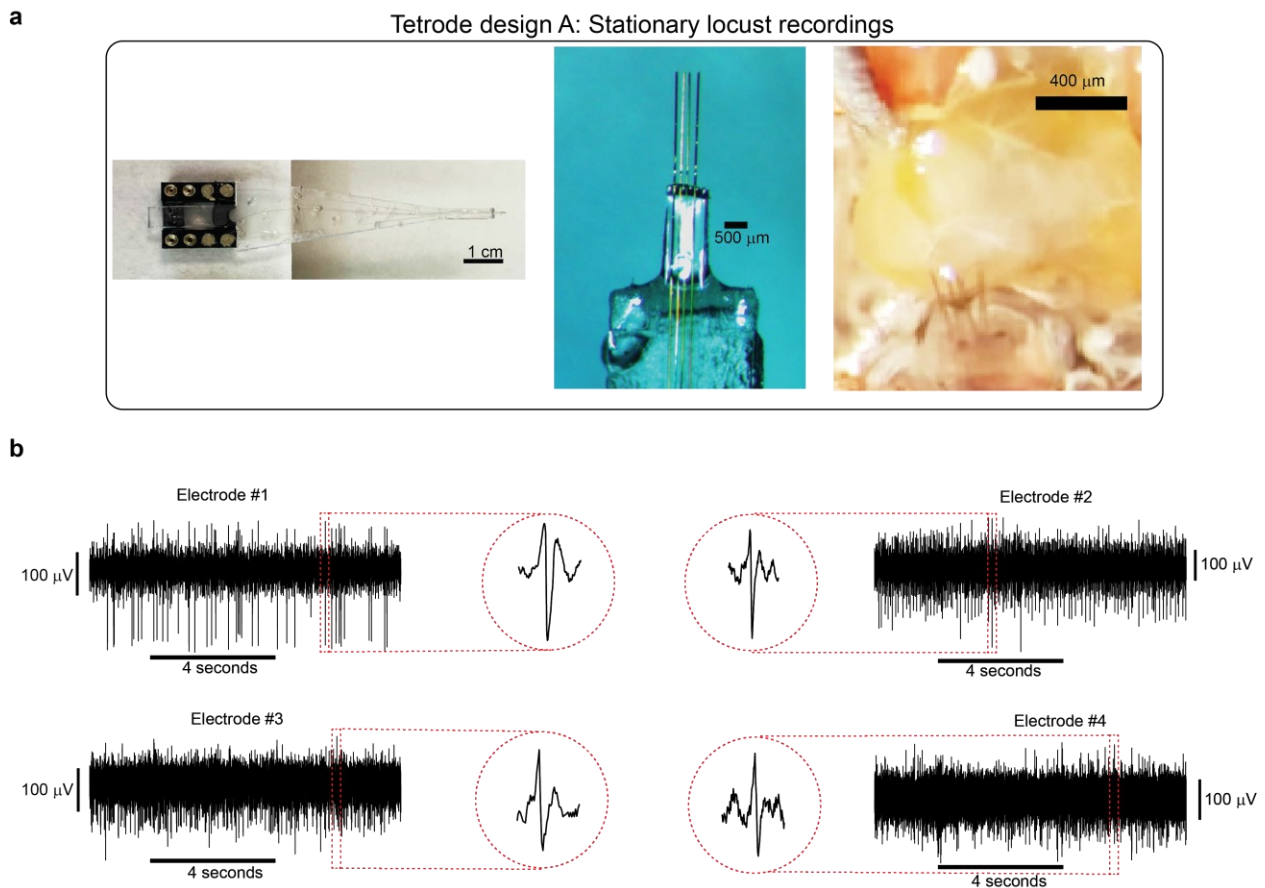


Figure 5.2: Custom tetrodes for minimally invasive recordings

a) Tetrode design A used for recording neural activity in stationary minimally invasive recordings. These electrodes were designed to span a large proportion of an antennal lobe using 4 independent NiCr wires (see Methods) with impedances in the 3-4 M Ω range.

b) Sample neural response traces. Sample neural response traces recorded simultaneously from a set of 4 electrodes (1 tetrode) from a single locust. Raw voltage traces showing distinct neural signals recorded from four electrodes (tetrode design A) on the same tetrode. All four channels pick up action potentials as

shown by the zoomed insets, and they are unique, as can be seen in the overall voltage traces as well as the insets.

The signals recorded from these electrodes were unique (**Fig. 5.2b**) and our overall preparation allowed the monitoring of antennal lobe activity over long periods of time (**Fig 5.3**), with strong odor-evoked responses observed for multiple hours after electrode implantation.

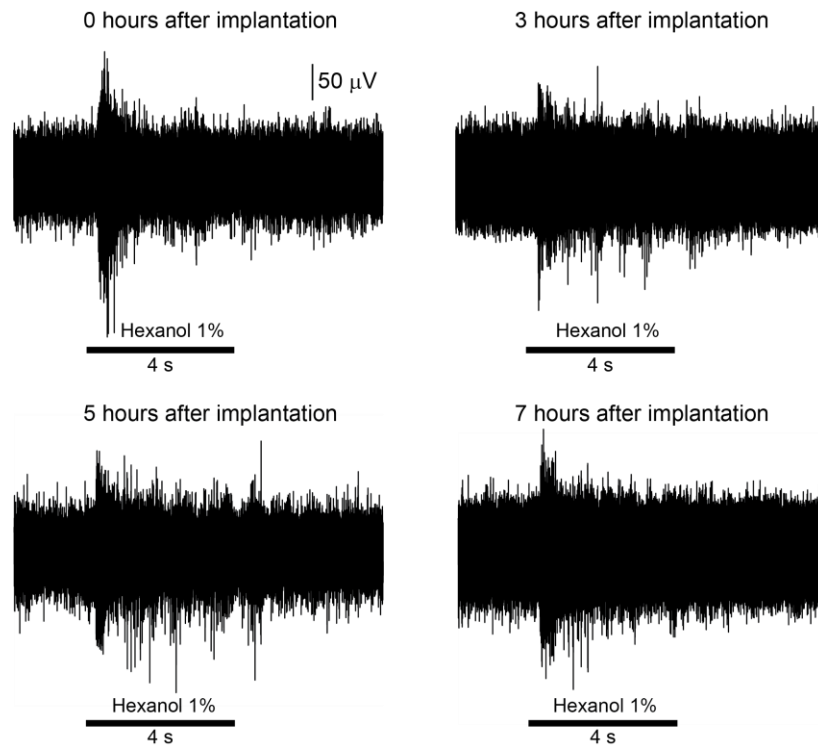


Figure 5.3: Long-term acquisition of odor-evoked signals

Neural responses to presentations of hexanol are shown as raw extracellular signals at four time points after electrode implantation (0 hours, 3 hours, 5 hours, and 7 hours) into the antennal lobe after minimally invasive surgery.

5.2.2 Effect of appetitive conditioning on odor representation

We wanted to understand how associative learning can affect the representation of innately appetitive and non-appetitive odorants at the level of antennal lobe projection neurons (PNs). For conditioning assays reported in Chapter 4, grass was used as the food reward and was

presented to the locust manually during the training phase. However, since the locust antennal lobe is located in close proximity to its mouthparts, this approach would compromise the acquired signals by inducing noise artifacts through the chewing of the grass as well as through motion of the experimenter. Hence, we switched to sugar water as a liquid food reward (glucose 1g/10 mL in water solution), which could be accepted by the locust without chewing, and be delivered in an automated fashion.

To ensure that sugar water is an appropriate unconditioned stimulus to induce palp-opening responses (PORs), we first performed a set of control experiments similar to the protocol in Chapter 4 (**Fig 4.3**). Hexanol was used as the conditioned stimulus for both ON-training and OFF-training (2 s gap) paradigms. Our results (**Fig 5.4a**) show that sugar water can also be used to induce PORs for hexanol in naïve locusts, and locusts trained under the OFF-training paradigm display delayed responses during the testing phase relative to ON-trained locusts (**Fig 5.4b**). These results indicate that sugar water could be substituted for grass for our proposed set of experiments.

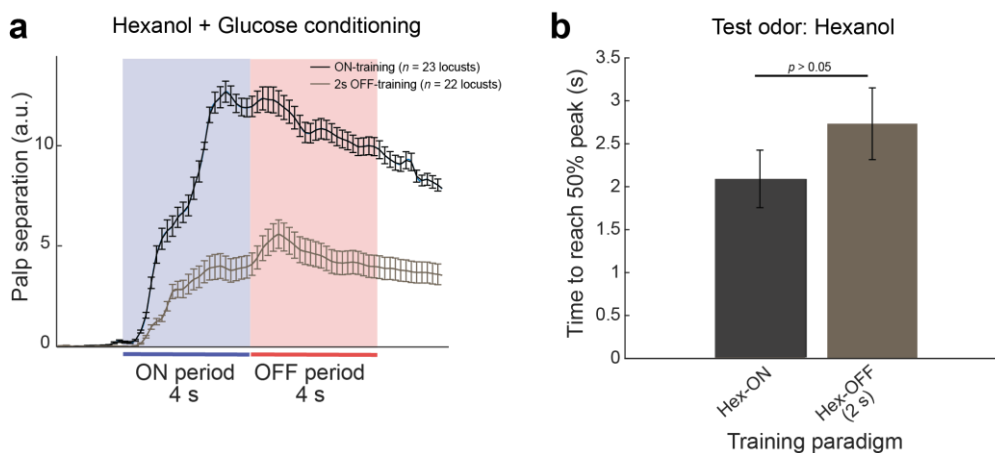


Figure 5.4: Using glucose as a food reward for appetitive conditioning

a) Results from conditioning experiments where glucose was used as food reward and hexanol was used as the conditioned stimulus are shown. We trained two sets of locusts, using both ON-training and OFF-

training paradigms (see Methods and Fig 4.3), and then tested them for POR responses to hexanol in an unrewarded phase. The mean (\pm s.e.m.) responses for both sets of experiments are shown and the blue bar indicates 4 s of odor presentation. Results from both paradigms are similar to grass-trained experiments (Chapter 4), with ON-trained locusts producing faster and stronger responses on average.

b) Latency of locust PORs to hexanol during the test phase are shown. Response latency here is defined as the time taken by locusts to reach 50% of the peak palp separation (time = 0 along the y-axis indicates odor onset). Each bar plot shows the mean latency across locusts, and error bars indicate s.e.m. These results are similar to those reported in Fig 4.10.

The setup used for the minimally invasive conditioning experiments is shown in **Fig 5.5a**.

Using the minimally invasive technique, a recording probe was inserted into the antennal lobe and a reference was placed just outside the lobe, an odorant line was placed near the antennae, and a tube to deliver sugar water was placed near the mouthparts. Note that for these set of experiments locusts were placed in small tubes to prevent their legs from displacing the food delivery system. Prior to the training phase, we recorded PN responses to a panel of 6 odorants – 3 appetitive (hexanol, isoamyl acetate, 2-octanol) and 3 non-appetitive (cyclohexanone, benzaldehyde, citral). Each stimulus was presented for 5 repetitions in a pulsatile fashion, with each pulse lasting 4 s, and the inter-pulse-interval was set to 56 s. The signals acquired from these experiments could not be reliably spike-sorted using the same approach as in previous Chapters and led to a loss of information. Instead, we used a recently published protocol⁹⁴ to extract the energy of the acquired signals by filtering and converting them to their root-mean-squared (RMS) values (see Methods). A brief schematic of how we performed this signal processing is illustrated in **Fig 5.5b**. We then performed conditioning using hexanol and benzaldehyde as the conditioned stimuli for two sets of 10 locusts using the ON-training protocol. After the training phase, we recorded PN responses to the same panel of 6 odorants as before.

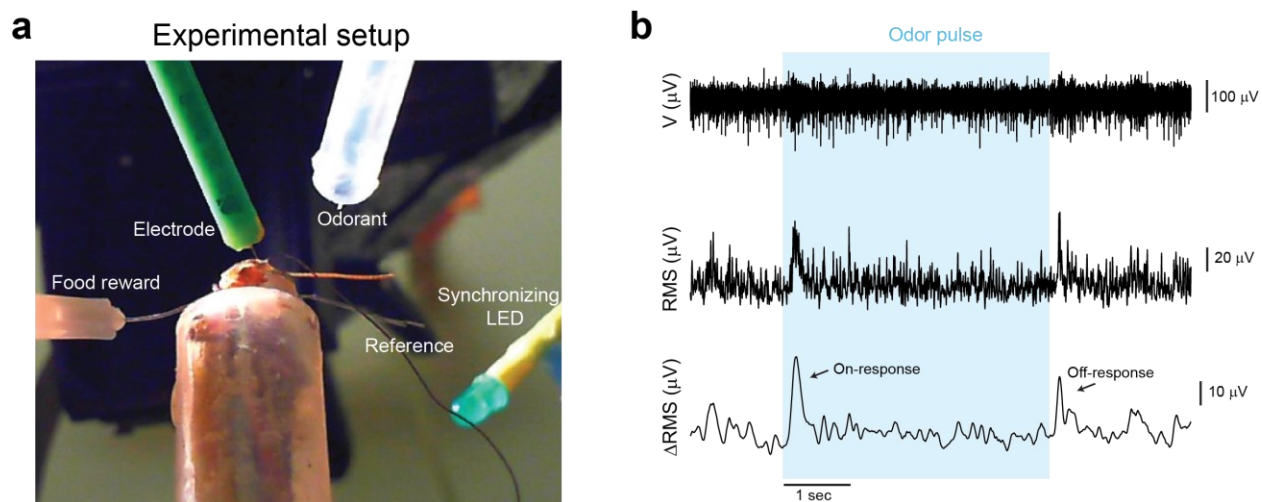


Figure 5.5: Simultaneous neural recordings and appetitive conditioning assay

a) The experimental setup for training locusts and monitoring their PN activity is shown. A small incision was made in the locust cuticle, a recording electrode was placed in the locust antennal lobe, and a reference (Ag/AgCl) wire was placed just outside. An automated sugar water (glucose 1g/10 mL water solution) dispenser was placed near the locust mouthparts, and a tube presenting the training odorant and carrier air stream was directed to both antennae.

b) A schematic showing the signal processing pipeline. The raw voltage traces were converted to a Δ RMS signal in 50 ms time-bins after smoothing and baseline subtraction (see Methods). Colored rectangle indicates 4 seconds of odor presentation. Increases in the RMS signal at the onset (on-response) and offset (off-response) of the stimulus can be seen, indicating stimulus-evoked ON and OFF responses.

To quantify the net effect of conditioning, we compared the PN responses prior to and after the training phase. Two sample sets of recordings obtained from these experiments are shown in **Fig 5.6a**. As can be seen, responses to odorants could increase, decrease, or remain unchanged after the training phase. In general, for individual experiments, we found the changes in responses to odors to be highly variable/unpredictable. Hence, we combined the results across all 20 conditioning experiments to obtain high-dimensional response matrices similar to PN recordings in Chapter 3 and performed PCA to visualize the population-level responses. Our results show that similar to **Fig 4.14**, appetitive and non-appetitive odorant responses were

organized to be primarily constrained in low-dimensional manifolds. Interestingly, prior to conditioning, these manifolds had considerable overlap (**Fig 5.6b**, left panel), but they became more separated after the training phase (**Fig 5.6b**, right panel). These results indicate that even in less constrained settings, PNs encode odorants in a similar manner as we observed in fully invasive preparations. While these neural responses cannot be directly mapped to behavior, the increase in separation between the appetitive and non-appetitive responses (as seen by the reduced overlap between the planes after conditioning) could be one potential mechanism by which naïve locusts (which did not produce any PORs) learn to perform PORs to appetitive odors after the training phase.

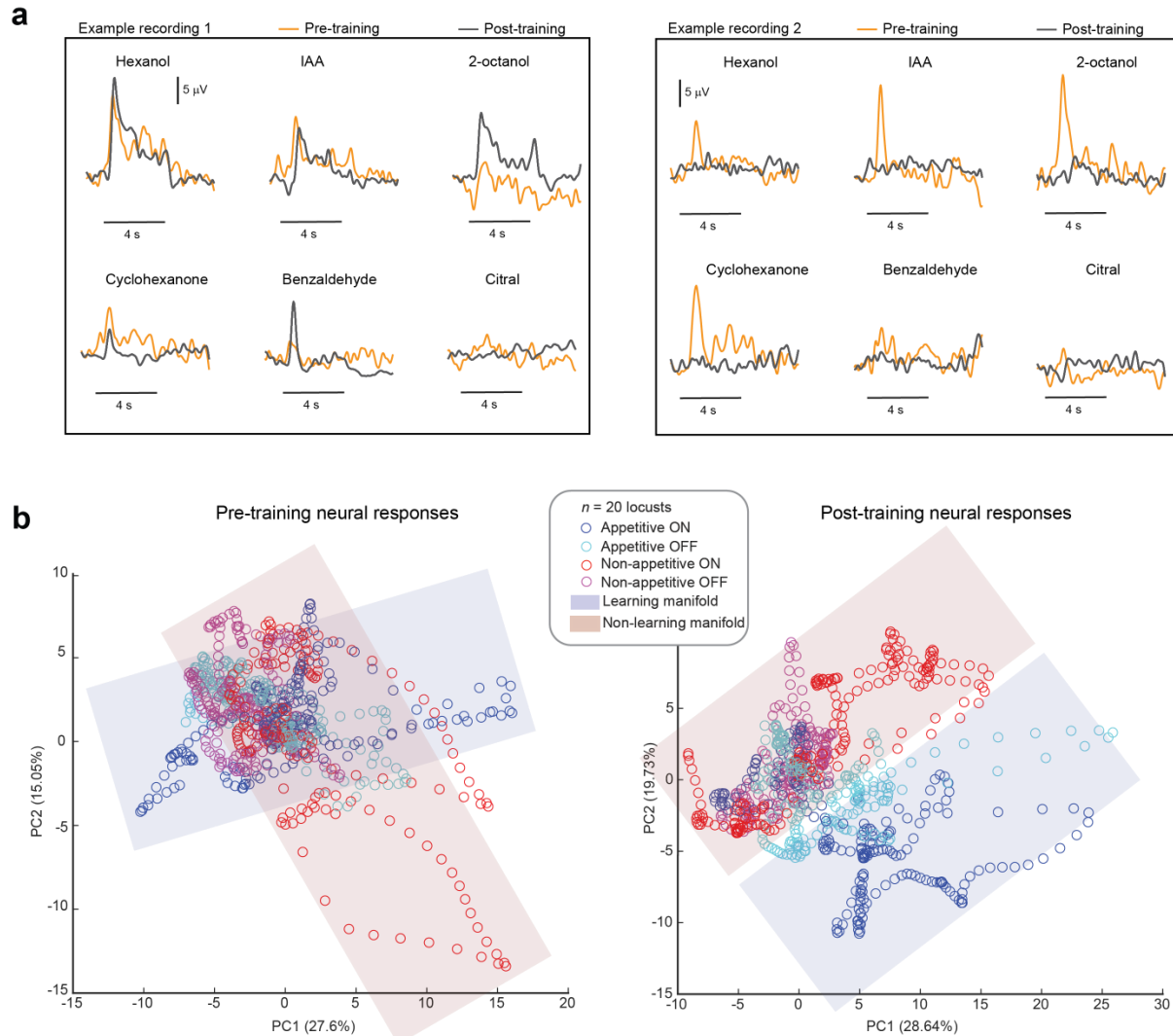


Figure 5.6: Neural response manifolds in behaving locusts

a) Representative recordings showing the average odor-evoked responses (see Methods) to the odor panel before (yellow) and after training (gray). In example 1 (left panel), hexanol was used as the training odorant, and in example 2, benzaldehyde was used as the training odorant (right panel). In each panel, the top row contains the appetitive odorants and the bottom row contains stimuli that were non-appetitive. Black bars below the plots indicate 4 s of odor presentation.

b) PCA visualization showing ensemble neural responses during both the ON- and the OFF- periods for all 6 odors are shown along the top 2 principal components ($n = 20$ locusts; see Methods). The data points were colored as follows: blue – appetitive odorants ON responses, cyan – appetitive odorants OFF responses, red – non-appetitive odorants ON responses, and magenta – non-appetitive odorants OFF responses. Variances in odor-evoked responses of appetitive odorants were not uniformly distributed but confined to a subspace and are schematically shown as using a linear plane (plane colored in blue that encompasses appetitive ON and appetitive OFF neural ensembles). Similarly, non-appetitive odorants

ensemble responses were confined to a distinct neural manifold schematically shown in red. Note that the two subspaces became less overlapping post-training (right panel versus left panel).

5.2.3 Neural activity in fully moving locusts

The innate olfactory preferences reported in Chapter 3 were assayed using immobilized locusts. Are behavioral results obtained in such stationary preparations also observed when a locust is freely moving? Do odorants evoke neural responses when they are encountered in more realistic plume-like presentations rather than sharp on-off pulses? To answer these questions, we adapted our minimally invasive technique to record neural activity in freely moving locusts.

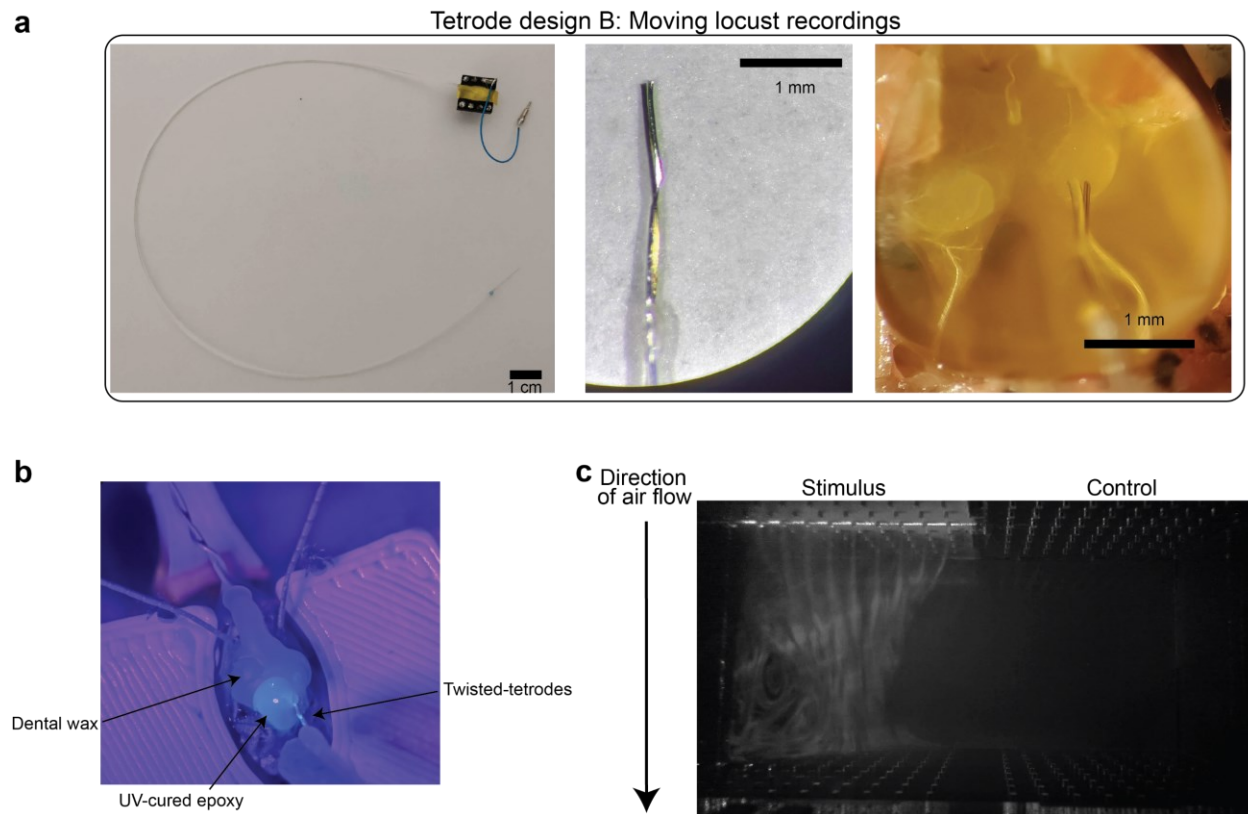


Figure 5.7: Setup for freely moving locust experiments

a) Tetrode design B used for recording neural activity in freely moving locusts. We adapted design A to a longer, more flexible tetrode to acquire PN activity from moving locusts. Similar to design A, we used four NiCr wires, but they were twisted together to provide greater mechanical stability. Additionally, the reference wire was also twisted with recording probes and placed into the antennal lobe to minimize mechanical noise artifacts during motion (rightmost picture).

b) We performed minimally invasive surgeries as described above and inserted the long, flexible tetrodes and reference wire into the locust antennal lobe. They were then secured in place using a combination of dental wax and UV-cured epoxy glue as shown here (under UV-light).

c) The behavior chamber used in walking experiments. We quantified the odor distribution dynamics using dry ice mixed in carrier air stream, and a laser light. Constant air was flown from the top to the bottom on both sides of the arena. The stimulus (dry ice in this case) was presented only to the left half and appears to be primarily contained to one side (more white smoke on the left side).

We designed longer, more flexible twister-wire tetrodes (**Fig 5.7a**; see Methods) using the same NiCr alloy wires as in **Fig 5.2**. After exposing the locust brain using the same minimally invasive technique as above, we implanted these tetrodes into the antennal lobe and covered the exposed cuticle with a combination of dental wax and epoxy glue (**Fig 5.7b**). Locusts were then released from the tether around their necks and moved into a behavioral arena (**Fig. 5.7c**) for a two-chamber exploration assay.

We used two chemical cues that were used across all previously reported results for ease of comparison – hexanol (innately appetitive) and benzaldehyde (innately non-appetitive). The behavior chamber was divided into two halves with independent and constant clean air flowing through two separate inlets. Odorants were pipetted onto KimWipes and placed in small chambers (**Fig. 5.8a**), and their vapors were introduced into the arena as air passed over them. Mixing chambers were designed to allow time for the odorant to diffuse uniformly into the air stream prior to introduction into the arena. Vacuum suction was placed beyond the arena to create a constant flow and clear out excess vapors, and the air flow rates were adjusted to ensure the odorant was primarily limited to one half of the arena (**Fig. 5.7b**). An overhead camera recorded the locust's movements while neural data were acquired using the same approach as above. An LED flash at the start of each recording was used to synchronize the neural and behavioral data offline.

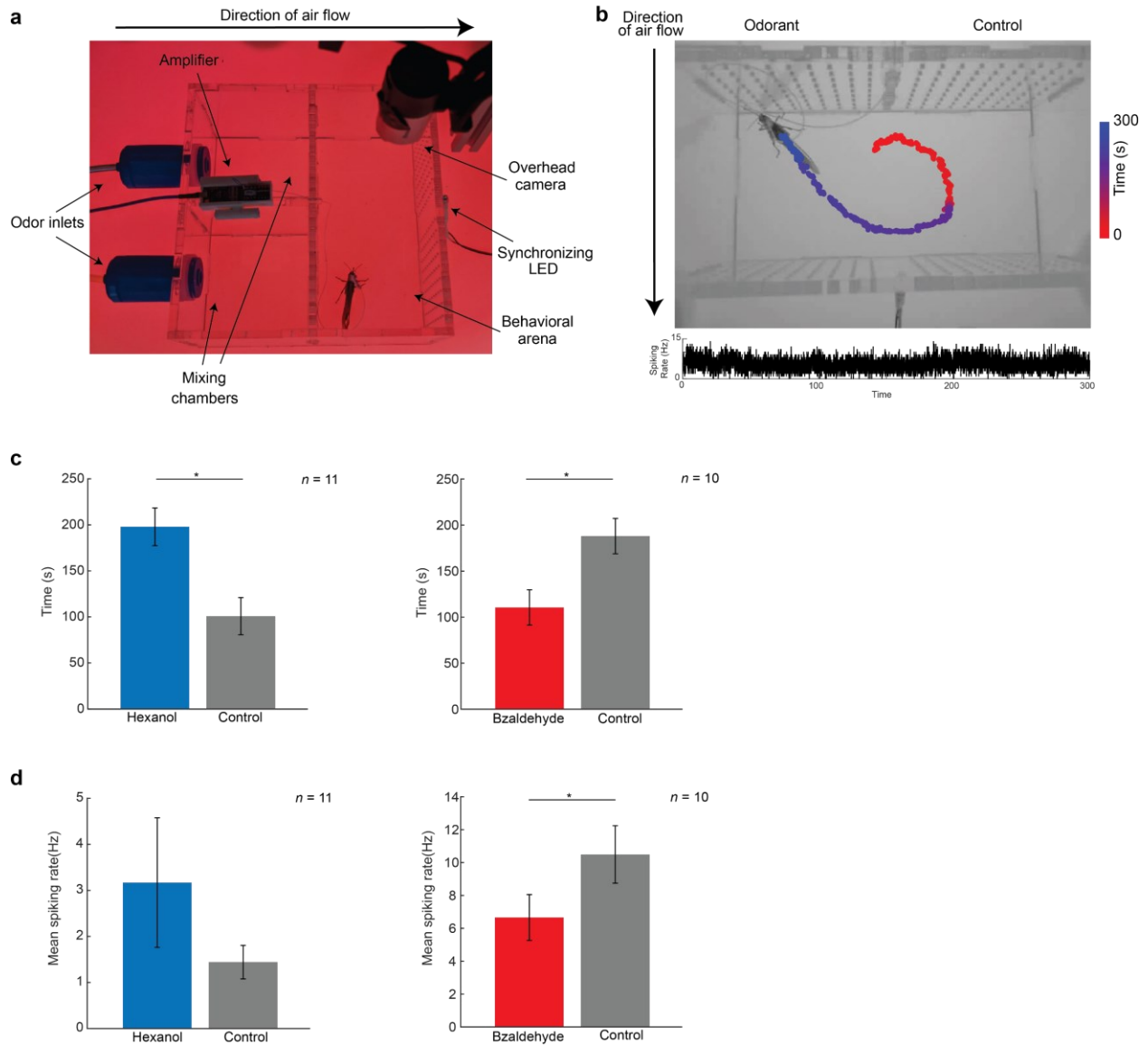


Figure 5.8: Neural recordings from freely moving locusts

a) Schematic showing a freely-moving locust implanted in the ‘behavioral arena’ with electrodes in its antennal lobe. A constant airflow was presented to both sides of the arena (entering from the left) and a vacuum suction (not visible) was placed beyond the right end to create constant flow. Odorants and control were introduced by pipetting them onto KimWipes placed in the ‘odor inlets’ and were allowed to mix with the background air in the ‘mixing chambers’ before being introduced into the arena. In each trial, the locust was placed at the center of the chamber and allowed to explore the arena for 5 minutes while its neural responses were recorded using the ‘amplifier’ and behavioral responses recorded using the ‘overhead camera’. The data were synchronized offline using a start flash signaled by the ‘synchronizing LED’.

b) Summary of a single 5-minute trial of a freely moving locust in the behavioral arena is shown. The top plot shows the arena as recorded by the overhead camera, with the position of the locust over time shown as dots going from red ($t = 0$ s) to blue ($t = 300$ s). The odorant was placed on the left half for this trial with the flow going from top to bottom. As can be seen, the locust starts in the center of the box, explores the control side (air stream with no odorant), and then moves into the side with the odorant. Bottom plot

shows the corresponding spiking rate recorded from the locust antennal lobe (see Methods) as a function of time.

c) Summary of behavioral responses (see Methods) recorded from locusts in the behavioral arena for two sets of experiments. Different sets of locusts were assayed for the behavioral preferences to hexanol (an innately appetitive odorant) and benzaldehyde (an innately non-appetitive odorant) in the behavioral arena while neural activity was recorded from the antenna lobe. In these plots, we show the average time spent by locusts in the halves containing the odorant and control, respectively. Locusts spent significantly more time near hexanol ($n = 11$ locusts) and away from benzaldehyde ($n = 10$ locusts) (* indicates $p < 0.05$, two-sampled t-test). Error bars indicate s.e.m.

d) Similar plots as **panel c**, but showing the average spiking activity recorded (see Methods) for the locusts in each set of experiments. Locusts had strong neural responses for hexanol compared to control but evoked significantly lesser responses when exposed to benzaldehyde. Error bars indicate s.e.m.

We performed multiple trials for the different odorants by randomly placing the odor in one inlet, with the other side serving as control. We then introduced the locust into the arena by placing it in the center and recording neural and behavioral activity for a period of 5 minutes. Note that to remove any visual biases, the arena was only dimly lit using a uniformly distributed array of red LED lights, which insects are primarily unable to see^{175,176}. The position of the locust over time was accurately tracked using a YOLOv4 convolutional neural network model (see Methods). As shown in **Fig. 5.8b**, we can see the locust start a trial at the center of the box, veer into the control half, and then spend time in the left half containing the odorant. Corresponding to the movement data, we also de-noised and extracted spiking events from the neural recordings (see Methods). In **Fig. 5.8b**, the bottom plot shows the spiking activity evolution for the corresponding trial.

The results from these set of experiments are summarized in **Fig. 5.8c, d**. Note that a different set of locusts was used for each odorant. For each trial, we compiled the time locusts spent on either side of the arena and computed the average spiking rate for the time spent in either half. We find that consistent with innate preferences obtained in stationary preparations, locusts preferred spending significantly more time near hexanol and away from benzaldehyde.

Interestingly, locusts also tended to have higher spiking activity when they were near hexanol (relative to control), whereas benzaldehyde appeared to reduce neural activity (relative to control), indicating that the odorants evoked unique neural responses.

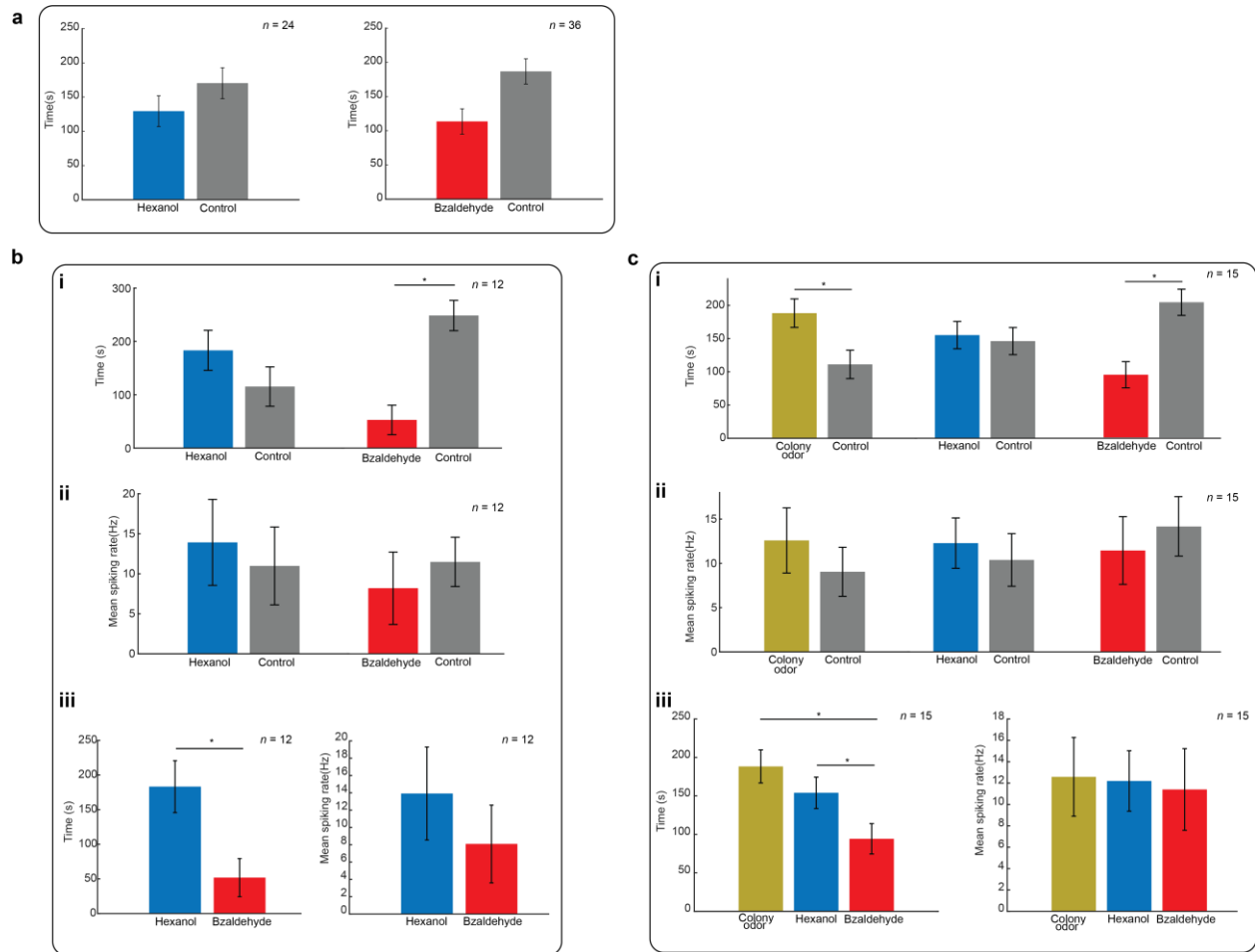


Figure 5.9: Controls for walking locust experiments

a) Locusts without surgical implantation of electrodes were used in two-choice assays using hexanol ($n = 24$ locusts) and benzaldehyde ($n = 36$ locusts) as the stimuli. The average time spent in each half is shown. Error bars indicate s.e.m. On average, locusts spent relatively more time near hexanol (130 seconds) vs benzaldehyde (113 seconds).

b) We performed similar walking locust experiments ($n = 12$ locusts) as in **Fig 5.8**, but tested the same locust using both hexanol and benzaldehyde as stimuli. The order in which the odors were presented was randomized for each locust. **i**) Locusts spent relatively more time near hexanol vs control but lesser time near benzaldehyde vs control. **ii**) On average, time spent in the hexanol half elicited stronger neural activity vs control. Benzaldehyde appeared to reduce spiking activity vs control. **iii**) Same results as **panels i** and **ii**, but only plotted for the odorants for comparison purposes (* indicates $p < 0.05$, t-test).

c) Similar results as **panel b**, but for locusts ($n = 15$) tested on three stimuli – colony odor, hexanol, and benzaldehyde.

Given the novelty of the assay and recording technique, we also performed multiple sets of control experiments to ensure the robustness of our results. Could our surgical methods have diminished or limited the locusts' olfactory sensing capabilities and alter their behavioral preferences? To control for this, we conducted these two-choice assays on a set of locusts with no surgical manipulations performed and found that these locusts also preferred to spend more time near hexanol relative to benzaldehyde (**Fig 5.9a**). We used different sets of locusts for each odor for results reported in **Fig. 5.8c, d**. To control for potential differences in behavioral preferences and neural responses across individuals, we collected two additional datasets where each locust was presented all the odorants in the panel (**Fig 5.9b, c**). For one dataset, we used hexanol and benzaldehyde as the odors, and for the second dataset, we used hexanol, benzaldehyde, and a colony odor (see Methods)¹⁷⁷. For both experiments, we found our results for time and spiking activity for hexanol and benzaldehyde to be similar to those in **Fig. 5.8c, d**. Taken together, these experiments helped validate our experimental approach and showed repeatability of our results across multiple datasets.

5.2.4 Explosive detection using minimally invasive recordings

Next, we wondered if our minimally invasive technique (**Fig 5.10a**) could be applied to solve a real-world problem of detecting explosive chemicals. For this set of experiments, we selected 6 chemicals of interest (**Fig 5.10b**). These chemicals have extremely low volatilities, and hence delivering them in their vapor phase to the locust antenna can be challenging. We placed small amounts of each chemical in independent bottles with an inlet and outlet, and placed the bottles in a water bath maintained at 50C. To deliver the chemical vapors, we simply pulsed clean, desiccated air into the bottles through the inlet and obtained vapors through the

outlet. This allowed us to deliver pure chemical vapors, and added only one additional control – a heated empty bottle to deliver ‘hot air’. Each stimulus was presented for 5 repetitions in a pulsatile fashion, with each pulse lasting 4 s, and the inter-pulse-interval was set to 56 s. Given the physical distance between the wires on these new electrodes, we again were unable to reliably spike sort without heavy loss in information. Hence, we used the RMS-based signal processing protocol described above to analyze this dataset. A sample set of neural responses collected from 1 recording electrode to all the odorants in the panel is shown in **Fig 5.10c**. Each curve is the average Δ RMS signal obtained in response to repeated presentations of the different chemicals over the five trials. Note that there are strong responses at the onset of three of the chemicals – TNT, DNT, and pATP, as well as moderate responses at the termination of TNT and pATP.

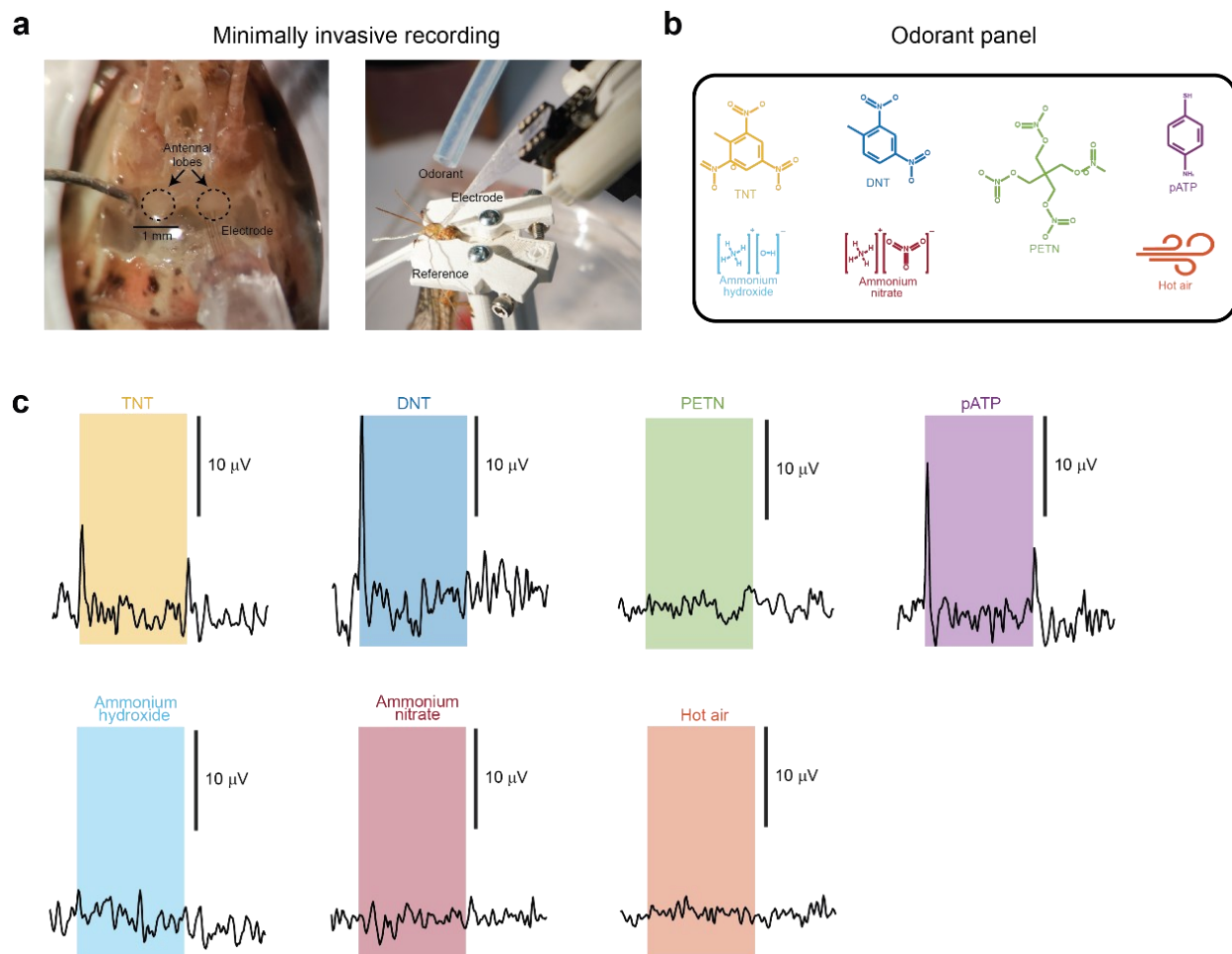


Figure 5.10: Minimally invasive procedure to record PN responses to different explosive chemicals

a) We applied the minimally invasive technique to implant custom-made tetrodes in the locust antennal lobe to record extracellular PN activity. In the left picture, the antennal lobes, tetrode wires, and reference electrode can be seen. In the right picture, an overall view of the recording setup including stimulus delivery can be seen.

b) The different explosive/precursor chemicals used in the odor panel are shown. Each of the 6 chemicals was heated to 50C prior to being presented and hence we also added hot air as a control stimulus.

c) A representative set of responses to all the stimuli used in the odor panel recorded from a single electrode are shown. Each stimulus was presented for 5 repetitions, the signals were converted to Δ RMS as shown in **Fig 5.5b**, and a mean across the trials was taken to obtain a single Δ RMS curve for each stimulus. Colored rectangles indicate 4 seconds of stimulus presentation. As can be seen, different stimuli evoked different levels of responses at both the onset and offset of the chemicals. In particular, TNT, DNT, and pATP elicited strong on-responses but with varying strengths, whereas the other stimuli had negligible responses relative to baseline activity.

How stable and unique are these responses to the different stimuli? To answer this, we recorded responses to the odorant panel from 12 electrode channels spread across 4 different locusts. To gauge the stability of the responses, we looked at the consistency of odor-evoked responses across all 5 repeated presentations of each chemical. We computed the average pairwise correlation across different trials for an odorant (see Methods) and found them to be highly correlated/consistent. The mean value for the distribution of correlations obtained for all such comparisons (**Fig 5.11a**, orange distribution) was 0.82, indicating that odor-evoked responses were very stable and repeatable across trials. To measure the uniqueness of responses, we computed similar pairwise correlations, but across the mean odor-responses for different odor pairs. We found that on average, comparisons of responses for different odors had a correlation of 0.40 (**Fig 5.11a**, blue distribution), which we found to be significantly lower than the within-odor correlations ($p < 10^{-50}$, two-sampled t-test). These results show that our novel surgical and recording methods were able to elicit stable as well as unique responses to different chemicals.

How distinct or separable are the odor responses? To visualize the high-dimensional data ($n = 12$ electrodes or dimensions), we performed principal component analysis (PCA) to reduce the dimensionality of the data to just the top three eigenvectors capturing the maximum variance. The result of this analysis is shown in **Fig 5.11b**, where each dot corresponds to a single 50 ms time-bin, and the different colors indicate different stimuli, as indicated by the corresponding colored text labels. The responses for each chemical appear to cluster into well-separated regions in this 3-D space. To help visualize this, we also fit a Gaussian distribution to each odor's responses and plotted the resulting 3-D ellipse using the same color convention. The PCA clusters indicated that odor responses were quite distinct. To quantify this, we used a quadratic discriminant classifier (see Methods) to accurately classify each time bin to its corresponding

odor. The results of this analysis are shown in **Fig. 5.11c**, where we show a confusion matrix of results from this classification approach. The confusion matrix appears largely diagonal, indicating that most of the target odorants were accurately identifiable, with an average accuracy of over 70%. Note that the chance level of accuracy for a naïve classifier would be 1-in-7 or approximately 14%.

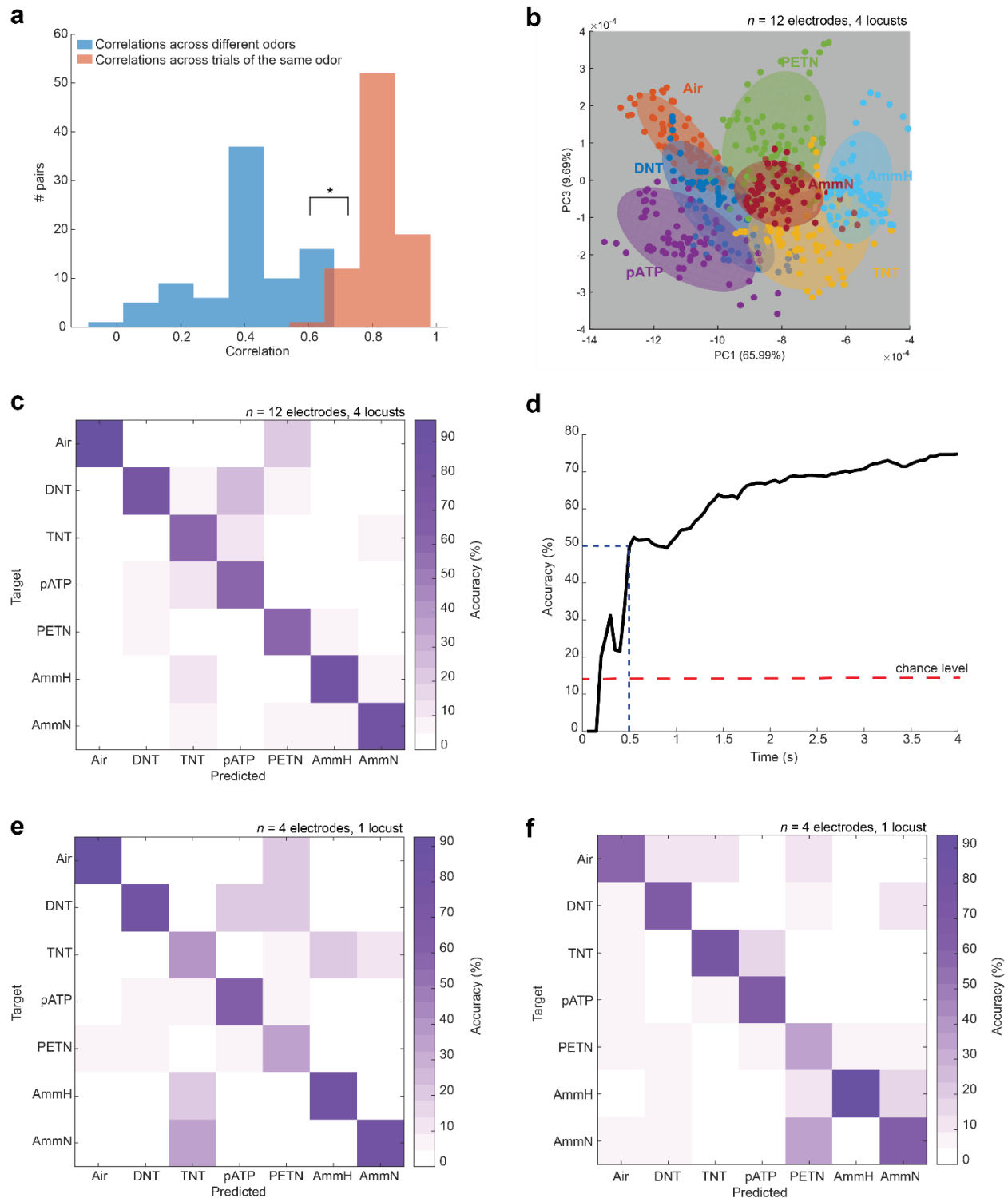


Figure 5.11: Neural responses can be used to decode chemical identity

a) The distribution of average pair-wise correlation of responses to a stimulus across five trials (see Methods) is shown in orange. The correlations are clustered around 0.8, indicating that the responses to a stimulus are robust and repeatable across trials. The distribution of pairwise correlations of mean responses to different odors is shown in blue. The correlations are clustered around 0.4, indicating a

weaker similarity across odors vs between repeated presentations of the same stimulus (orange distribution). The two distributions were found to be significantly different ($p < 10^{-50}$, t-test).

b) Clustering of neural responses ($n = 12$ electrodes from 4 locusts) after PCA dimensionality reduction is shown for all 7 stimuli (see Methods). Each colored dot indicates a 50 ms time-bin during the odor presentation period, and the identity of the stimulus is indicated using the same color. A Gaussian ellipse was fit to each cluster corresponding to an odorant and is plotted using the same color as the stimulus for visualization purposes. Note that the odors appear to form well-separated clusters in this reduced space.

c) Confusion matrix showing the results of fitting quadratic discriminants (see Methods, $n = 12$ electrodes from 4 locusts) to the odorant responses after PCA analysis. The y-axis shows the target labels, and the x-axis shows the predicted labels. Note that the matrix is primarily diagonal, indicating that each target stimulus can be accurately predicted from its neural responses.

d) Curve showing the performance of the quadratic classifier as a function of increased duration of neural responses used for training. We computed the accuracy of predictions for each odor (diagonal values along the confusion matrix) and the average accuracy across all 7 classes is shown for each time point. As can be seen, the accuracy of the classifier increases as more data is provided for training. The performance accuracy exceeds chance levels (indicated in red; 1-in-7 or 14%) within 250 ms and reaches 50% in 500 ms.

e) Similar plot as in **panel c** but using only data from 4 electrodes recorded from an individual locust.

f) Similar plot as in **panel c** but using only data from 4 electrodes recorded from a different locust.

The results shown in **Fig. 5.11c** were obtained using all 4 seconds of odor-evoked responses. However, it is well-established^{22,23} (also refer to rasters in **Fig 3.3c**) that PNs in the antennal lobe can start responding to an external cue within hundreds of milliseconds. Thus, we wondered how the accuracy of the classifier would look like if we systematically altered the amount or duration of odor responses used to fit the discriminants. To test this, we trained the model using n bins (n ranging from 4 to 80; 4 being the minimum requirement of the classifier) of size 50 ms each, and then tested the accuracy of classifying all 80 bins of data. The results of this approach are shown in **Fig. 5.11d**, where we found that the accuracy of this approach increased as more data was used to learn the parameters. Remarkably, however, the classifier reached above-chance levels of performance within the first few hundred milliseconds and achieved 50% accuracy using just the first 500 ms of data.

Could neural responses from a single locust be used to detect and classify these different chemicals? We designed our new recording tetrodes to allow recording from up to four distinct regions within a single antennal lobe. For two locusts in our experiments, we were able to successfully pick neural activity on all four of these electrodes simultaneously (**Fig 5.2**). We used data from these sets of recordings to test the capabilities of our tetrodes as well as single locusts in solving this identity decoding task. We repeated the discriminant classifier analyses as described above, but using only data from single locusts where all four channels picked up neural activity. The results of these analyses (**Fig. 5.11e, f**) show that even 4 channels from a single locust can successfully classify chemicals well above chance levels (values along diagonals > 35% for all chemicals for both classifiers; chance level = 14%).

Finally, we wanted to test if locusts displayed any behavioral preferences for explosives (chemicals typically not encountered by locusts). We performed recordings in freely moving locusts by introducing ammonium hydroxide into the behavioral arena. Similar to benzaldehyde, locusts appeared to significantly prefer spending time away from ammonium hydroxide, but unlike benzaldehyde, maintained a higher spiking activity when nearer to it (relative to control).

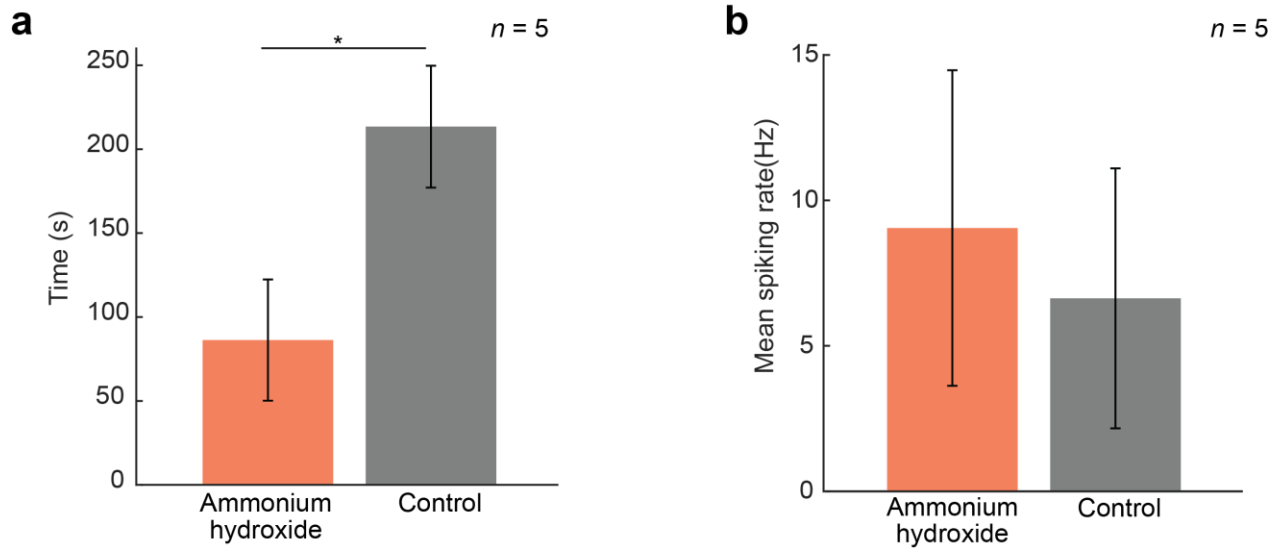


Figure 5.12: Freely moving locust responses to an explosive precursor

a) Similar plot as **Fig 5.8c**, but for ammonium hydroxide. Locusts spent significantly more time away from ammonium hydroxide ($n = 5$ locusts).

b) Similar plot as **Fig. 5.8d**, but for ammonium hydroxide. Despite spending lesser time near the odorant, locusts had stronger neural responses when near ammonium hydroxide relative to control.

5.3 Discussion

How do classical conditioning assays drive changes in behavioral preferences? *In vivo* imaging of insect brains monitoring odorant responses before, during, and after associative learning has implicated higher centers of processing such as the mushroom body (directly downstream from the antennal lobe) in driving the observed behavioral changes. Indeed, the mushroom body is believed to be the primary center of the insect brain that is responsible for forming and maintaining memories^{178–180}. However, recent studies indicate that we could observe reinforcement-induced changes at the level of the antennal lobe itself. In moths, olfactory conditioning was shown to recruit additional neural responses in the antennal lobe¹⁸¹. Odor representation was also altered in the projection neurons of *Drosophila* during positive reinforcement assays¹⁸², while in honeybees, injection of a neuromodulator into the antennal lobe was shown to affect memory formation¹⁸³. In this study, we applied our newly developed

minimally invasive surgical protocol to test the validity of our manifold-based organization of odor responses and to gauge the effect of classical conditioning on odor responses in the locust antennal lobe.

Using a panel of six odorants (3 appetitive and 3 non-appetitive) we observed PN responses in naïve (untrained) locusts to organize similarly to the structure obtained in Chapter 4 (Fig 4.14). Interestingly, this organization was altered after conditioning assays to decrease the overlap between the appetitive and non-appetitive manifolds while still constraining odor-responses primarily to these latent structures. At the neural level, this indicates a reduction in the amount of overlapping PNs that respond to odorants from both groups – potentially informing how naïve locusts with no behavioral responses to appetitive odors can produce PORs after being conditioned. Whether this phenomenon is achieved via suppression of commonly activated PNs or through recruitment of additional uniquely responsive PNs as a consequence of conditioning remains to be tested. Additionally, due to the duration of the overall experiment, we were limited to studying six odorants. Whether these results are observed more generally (such as 22 odors in Chapters 3-4) or are specific to these chemicals also remains an open question.

Next, we adapted the procedure to allow the locust to fully recover, move and sample its environment while we continued to monitor its neural responses. Our results indicate that behavioral preferences obtained from stationary locusts are also observed in freely moving locusts. We recorded the movements of the locusts and tracked their position using a deep learning framework to allow fast inference and validated the overall approach by collecting multiple datasets using traditional biological chemicals. This protocol can be further enhanced in future iterations by using machine learning and 3D pose estimation algorithms to classify idiosyncratic behavioral motifs of locusts in response to chemicals in their surroundings such as

antennal flicking and grooming, which can provide an additional axis of chemical readout^{88,89,184-188}.

These initial sets of experiments indicate that odor encoding patterns appear to remain conserved as we move from fully invasive preparations with fixed antennal positions to minimally invasive techniques with actively sampling antennae. The new procedure not only minimizes harm to the locust, but is also significantly faster to perform (~2 hours for fully invasive vs. 15 minutes for minimally invasive procedure). Hence, we next wanted to use this preparation to solve a real-world chemical detection problem. Combined with the fabrication of tetrodes that allow monitoring activity from distinct regions of the antennal lobe, we showed that even a single locust could be used to classify six different chemicals of interest within hundreds of milliseconds. These results, combined with the long-term stability of our preparations (up to 3 days shown in **Fig. 5.13**) open up the potential for applying our approach to develop low-cost, minimal-maintenance chemical detectors with applications in homeland security and environmental monitoring¹⁸⁹⁻¹⁹³.

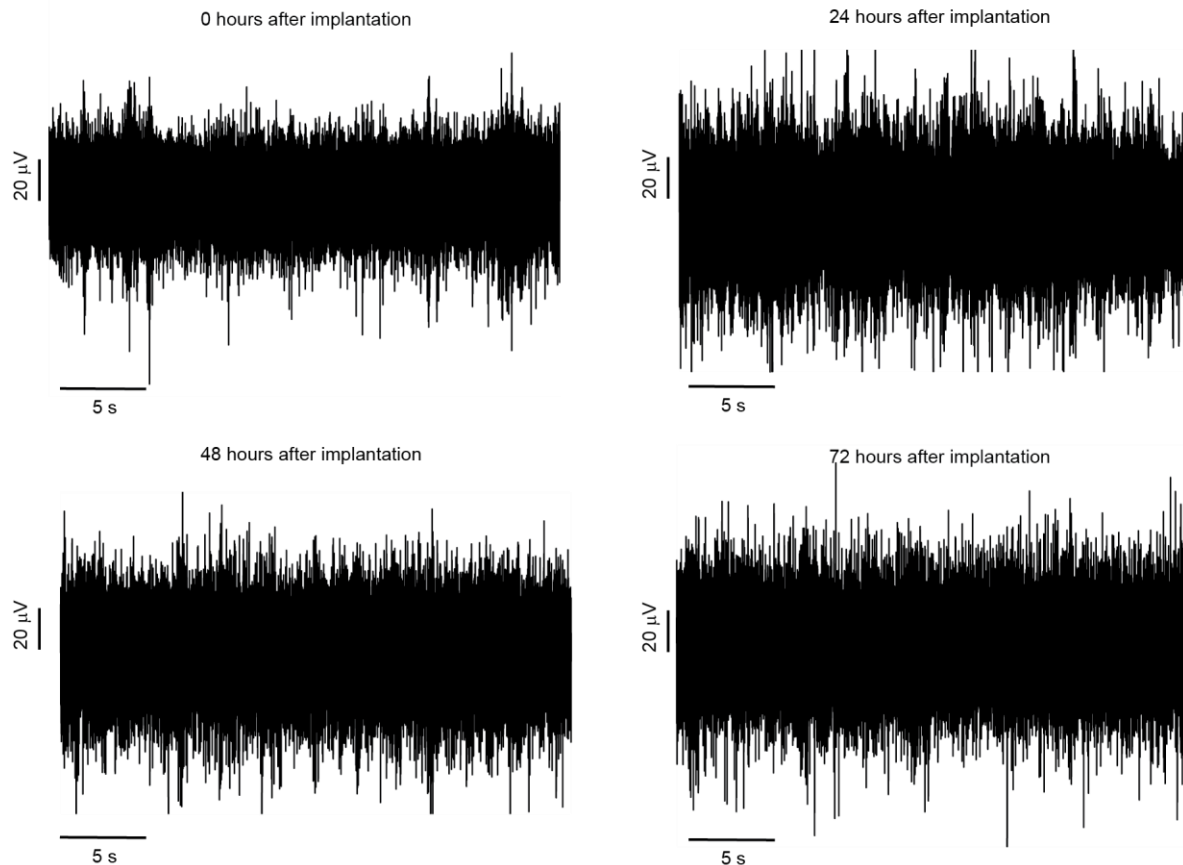


Figure 5.13: Long-term recording from walking locusts

Spiking activity recorded from a single freely moving locust recorded at 4 time points – 0, 24, 48, and 72 hours after electrode implantation.

5.4 Acknowledgments and author contributions

We would like to thank Michael Traner, Avishek Debnath, and Grayson Derossi for their contributions to this study. R.C and M.T. co-developed the minimally invasive surgery and designed the tetrodes. A.D. helped fabricate tetrode design A. G.D. helped design the behavioral arena and perform control experiments in Fig 5.9a. R.C performed all other experiments and analyzed all the datasets. R.C and B.R co-wrote this study.

This research was supported by Office of Naval Research grants (N00014-16-1-2426, N00014-19-1-2049) to B.R.

Chapter 6: Conclusion

Understanding how the brain encodes for stimuli to drive appropriate behavioral responses is a fundamental goal of neuroscience. In this work, we aimed to gain an understanding of the organization of olfactory information in the locust antennal lobe and how it relates to innate and acquired behaviors. We developed novel experimental approaches to validate the robustness of our results as we move from tightly controlled laboratory settings to more naturalistic scenarios. Finally, we demonstrated how these tools can be applied to solve real-world challenges such as the detection of explosive chemicals.

6.1 Summary of findings

We began by assaying the innate appetitive preferences of locusts to a panel of chemically diverse and biologically relevant odorants. Understanding these appetitive preferences is important since innate behaviors are genetically encoded in an organism and are a direct consequence of evolution. For locusts, the fast and accurate determination of whether an encountered stimulus is favorable or harmful is key for survival. We used a well-characterized behavior, the palp-opening response (POR), to classify odorants as being innately appetitive or non-appetitive. By pooling results across multiple locusts, we obtained a range of preferences where a green-leaf volatile found in the food locusts consume was classified as the most appetitive odorant, whereas a chemical used in pesticides against locusts was classified as being least appetitive. Our attempts to explain these results as a consequence of our experimental design or the chemical features of the stimuli proved unsuccessful, and hence, we hypothesized that the locust olfactory pathway must be playing an active role in producing these results.

To test this, we probed projection neurons (PNs) in the locusts' antennal lobe using extracellular electrophysiological recordings to observe their responses to all the assayed odorants. Once again, we pooled results from multiple locusts to obtain PN responses from a large fraction of neurons in the antennal lobe (~10% of all PNs). Each odorant evoked strong excitatory responses across multiple PNs when it was presented (i.e., an ON response). The subsets and number of neurons that were activated varied across stimuli. However, at the population level, we found that the subsets of PNs that were activated by odorants with similar innate valence had significant overlap. We wondered then if neural responses from PNs could be used to make predictions about an odorant's behavioral outcome. We found that a simple linear classifier that was trained to predict an odorant's behavioral outcome from its neural responses produced results that correlated strongly to observed behavioral results. These results indicate that computations in the locust antennal lobe produce PN responses that are encoding for the onset of stimuli in a valence-dependent manner.

Projection neurons have been shown to produce responses not only at the onset of stimuli but also at their offset (i.e., OFF response). These OFF responses tend to be almost as strong and spatiotemporally diverse as ON responses, but their exact functional role remains to be elucidated. We found PNs to elicit strong responses at the termination of all odorants in our dataset. Different subsets of PNs were activated by different odorants, and there was minimal overlap between the subsets of PNs that responded to the onset and offset of an odorant. We applied our linear classifier approach to predict behavioral outcomes using the OFF responses of PNs and found surprisingly accurate predictions, indicating that these bouts of activity are also information-rich. We confirmed that the two classification approaches used were not redundant and were combining information across PNs using very dissimilar weighting schemes. These

results indicate that computations in the locust antennal lobe produce PN responses that are encoding for the onset and offset of stimuli in a distinct yet valence-dependent manner.

In a small subset of PNs, the odor-evoked ON or OFF responses were highly correlated with innate preferences. Could these individual neurons be sufficient to encode the preferences of all stimuli (akin to the ‘labeled-line’ approach discussed in Chapter 1)? Individual PN responses to encounters of the same stimulus under different perturbations were found to be highly variable. The ambient humidity conditions and recent history prior to encountering a stimulus altered how PNs responded to an odorant (hexanol). However, we found that locusts could produce robust behavioral responses to the odorant under the same perturbations. Hence, while we cannot definitively rule it out, we deem it extremely unlikely that individual PNs could be used to encode such amounts of information. Instead, we propose a flexible coding approach, which does not rely on any fixed sets of PNs to produce behavioral outputs. Briefly, this approach requires activation of only subsets of neurons in response to different encounters of a stimulus (any ‘m’ activated neurons in an encounter out of ‘n’ total responders when the stimulus is encountered solitarily; $m < n$). Classification results using this scheme and combining activity from both ON- and OFF-responsive PNs produced behavioral predictions that were highly correlated with observed results. Taken together, these results provide insight into how the antennal lobe network could encode for the onset and offset of stimuli to signify their valence and how the information-rich OFF-responsive neurons could contribute to producing behavioral dynamics.

During the behavior experiments, not all locusts produced PORs to an odorant. We wondered then if we could apply an appetitive conditioning assay to induce PORs in locusts that originally did not respond to a stimulus. We attempted to condition locusts to both appetitive and

non-appetitive odorants by pairing them with food rewards. Locusts produced PORs to appetitive odorants after conditioning, but no responses could be induced for non-appetitive odorants. Interestingly, the learned responses for an appetitive odorant appeared to generalize to other appetitive odorants. Moreover, locusts conditioned on non-appetitive odorants also produced responses to appetitive odorants during the test phase.

Finally, given that the ON- and OFF-responsive PNs for an odorant appear to have minimal overlap, we wondered if delaying the food reward till after odor termination would produce differences in learned responses. Indeed, the pairing of the offset of appetitive odorants with food rewards significantly delayed behavioral responses, indicating that not only the identity of the stimulus but the temporal delay could also potentially be conditioned. The efficacy of this offset-conditioning weakened as the gap between the stimulus and food reward was extended, with almost no learning observed in locusts trained with the longest gap. This result served as an in-built control that our assay was not simply producing trivial innate responses upon sufficient encounters with an odorant and that pairing the conditioned stimulus sufficiently closely with food rewards was essential. Indeed, the lack of any increase in responses to non-appetitive odorants (even to their innate levels) also refutes this potential pitfall.

For these behavioral experiments, we trained a deep neural network to accurately track the position of the locusts' palps over time. This allowed us to make comparisons pertaining to the strength and efficacy of the learned responses to different odorants as well as the temporal delays introduced by delaying the food reward during training. Using linear models (with added sparsity constraints) we found that responses from only half the PNs we recorded from were sufficient to faithfully capture the behavioral results obtained across all paradigms.

Finally, we visualized the ON and OFF PN responses evoked by all odorants using a dimensionality reduction technique (PCA). In this latent 3D space, we observed two planes (neural manifolds) along which the odor-evoked response trajectories appeared to align. Trajectories that lay on/were closer to the first plane appeared to be for innately attractive odorants and locusts could be trained to respond to them, whereas trajectories on/near the second plane were for odorants that were innately less attractive, which locusts could not learn to respond to. These results were further validated using a clustering analysis, which produced similar results using the high-dimensional data (information from all recorded PNs).

The results thus far were obtained from different sets of locusts used in behavioral and electrophysiological experiments, precluding any causal links. Additionally, we wanted to understand if the results we observed in tightly controlled experimental settings would still be conserved as we tested locusts in more realistic/practical scenarios. To address these concerns, we first developed a novel surgical method that allowed us to probe PN responses while the locust retained full movement of its limbs and antenna, and could continue to accept food. Next, we demonstrated that sugar water (glucose) is an effective food reward to induce PORs through conditioning. These advances allowed us to perform conditioning assays in locusts while recording the activity of their PNs.

We conditioned locusts using both appetitive and non-appetitive odorants. In order to gauge the effects of this assay at the neural level, we recorded PN responses to a panel of odorants prior to and after the conditioning. We observed that prior to conditioning, the PN responses in naïve (untrained) locusts organized into similar neural manifolds as our earlier results (appetitive and non-appetitive). This indicated that odor representation principles in this less restricted protocol agreed with those observed in fully invasive preparations. Interestingly,

after conditioning, we found the neural manifold structure to remain conserved, but the appetitive and non-appetitive manifolds became segregated and were almost non-overlapping. At the neural level, this implied that the PN responses for appetitive and non-appetitive odorants became less correlated. Whether these results were due to commonly activated neurons becoming suppressed, or as a result of new uniquely responding PNs being recruited due to conditioning remains to be tested. However, these results do indicate a potential mechanism by which conditioning can alter innate odor representation in the antennal lobe. Whether these alterations drive the gain in POR responses after conditioning and the generalization of POR responses across multiple similarly encoded stimuli remains to be elucidated. Further experiments using different conditioning odorants as well as a larger panel of test odorants would also be useful in estimating how generalizable these preliminary results are.

Next, we wondered if locusts implanted with electrodes could freely move around, explore, and detect chemicals in their surroundings. This would open up the potential for open-field studies and have applications in remote sensing and environmental monitoring. We modified our custom electrode design to make them longer and more flexible to allow locusts to freely move while implanted. We found locusts to recover very quickly (on the order of few minutes) after electrodes were placed in their antennal lobe and secured to their cuticle. After recovery locusts moved freely, and we were able to acquire stable neural activity over multiple days. A simple two-choice behavioral assay was used to validate this recording approach and to understand locust olfactory preferences in more mobile settings. We introduced odorants with strong innate behavioral and neural responses into one half of the behavioral arena (other half with just background air serving as control) and recorded the locusts' movements and neural activity. A deep neural network was trained and applied to allow fast and accurate inference of

the locusts' position in the arena. We found that consistent with our results from previous experiments where the locusts were stationary, locusts spent significantly more time closer to hexanol (innately appetitive) versus benzaldehyde (innately non-appetitive) and the spiking responses elicited near these odorants was also much higher for hexanol. These results were replicated in multiple datasets to ensure their robustness. Taken together, these results indicated that freely moving locusts with implanted electrodes were still able to produce unique behavioral and neural activity to different stimuli even when they were encountered in these more realistic (constant and plume-like vs periodic and pulsatile) scenarios.

The minimally invasive technique produced odor-evoked PN responses similar to those observed in traditional preparations. Not only was this preparation less harmful to the locust, but it was also significantly faster than fully invasive techniques (~15 minutes vs ~2 hours to prepare locust for electrode implantation). Hence, we wondered if this approach could be applied to solve a real-world challenge of detecting explosive chemicals (and their precursors). Using data from just 4 locusts, we found that locust PNs could produce highly discriminable responses to different chemicals of interest. A quadratic classifier trained to classify the chemicals produced results above chance levels within just 250 ms of odorant exposures, reached 50% accuracy in just 500 ms, and finally peaked close to 75%. By designing new electrodes that could sample PNs from distinct regions of the antennal lobe, we were able to produce well above chance level classifications using neural responses from just individual locusts. These results show how we can apply this new recording technique to use the locust's neural network as an inexpensive and efficient biological sensor. Finally, we tested an explosive precursor in the behavioral arena and recorded neural activity in freely moving locusts. Locusts behaviorally preferred to spend less

time near this chemical (ammonium hydroxide; compared to control) but still produced very strong neural responses when they were closer.

In this work, we gained an understanding about how the locust antennal lobe encodes for olfactory cues to facilitate quick and robust behavioral decisions. We demonstrated how results obtained from tightly controlled, invasive experiments are also observed in more realistic/practical experimental setups. Finally, using minimally invasive techniques, we establish the potential of locusts to be used as inexpensive, real-time sensors to detect chemicals at levels that are challenging for silicon-based counterparts. In the next section, I discuss how the experimental and analytical pipelines created to achieve these results can be further enhanced for specific applications.

6.2 Future work

6.2.1 Mechanisms in the antennal lobe

Neural recordings from PNs and preliminary results from ORNs indicate that information relayed from sensory neurons is re-formatted by the antennal lobe (AL) network to represent innate appetitive preferences for a diverse panel of chemicals. Intriguingly, the ORNs are not known to produce significant OFF-responses at the termination of stimuli, but our results show that OFF-responses across ensembles of PNs are generated for all stimuli and also contain valence information. The mechanism underlying how the AL network reshapes its input and how it produces stimulus-specific OFF-responses remains to be elucidated. In particular, the role of AL-intrinsic, inhibitory local neurons (LNs) is not well understood.

Similar to PNs, LNs have been shown to generate stimulus-specific responses. However, unlike PNs, these neurons do not fire full-blown sodium spikes, which can be recorded

extracellularly, but instead produce calcium spikelets. Additionally, the primary neurotransmitter they release is GABA, whereas PNs release acetylcholine. Given the current lack of genetic labeling tools in locusts, LNs are typically studied individually using intracellular recordings. Recent work has shown that LNs come in two flavors – those with high and low baseline activity levels¹⁹⁴. Whether one or both of these subsets are differentially activated for innately appetitive and non-appetitive odorants remains to be analyzed. Similar anatomical/morphological studies can also be performed in PNs to study their distribution in the AL as well as their downstream projections in the lateral horn and mushroom body. This can inform us if, similar to results in *Drosophila*¹⁹⁵, the locust AL also exhibits spatial segregation to encode for innately appetitive versus non-appetitive odorants.

6.2.2 The functional role of opponent PN ensembles

In Chapters 3 and 4, we demonstrated how population-level PN responses for appetitive and non-appetitive odorants aligned in different neural manifolds. Behaviorally, odorants aligning with the appetitive manifold produced more frequent innate POR responses and only these odors could be conditioned using reinforcement with food rewards to induce behavior. Here, we re-analyze these PN responses and observe the emergence of “opponent” subsets or ensembles.

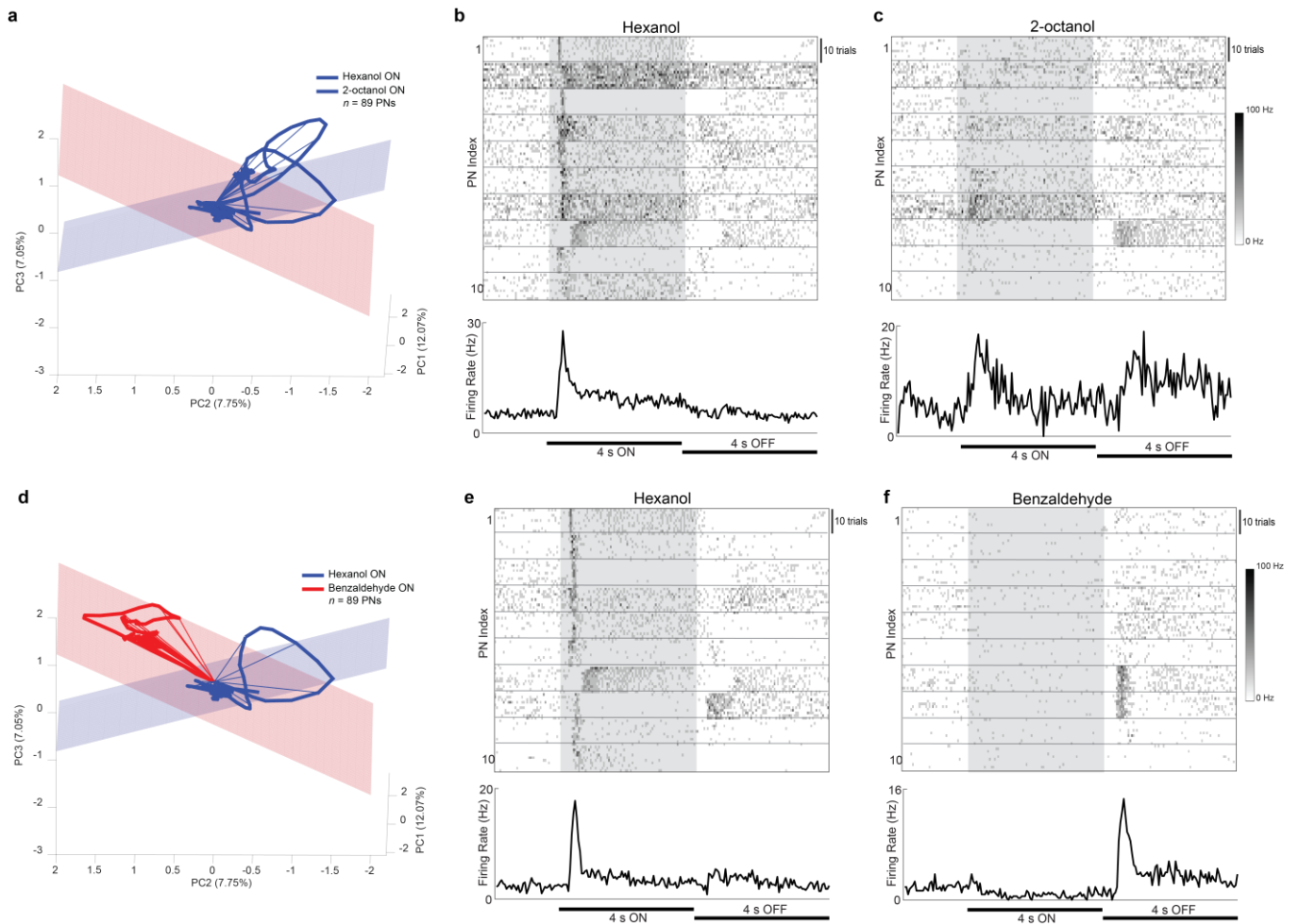


Figure 6.1: Opponent PN ensembles for behaviorally distinct odors

a) PCA trajectories of hexanol and 2-octanol (both appetitive) odorant responses re-plotted from **Fig. 4.14a**. Blue plane shows the learning manifold and red plane represents the non-learning manifold. The trajectories of both odorants lie close to the blue manifold and are similar to each other.

b) Raster plots showing the PN spiking activity across all ten trials for hexanol presentations in ten representative PNs (described in text). Gray rectangle indicates 4 s of odor presentations. Bottom plot shows the PSTH for these ten PNs with the ON and OFF periods indicated.

c) Similar plot as **panel b**, showing the responses of the same PNs but for 2-octanol.

d) Similar plot as **panel a** but for hexanol and benzaldehyde.

e) Raster plots for PN responses to ten trials of hexanol presentations in a different set of ten PNs. Similar convention as **panel b**.

f) Similar plot as **panel e**, showing the responses of the same PNs but for benzaldehyde.

We analyzed the PN responses for different odor pairs – some pairs belonging to the same category (i.e., both appetitive or both non-appetitive) and others containing one odorant

from each category. For each pair, we looked to extract the top ten PNs that had the most distinct responses for the two odors – i.e., the PNs that could discriminate between these odors the best. We achieved this by sorting the PNs based on the difference in average firing rates evoked by the two odors during the ON period – PNs with the highest difference would encode the two odors with the highest discriminability. Our results show that for odorants belonging to the same group, even the most discriminable PNs had similar responses. In **Figs. 6.1a-c**, we show the results for hexanol and 2-octanol, which are both innately appetitive (**Fig. 6.1a**). The activity across the top ten PNs with maximal differences in firing rates for these odors are shown in **Fig. 6b, c** (individual PN rasters for ten trials for each odor on top, PSTH for all ten PNs on the bottom). As can be seen, even these most unique neurons appear to be ON-responsive for both odors. In contrast, the results from comparing hexanol and benzaldehyde, two odors with different innate preferences are shown in **Figs. 6d-f**. Here, the most unique PNs appear to have contrasting responses, being primarily ON-responsive for hexanol, and OFF-responsive for benzaldehyde. These results were not unique for these odorants but were also found when comparing other pairs belonging to the same group (hexanol-hexanal, cyclohexanone-citral) and across groups (hexanal-linalool, cyclohexanone-isoamyl acetate). Taken together, these results indicate the existence of these “opponent” ensembles that are observed only when making comparisons between odors with opposing behavioral outputs.

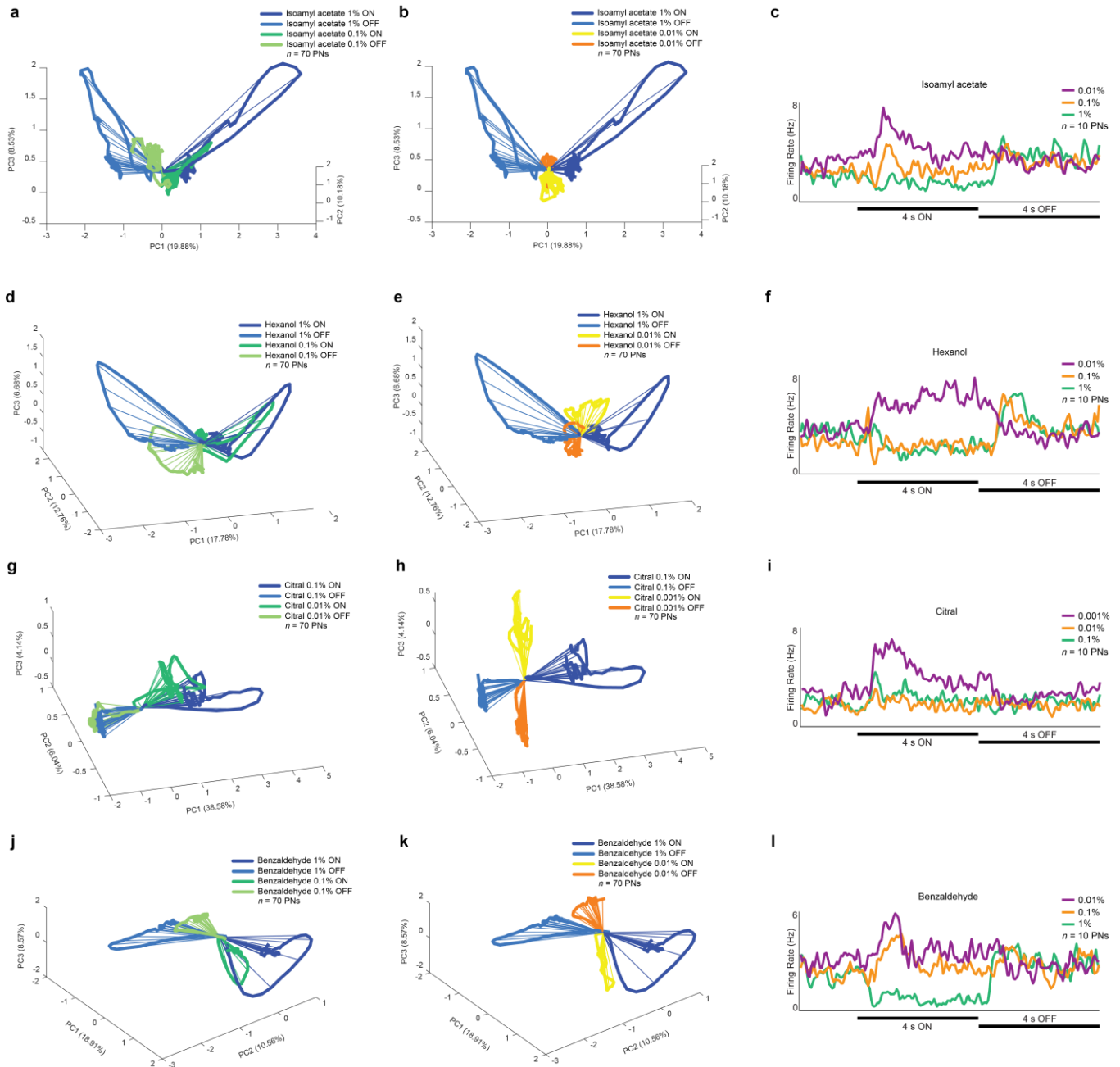


Figure 6.2: Concentration coding in PNs

a) PCA trajectories showing the ON- and OFF- response trajectories for *iaa* presented at two concentrations (1% and 0.1%; $n = 70$ PNs). The trajectories corresponding to the same odor period evolve in similar directions, indicating similar ensembles of PNs being activated. The length of the trajectories indicates the strength of the responses.

b) Similar plot as **panel a** but for iaa presented at 1% and 0.01%. Note that the yellow and orange trajectories now deviate from the higher-concentration trajectories, indicating a change in the underlying PN ensembles.

c) PSTH plots for representative PNs ($n = 10$) showing responses to 1%, 0.1% and 0.01% iaa. Note that the responses for the lowest concentration of iaa (0.01%, magenta) is significantly different from responses for the highest concentration (1%, green).

d-f) Similar plots as **a-c** but for hexanol at 1%, 0.1% and 0.01%.

g-i) Similar plots as **a-c** but for citral at 0.1%, 0.01% and 0.001%.

j-l) Similar plots as **a-c** but for benzaldehyde at 1%, 0.1%, and 0.01%. [Dataset in this figure was collected by Srinath Nizampatnam and re-analyzed by R.C.]

Are these opponent ensembles unique for this dataset or behavioral axis? We re-analyzed unpublished datasets from our laboratory where PN responses across multiple concentrations of the same odorant were recorded. For every odorant, we visualized PN ON- and OFF- responses across different concentrations (separated by one order of magnitude) using PCA. We observed that for the two closest concentrations, the ON- and OFF-trajectories evolved in similar directions, indicating that these concentrations were evoking responses across similar subsets of PNs. This is shown in **Fig 6.2 a,d,g,j** (left panels), where the blue and green trajectories align in similar directions. Interestingly, when making similar comparisons across PN responses for concentrations separated by two orders of magnitude, we see significant differences. Both the ON- and OFF-response trajectories for these two concentrations evolve in different directions, indicating a change in the subsets of PNs activated. This is shown in **Fig 6.2 b,e,h,k** (middle panels) where relative to the left panels, the blue trajectories are much more distinct from the yellow/orange trajectories for every odorant. For these odors, we looked for the top ten PNs which had the maximum discriminability for these different concentrations (**Fig 6.2**, right panels; similar as analysis in **Fig 6.1**). We observed that PNs that were strongly activated at the lowest concentrations (magenta curves) were primarily inhibited for the highest concentrations (green curves) and produced OFF-responses. Similar results were also observed when looking at

concentration-based responses in humid ambient conditions (**Fig 6.3**), indicating that this phenomenon may be conserved across external perturbations.

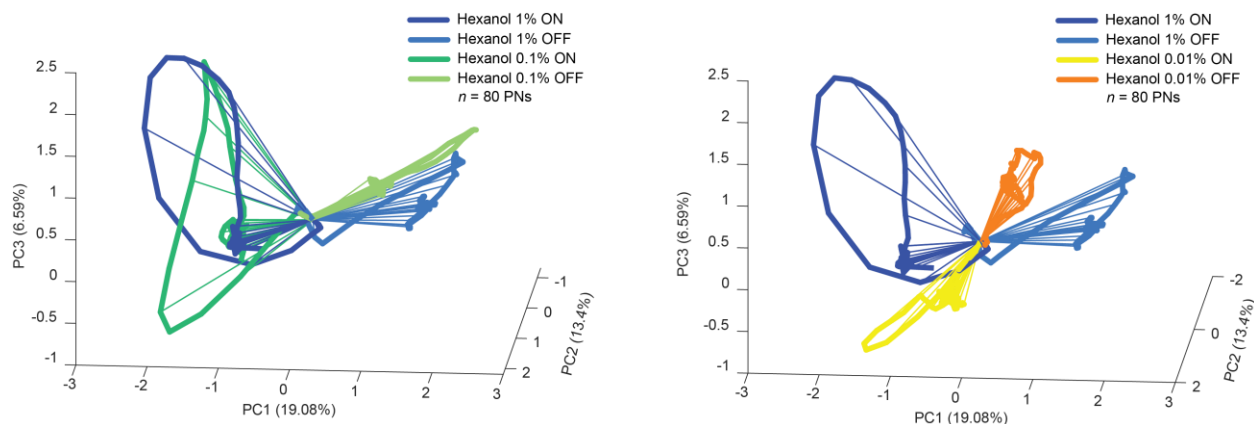


Figure 6.3: Concentration coding in humid ambient conditions

PCA plots showing hexanol responses for 1%, 0.1% and 0.01% hexanol ($n = 80$ PNs) recorded in humid conditions. Similar color convention as used in **Fig. 6.2**. 1% and 0.1% hexanol have much higher overlap compared to 1% and 0.01% hexanol responses, indicating a similar change in subsets of PNs encoding these concentrations as observed in dry conditions reported in **Fig 6.2**. [Dataset in this figure was collected by Srinath Nizampatnam and re-analyzed by R.C.]

These results are unintuitive if we extend the mechanism of concentration coding from the level of ORNs to PNs. At the sensory level, an increase in the concentration of a stimulus typically leads to a monotonic increase in the spiking rate of activated ORNs as well as the recruitment of additional ORNs^{196,197}. However, our results indicate that at sufficiently different concentrations, the ensembles of PNs that are activated are altered. Instead, these results are similar to those shown in **Fig 6.1** where nearby concentrations of an odorant are encoded similar to odors from the same innate group (both appetitive), whereas odors separated by two orders of magnitude are encoded similar to odors from different innate groups. Whether the behavioral responses at extreme concentrations are also switched similar to innate valence remains to be investigated – concentration-based changes in an odorant’s valence have been reported in

*Drosophila*¹⁹⁸, but the neural mechanism underlying those observations also remains unexplained. Additionally, whether this mechanism of encoding behaviorally different stimuli with opposing ensembles is a more generalized feature of the antennal lobe (such as for encoding acids vs. bases, pheromones vs. non-pheromones) is also an interesting direction for future work.

6.2.3 Understanding behavioral readout of olfactory inputs

In this work, we found that applying Pavlovian conditioning techniques could induce POR responses for innately appetitive odorants and not for non-appetitive odorants. However, these induced responses were not unique to an odorant but appeared to generalize to other innately appetitive odorants (hex-trained locusts responded to iaa and vice versa).

Can locusts be trained to selectively respond to only one chemical and not others (respond to hexanol but not to isoamyl acetate), or are learned responses always generalized? Differential conditioning is an adaptation of classical conditioning where two stimuli are presented during training but only one is paired with a food reward, with the goal being the selective reinforcement of one chemical versus another. Combining this approach with our minimally invasive recording techniques can be used to test whether learning in locusts is always generalized and how neural responses to rewarded and unrewarded odorants are uniquely affected through this paradigm.

Our classical conditioning results were obtained using four odorants – two appetitive and two non-appetitive. In Chapter 4, we also showed preliminary results when applying operant conditioning techniques to increase PORs to the same panel of four odorants. Extending these experiments to additional appetitive and non-appetitive odorants would be useful in demonstrating the robustness of the conclusions drawn in this work and understanding how these

two popular conditioning techniques produce similar or distinct results – including changes observed in odor coding at the level of PNs via minimally invasive recordings.

6.2.4 Real-world chemical detection using locusts

In this work, we demonstrated how PN responses can uniquely encode for different explosive chemicals within just hundreds of milliseconds. We developed a freely moving locust preparation that allows monitoring of PN responses as locusts explore a behavioral arena. Our results indicate that this approach does not appear to alter the innate olfactory preferences of locusts and can be used to record neural and behavioral activity across multiple days. Here, we discuss how these developments can be enhanced for practical applications such as open-field detection of chemicals of interest.

Our current recording apparatus comprises long and flexible tetrodes that are connected to an amplifier/recording computer using physical wiring. For open-field experiments, we could adapt this setup to a wireless neural acquisition system that can either transmit data in real-time with minimal loss/lag, or can log the data on-board for retrieval and offline analysis. This would require the design of lightweight amplification systems that can be directly mounted on the back of the locust – given the payload carrying capacity of locusts and the physical recovery observed after electrode implantations, this approach should be feasible with sufficient advances in miniaturized fabrication of circuits. A reduction in the distance between the antennal lobe and amplifier (through a reduction in length of electrodes that would only be required to attach to the back of the locust) would also reduce external noise being introduced into the recordings.

In laboratory experiments, the concentrations and timing of stimuli are predictable and tunable – luxuries that are not afforded in open-field explorations. It is also possible that neural responses are weakened to the level of the noise floor. In such instances, simultaneous

monitoring of behavioral responses can provide a second axis along which stimuli can be detected and classified. Our current analytical pipeline has a deep learning framework that can detect locusts in each frame. The output of this model can easily be fed into a secondary network that can then classify different behavioral motifs (such as grooming, antennal flicking; **Fig. 6.4**), which can be used to predict not only the presence of a chemical in the locust's vicinity but also the identity of the stimulus.

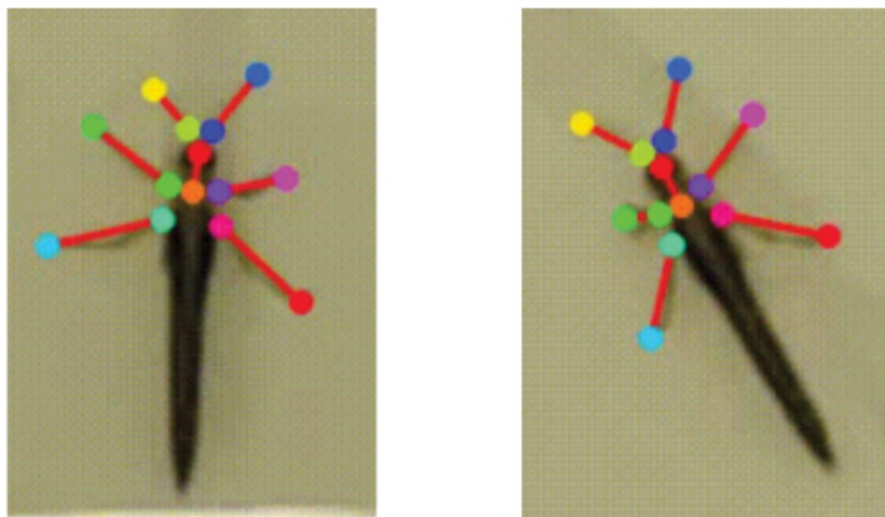


Figure 6.4: Markerless tracking for pose estimation in locusts

A neural network⁸⁸ was trained to perform markerless tracking of locust body positions in a behavioral arena. The network's output labels each body part by a different colored dot, with connections between parts indicated by red lines. The relative positions of body parts can be constructed into postures over time, and the sequence of postures can be used to construct complex behavioral motifs.

Finally, we optimized our protocol to allow a locust to be implanted with electrodes and ready for movement within 30 minutes. This turnaround time combined with the long-term stability of recordings can be used to perform experiments using groups or swarms of locusts, such as releasing multiple locusts into a large field to sample different regions. Miniaturized cameras can also be mounted on the back of the locusts to obtain a visual map of unexplored

regions. Locusts undergo a marked phase change (from solitary to gregarious) when they are assembled into groups¹⁹⁹. Our protocol can be directly applied to study any neural changes that take place as locusts undergo phase changes in group settings and whether odor coding principles remain conserved as they transition from the solitary phase to the gregarious phase²⁰⁰.

References

1. Herz RS. The Role of Odor-Evoked Memory in Psychological and Physiological Health. *Brain Sci.* 2016;6(3):22. doi:10.3390/brainsci6030022
2. Arshamian A, Iannilli E, Gerber JC, et al. The functional neuroanatomy of odor evoked autobiographical memories cued by odors and words. *Neuropsychologia.* 2013;51(1):123-131. doi:10.1016/j.neuropsychologia.2012.10.023
3. Santos DV, Reiter ER, DiNardo LJ, Costanzo RM. Hazardous Events Associated With Impaired Olfactory Function. *Archives of Otolaryngology–Head & Neck Surgery.* 2004;130(3):317-319. doi:10.1001/archotol.130.3.317
4. Velayudhan L. Smell identification function and Alzheimer’s disease: a selective review. *Curr Opin Psychiatry.* 2015;28(2):173-179. doi:10.1097/YCO.0000000000000146
5. Doty RL. Olfaction in Parkinson’s disease and related disorders. *Neurobiol Dis.* 2012;46(3):527-552. doi:10.1016/j.nbd.2011.10.026
6. Fleischer J, Krieger J. Insect Pheromone Receptors – Key Elements in Sensing Intraspecific Chemical Signals. *Front Cell Neurosci.* 2018;12:425. doi:10.3389/fncel.2018.00425
7. Takahashi LK. Olfactory systems and neural circuits that modulate predator odor fear. *Front Behav Neurosci.* 2014;8:72. doi:10.3389/fnbeh.2014.00072
8. Detrain C, Deneubourg JL. Collective Decision-Making and Foraging Patterns in Ants and Honeybees. In: Simpson SJ, ed. *Advances in Insect Physiology.* Vol 35. Academic Press; 2008:123-173. doi:10.1016/S0065-2806(08)00002-7
9. Chalissery JM, Renyard A, Gries R, Hoefele D, Alamsetti SK, Gries G. Ants Sense, and Follow, Trail Pheromones of Ant Community Members. *Insects.* 2019;10(11):383. doi:10.3390/insects10110383
10. David Morgan E. Trail pheromones of ants. *Physiological Entomology.* 2009;34(1):1-17. doi:10.1111/j.1365-3032.2008.00658.x
11. Bortolotti L, Costa C. Chemical Communication in the Honey Bee Society. In: Mucignat-Caretta C, ed. *Neurobiology of Chemical Communication.* Frontiers in Neuroscience. CRC Press/Taylor & Francis; 2014. Accessed December 16, 2021. <http://www.ncbi.nlm.nih.gov/books/NBK200983/>
12. Sengupta S, Smith DP. How *Drosophila* Detect Volatile Pheromones: Signaling, Circuits, and Behavior. In: Mucignat-Caretta C, ed. *Neurobiology of Chemical Communication.*

- Frontiers in Neuroscience. CRC Press/Taylor & Francis; 2014. Accessed December 16, 2021. <http://www.ncbi.nlm.nih.gov/books/NBK200999/>
13. Guo X, Yu Q, Chen D, et al. 4-Vinylanisole is an aggregation pheromone in locusts. *Nature*. 2020;584(7822):584-588. doi:10.1038/s41586-020-2610-4
 14. Buck L, Axel R. A novel multigene family may encode odorant receptors: a molecular basis for odor recognition. *Cell*. 1991;65(1):175-187. doi:10.1016/0092-8674(91)90418-x
 15. Poncelet G, Shimeld SM. The evolutionary origins of the vertebrate olfactory system. *Open Biology*. 10(12):200330. doi:10.1098/rsob.200330
 16. Niimura Y, Nei M. Evolution of olfactory receptor genes in the human genome. *PNAS*. 2003;100(21):12235-12240. doi:10.1073/pnas.1635157100
 17. Ache BW, Young JM. Olfaction: Diverse Species, Conserved Principles. *Neuron*. 2005;48(3):417-430. doi:10.1016/j.neuron.2005.10.022
 18. Cassenaer S, Laurent G. Conditional modulation of spike-timing-dependent plasticity for olfactory learning. *Nature*. 2012;482(7383):47-52. doi:10.1038/nature10776
 19. Ito I, Ong RC ying, Raman B, Stopfer M. Sparse odor representation and olfactory learning. *Nat Neurosci*. 2008;11(10):1177-1184. doi:10.1038/nn.2192
 20. Laurent G, Davidowitz H. Encoding of olfactory information with oscillating neural assemblies. *Science*. 1994;265(5180):1872-1875. doi:10.1126/science.265.5180.1872
 21. Raman B, Joseph J, Tang J, Stopfer M. Temporally Diverse Firing Patterns in Olfactory Receptor Neurons Underlie Spatiotemporal Neural Codes for Odors. *J Neurosci*. 2010;30(6):1994-2006. doi:10.1523/JNEUROSCI.5639-09.2010
 22. Stopfer M, Jayaraman V, Laurent G. Intensity versus identity coding in an olfactory system. *Neuron*. 2003;39(6):991-1004. doi:10.1016/j.neuron.2003.08.011
 23. Saha D, Leong K, Li C, Peterson S, Siegel G, Raman B. A spatiotemporal coding mechanism for background-invariant odor recognition. *Nat Neurosci*. 2013;16(12):1830-1839. doi:10.1038/nn.3570
 24. Wilson RI. Early Olfactory Processing in *Drosophila*: Mechanisms and Principles. *Annu Rev Neurosci*. 2013;36:217-241. doi:10.1146/annurev-neuro-062111-150533
 25. Laurent G. A systems perspective on early olfactory coding. *Science*. 1999;286(5440):723-728. doi:10.1126/science.286.5440.723
 26. Wilson RI, Turner GC, Laurent G. Transformation of Olfactory Representations in the *Drosophila* Antennal Lobe. *Science*. 2004;303(5656):366-370. doi:10.1126/science.1090782

27. Rajagopalan A, Assisi C. Effect of Circuit Structure on Odor Representation in the Insect Olfactory System. *eNeuro*. 2020;7(3):ENEURO.0130-19.2020. doi:10.1523/ENEURO.0130-19.2020
28. Gupta N, Stopfer M. Functional analysis of a higher olfactory center, the lateral horn. *J Neurosci*. 2012;32(24):8138-8148. doi:10.1523/JNEUROSCI.1066-12.2012
29. Oya S, Kohno H, Kainoh Y, Ono M, Kubo T. Increased complexity of mushroom body Kenyon cell subtypes in the brain is associated with behavioral evolution in hymenopteran insects. *Sci Rep*. 2017;7(1):13785. doi:10.1038/s41598-017-14174-6
30. Gupta N, Stopfer M. Insect Olfaction: a Model System for Neural Circuit Modeling. In: Jaeger D, Jung R, eds. *Encyclopedia of Computational Neuroscience*. Springer; 2015:1436-1441. doi:10.1007/978-1-4614-6675-8_338
31. Zhao B, Sun J, Zhang X, et al. Long-term memory is formed immediately without the need for protein synthesis-dependent consolidation in *Drosophila*. *Nat Commun*. 2019;10(1):4550. doi:10.1038/s41467-019-12436-7
32. Heimbeck G, Bugnon V, Gendre N, Keller A, Stocker RF. A central neural circuit for experience-independent olfactory and courtship behavior in *Drosophila melanogaster*. *Proc Natl Acad Sci U S A*. 2001;98(26):15336-15341. doi:10.1073/pnas.011314898
33. Ochieng SA, Hallberg E, Hansson BS. Fine structure and distribution of antennal sensilla of the desert locust, *Schistocerca gregaria* (Orthoptera: Acrididae). *Cell and Tissue Research*. 1998;291(3):525-536. doi:10.1007/s004410051022
34. Katz B, Schmitt OH. Electric interaction between two adjacent nerve fibres. *J Physiol*. 1940;97(4):471-488.
35. Van der Goes van Naters W. Inhibition among olfactory receptor neurons. *Front Hum Neurosci*. 2013;7:690. doi:10.3389/fnhum.2013.00690
36. Su CY, Menuz K, Reisert J, Carlson JR. Non-synaptic inhibition between grouped neurons in an olfactory circuit. *Nature*. 2012;492(7427):66-71. doi:10.1038/nature11712
37. Jones WD, Cayirlioglu P, Kadow IG, Vosshall LB. Two chemosensory receptors together mediate carbon dioxide detection in *Drosophila*. *Nature*. 2007;445(7123):86-90. doi:10.1038/nature05466
38. Min S, Ai M, Shin SA, Suh GSB. Dedicated olfactory neurons mediating attraction behavior to ammonia and amines in *Drosophila*. *Proc Natl Acad Sci U S A*. 2013;110(14):E1321-1329. doi:10.1073/pnas.1215680110
39. Ai M, Min S, Grosjean Y, et al. Acid sensing by the *Drosophila* olfactory system. *Nature*. 2010;468(7324):691-695. doi:10.1038/nature09537

40. Suh GSB, Wong AM, Hergarden AC, et al. A single population of olfactory sensory neurons mediates an innate avoidance behaviour in *Drosophila*. *Nature*. 2004;431(7010):854-859. doi:10.1038/nature02980
41. McMeniman CJ, Corfas RA, Matthews BJ, Ritchie SA, Vosshall LB. Multimodal integration of carbon dioxide and other sensory cues drives mosquito attraction to humans. *Cell*. 2014;156(5):1060-1071. doi:10.1016/j.cell.2013.12.044
42. Malnic B, Hirono J, Sato T, Buck LB. Combinatorial receptor codes for odors. *Cell*. 1999;96(5):713-723. doi:10.1016/s0092-8674(00)80581-4
43. Hallem EA, Ho MG, Carlson JR. The molecular basis of odor coding in the *Drosophila* antenna. *Cell*. 2004;117(7):965-979. doi:10.1016/j.cell.2004.05.012
44. Saha D, Sun W, Li C, et al. Engaging and disengaging recurrent inhibition coincides with sensing and unsensing of a sensory stimulus. *Nature Communications*. 2017;8(1):15413. doi:10.1038/ncomms15413
45. Nizampatnam S, Zhang L, Chandak R, Katta N, Raman B. Invariant Odor Recognition with ON-OFF Neural Ensembles. *bioRxiv*. Published online November 8, 2020:2020.11.07.372870. doi:10.1101/2020.11.07.372870
46. Nizampatnam S, Saha D, Chandak R, Raman B. Dynamic contrast enhancement and flexible odor codes. *Nature Communications*. 2018;9(1):3062. doi:10.1038/s41467-018-05533-6
47. Saha D, Raman B. Relating early olfactory processing with behavior: a perspective. *Current Opinion in Insect Science*. 2015;12:54-63. doi:10.1016/j.cois.2015.09.009
48. Traner M, Chandak R, Raman B. Recent approaches to study the neural bases of complex insect behavior. *Current Opinion in Insect Science*. 2021;48:18-25. doi:10.1016/j.cois.2021.07.004
49. Biology NRC (US) C on RO in. *The Nervous System and Behavior*. National Academies Press (US); 1989. Accessed December 8, 2021. <https://www.ncbi.nlm.nih.gov/books/NBK217810/>
50. Blanco-Hernández E, Valle-Leija P, Zomosa-Signoret V, Drucker-Colín R, Vidaltamayo R. Odor memory stability after reinnervation of the olfactory bulb. *PLoS One*. 2012;7(10):e46338. doi:10.1371/journal.pone.0046338
51. Rodriguez I, Boehm U. Pheromone sensing in mice. *Results Probl Cell Differ*. 2009;47:77-96. doi:10.1007/400_2008_8
52. Stensmyr MC, Dweck HKM, Farhan A, et al. A Conserved Dedicated Olfactory Circuit for Detecting Harmful Microbes in *Drosophila*. *Cell*. 2012;151(6):1345-1357. doi:10.1016/j.cell.2012.09.046

53. Pavlov IP. *Conditioned Reflexes: An Investigation of the Physiological Activity of the Cerebral Cortex*. Oxford Univ. Press; 1927:xv, 430.
54. Thorndike EL. Animal Intelligence: An Experimental Study of the Associative Processes in Animals. *Psychological Review*. 1898;5(5):551-553. doi:10.1037/h0067373
55. Skinner BF. *The Behavior of Organisms: An Experimental Analysis*. Appleton-Century; 1938:457.
56. Hollis KL, Guillette LM. What Associative Learning in Insects Tells Us about the Evolution of Learned and Fixed Behavior. *IJCP*. 2015;28. doi:10.46867/ijcp.2015.28.01.07
57. Yu D, Ponomarev A, Davis RL. Altered Representation of the Spatial Code for Odors after Olfactory Classical Conditioning: Memory Trace Formation by Synaptic Recruitment. *Neuron*. 2004;42(3):437-449. doi:10.1016/S0896-6273(04)00217-X
58. Vergoz V, Roussel E, Sandoz JC, Giurfa M. Aversive Learning in Honeybees Revealed by the Olfactory Conditioning of the Sting Extension Reflex. *PLOS ONE*. 2007;2(3):e288. doi:10.1371/journal.pone.0000288
59. Hansson B, Society MP, Fan R jane, Hansson BS. Olfactory discrimination conditioning in the moth *Spodoptera littoralis*. *Physiol Behav*. Published online 2001:159-165.
60. Daly KC, Smith BH. Associative olfactory learning in the moth *Manduca sexta*. *J Exp Biol*. 2000;203(Pt 13):2025-2038.
61. Menzel R. Associative learning in honey bees. *Apidologie*. 1993;24(3):157-168. doi:10.1051/apido:19930301
62. Giurfa M. Associative Mechanosensory Conditioning of the Proboscis Extension Reflex in Honeybees. *Learning & Memory*. 2004;11(3):294-302. doi:10.1101/lm.63604
63. Chabaud MA, Devaud JM, Pham-Delègue MH, Preat T, Kaiser L. Olfactory conditioning of proboscis activity in *Drosophila melanogaster*. *J Comp Physiol A Neuroethol Sens Neural Behav Physiol*. 2006;192(12):1335-1348. doi:10.1007/s00359-006-0160-3
64. Simões P, Ott SR, Niven JE. Associative olfactory learning in the desert locust, *Schistocerca gregaria*. *Journal of Experimental Biology*. 2011;214(15):2495-2503. doi:10.1242/jeb.055806
65. Algorithms for Olfactory Search across Species | Journal of Neuroscience. Accessed December 8, 2021. <https://www.jneurosci.org/content/38/44/9383>
66. Chen TW, Wardill TJ, Sun Y, et al. Ultrasensitive fluorescent proteins for imaging neuronal activity. *Nature*. 2013;499(7458):295-300. doi:10.1038/nature12354

67. Tian L, Hires SA, Mao T, et al. Imaging neural activity in worms, flies and mice with improved GCaMP calcium indicators. *Nat Methods*. 2009;6(12):875-881. doi:10.1038/nmeth.1398
68. Klapoetke NC, Murata Y, Kim SS, et al. Independent optical excitation of distinct neural populations. *Nat Methods*. 2014;11(3):338-346. doi:10.1038/nmeth.2836
69. Costa L, Nunes-Silva P, Galaschi-Teixeira JS, et al. RFID-tagged amazonian stingless bees confirm that landscape configuration and nest re-establishment time affect homing ability. *Insect Soc*. 2021;68(1):101-108. doi:10.1007/s00040-020-00802-4
70. Kumari M, Hasan SMR. A New CMOS Implementation for Miniaturized Active RFID Insect Tag and VHF Insect Tracking. *IEEE Journal of Radio Frequency Identification*. 2020;4(2):124-136. doi:10.1109/JRFID.2020.2964313
71. Nunes-Silva P, Costa L, Campbell AJ, et al. Radiofrequency identification (RFID) reveals long-distance flight and homing abilities of the stingless bee *Melipona fasciculata*. *Apidologie*. 2020;51(2):240-253. doi:10.1007/s13592-019-00706-8
72. Susanto F, Gillard T, Souza PD, et al. Addressing RFID Misreadings to Better Infer Bee Hive Activity. *IEEE Access*. 2018;6:31935-31949. doi:10.1109/ACCESS.2018.2844181
73. Van Geystelen A, Benaets K, de Graaf DC, Larmuseau MHD, Wenseleers T. Track-a-Forager: a program for the automated analysis of RFID tracking data to reconstruct foraging behaviour. *Insect Soc*. 2016;63(1):175-183. doi:10.1007/s00040-015-0453-z
74. Fiala M. ARTag, a fiducial marker system using digital techniques. In: *2005 IEEE Computer Society Conference on Computer Vision and Pattern Recognition (CVPR '05)*. Vol 2. ; 2005:590-596 vol. 2. doi:10.1109/CVPR.2005.74
75. Celozzi C, Paravati G, Sanna A, Lamberti F. A 6-DOF ARTag-based tracking system. *IEEE Transactions on Consumer Electronics*. 2010;56(1):203-210. doi:10.1109/TCE.2010.5439146
76. Crall JD, Gravish N, Mountcastle AM, Combes SA. BEEtag: A Low-Cost, Image-Based Tracking System for the Study of Animal Behavior and Locomotion. *PLOS ONE*. 2015;10(9):e0136487. doi:10.1371/journal.pone.0136487
77. Jacob M. Graving. *Pinpoint: Behavioral Tracking Using 2D Barcode Tags v0.0.1-Alpha*. Zenodo; 2017. doi:10.5281/zenodo.1008970
78. Wario F, Wild B, Couvillon MJ, Rojas R, Landgraf T. Automatic methods for long-term tracking and the detection and decoding of communication dances in honeybees. *Front Ecol Evol*. 2015;3. doi:10.3389/fevo.2015.00103
79. Gal A, Saragosti J, Kronauer DJ. anTraX, a software package for high-throughput video tracking of color-tagged insects. Berman GJ, Dulac C, Shaevitz JW, Perez-Escudero A, eds. *eLife*. 2020;9:e58145. doi:10.7554/eLife.58145

80. Shoji K. Individual Activity Level and Mobility Patterns of Ants Within Nest Site. In: Dorigo M, Birattari M, Blum C, Christensen AL, Reina A, Trianni V, eds. *Swarm Intelligence*. Lecture Notes in Computer Science. Springer International Publishing; 2018:378-384. doi:10.1007/978-3-030-00533-7_32
81. Modlmeier AP, Colman E, Hanks EM, Bringenberg R, Bansal S, Hughes DP. Ant colonies maintain social homeostasis in the face of decreased density. Gordon DM, Baldwin IT, Crall JD, Davidson J, eds. *eLife*. 2019;8:e38473. doi:10.7554/eLife.38473
82. Garrison LK, Kleineidam CJ, Weidenmüller A. Behavioral flexibility promotes collective consistency in a social insect. *Scientific Reports*. 2018;8(1):15836. doi:10.1038/s41598-018-33917-7
83. Crall JD, Switzer CM, Oppenheimer RL, et al. Neonicotinoid exposure disrupts bumblebee nest behavior, social networks, and thermoregulation. *Science*. 2018;362(6415):683-686. doi:10.1126/science.aat1598
84. Crall JD, de Bivort BL, Dey B, Ford Versypt AN. Social Buffering of Pesticides in Bumblebees: Agent-Based Modeling of the Effects of Colony Size and Neonicotinoid Exposure on Behavior Within Nests. *Front Ecol Evol*. 2019;7. doi:10.3389/fevo.2019.00051
85. Crall JD, Gravish N, Mountcastle AM, et al. Spatial fidelity of workers predicts collective response to disturbance in a social insect. *Nature Communications*. 2018;9(1):1201. doi:10.1038/s41467-018-03561-w
86. Knebel D, Ayali A, Guershon M, Ariel G. Intra- versus intergroup variance in collective behavior. *Science Advances*. 2019;5(1):eaav0695. doi:10.1126/sciadv.aav0695
87. Crall JD, Souffrant AD, Akandwanaho D, et al. Social context modulates idiosyncrasy of behaviour in the gregarious cockroach *Blaberus discoidalis*. *Animal Behaviour*. 2016;111:297-305. doi:10.1016/j.anbehav.2015.10.032
88. DeepPoseKit, a software toolkit for fast and robust animal pose estimation using deep learning | eLife. Accessed January 12, 2021. <https://elifesciences.org/articles/47994>
89. Mathis A, Mamidanna P, Cury KM, et al. DeepLabCut: markerless pose estimation of user-defined body parts with deep learning. *Nature Neuroscience*. 2018;21(9):1281-1289. doi:10.1038/s41593-018-0209-y
90. Nath T, Mathis A, Chen AC, Patel A, Bethge M, Mathis MW. Using DeepLabCut for 3D markerless pose estimation across species and behaviors. *Nat Protoc*. 2019;14(7):2152-2176. doi:10.1038/s41596-019-0176-0
91. Kaushik PK, Renz M, Olsson SB. Characterizing long-range search behavior in Diptera using complex 3D virtual environments. *PNAS*. 2020;117(22):12201-12207. doi:10.1073/pnas.1912124117

92. Richie JM, Patel PR, Welle EJ, et al. Benchtop Carbon Fiber Microelectrode Array Fabrication Toolkit. *bioRxiv*. Published online March 22, 2021:2021.03.22.436422. doi:10.1101/2021.03.22.436422
93. Guo P, Pollack AJ, Varga AG, Martin JP, Ritzmann RE. Extracellular Wire Tetrode Recording in Brain of Freely Walking Insects. *JoVE (Journal of Visualized Experiments)*. 2014;(86):e51337. doi:10.3791/51337
94. Saha D, Mehta D, Altan E, et al. Explosive sensing with insect-based biorobots. *Biosensors and Bioelectronics: X*. 2020;6:100050. doi:10.1016/j.biosx.2020.100050
95. Thomas SJ, Harrison RR, Leonardo A, Reynolds MS. A Battery-Free Multichannel Digital Neural/EMG Telemetry System for Flying Insects. *IEEE Transactions on Biomedical Circuits and Systems*. 2012;6(5):424-436. doi:10.1109/TBCAS.2012.2222881
96. Harrison RR, Fotowat H, Chan R, et al. Wireless Neural/EMG Telemetry Systems for Small Freely Moving Animals. *IEEE Transactions on Biomedical Circuits and Systems*. 2011;5(2):103-111. doi:10.1109/TBCAS.2011.2131140
97. Berényi A, Somogyvári Z, Nagy AJ, et al. Large-scale, high-density (up to 512 channels) recording of local circuits in behaving animals. *Journal of Neurophysiology*. 2014;111(5):1132-1149. doi:10.1152/jn.00785.2013
98. Strauch M, Lüdke A, Münch D, et al. More than apples and oranges - Detecting cancer with a fruit fly's antenna. *Sci Rep*. 2014;4(1):3576. doi:10.1038/srep03576
99. Rains GC, Utley SL, Lewis WJ. Behavioral monitoring of trained insects for chemical detection. *Biotechnol Prog*. 2006;22(1):2-8. doi:10.1021/bp050164p
100. Pramanik C, Saha H, Gangopadhyay U. Design optimization of a high performance silicon MEMS piezoresistive pressure sensor for biomedical applications. *Journal of Micromechanics and Microengineering*. 2006;16:2060-2066. doi:10.1088/0960-1317/16/10/019
101. Santos HA, ed. Front matter. In: *Porous Silicon for Biomedical Applications*. Woodhead Publishing; 2014:i-iii. doi:10.1016/B978-0-85709-711-8.50021-0
102. Xu Y, Hu X, Kundu S, et al. Silicon-Based Sensors for Biomedical Applications: A Review. *Sensors (Basel)*. 2019;19(13):2908. doi:10.3390/s19132908
103. Harraz FA. Porous silicon chemical sensors and biosensors: A review. *Sensors and Actuators B: Chemical*. 2014;202:897-912. doi:10.1016/j.snb.2014.06.048
104. Terutsuki D, Uchida T, Fukui C, Sukekawa Y, Okamoto Y, Kanzaki R. Electroantennography-based Bio-hybrid Odor-detecting Drone using Silkmoth Antennae for Odor Source Localization. *J Vis Exp*. 2021;(174). doi:10.3791/62895

105. Martinez D, Moraud EM. Reactive and Cognitive Search Strategies for Olfactory Robots. In: Persaud KC, Marco S, Gutiérrez-Gálvez A, eds. *Neuromorphic Olfaction*. Frontiers in Neuroengineering. CRC Press/Taylor & Francis; 2013. Accessed December 16, 2021. <http://www.ncbi.nlm.nih.gov/books/NBK298821/>
106. Anderson MJ, Sullivan JG, Horiuchi TK, Fuller SB, Daniel TL. A bio-hybrid odor-guided autonomous palm-sized air vehicle. *Bioinspir Biomim*. 2020;16(2):026002. doi:10.1088/1748-3190/abbd81
107. Vouloutsi V, Lopez-Serrano LL, Mathews Z, et al. The Synthetic Moth: A Neuromorphic Approach toward Artificial Olfaction in Robots. In: Persaud KC, Marco S, Gutiérrez-Gálvez A, eds. *Neuromorphic Olfaction*. Frontiers in Neuroengineering. CRC Press/Taylor & Francis; 2013. Accessed December 16, 2021. <http://www.ncbi.nlm.nih.gov/books/NBK298818/>
108. Sato H, Berry C, Peeri Y, et al. Remote radio control of insect flight. *Frontiers in Integrative Neuroscience*. 2009;3:24. doi:10.3389/neuro.07.024.2009
109. The Good Scents Company - Aromatic/Hydrocarbon/Inorganic Ingredients Catalog information. Accessed July 22, 2021. <http://www.thegoodscentcompany.com/data/rw1002711.html>
110. Saha D, Leong K, Katta N, Raman B. Multi-unit Recording Methods to Characterize Neural Activity in the Locust (*Schistocerca Americana*) Olfactory Circuits. *JoVE (Journal of Visualized Experiments)*. 2013;(71):e50139. doi:10.3791/50139
111. Pouzat C, Mazor O, Laurent G. Using noise signature to optimize spike-sorting and to assess neuronal classification quality. *Journal of Neuroscience Methods*. 2002;122(1):43-57. doi:10.1016/S0165-0270(02)00276-5
112. Ronneberger O, Fischer P, Brox T. U-Net: Convolutional Networks for Biomedical Image Segmentation. *arXiv:150504597 [cs]*. Published online May 18, 2015. Accessed July 22, 2021. <http://arxiv.org/abs/1505.04597>
113. Saha D, Mehta D, Altan E, et al. Explosive sensing with insect-based biorobots. *Biosensors and Bioelectronics: X*. 2020;6:100050. doi:10.1016/j.biosx.2020.100050
114. Twister. Open Ephys. Accessed December 22, 2021. <https://open-ephys.org/twister>
115. Alexey. *Yolo v4, v3 and v2 for Windows and Linux*.; 2021. Accessed December 13, 2021. <https://github.com/AlexeyAB/darknet>
116. Bochkovskiy A, Wang CY, Liao HYM. YOLOv4: Optimal Speed and Accuracy of Object Detection. *arXiv:200410934 [cs, eess]*. Published online April 22, 2020. Accessed December 13, 2021. <http://arxiv.org/abs/2004.10934>

117. Grosjean Y, Rytz R, Farine JP, et al. An olfactory receptor for food-derived odours promotes male courtship in *Drosophila*. *Nature*. 2011;478(7368):236-240. doi:10.1038/nature10428
118. Semmelhack JL, Wang JW. Select *Drosophila* glomeruli mediate innate olfactory attraction and aversion. *Nature*. 2009;459:218-223. doi:10.1038/nature07983
119. Knaden M, Strutz A, Ahsan J, Sachse S, Hansson BS. Spatial representation of odorant valence in an insect brain. *Cell Rep*. 2012;1(4):392-399. doi:10.1016/j.celrep.2012.03.002
120. Kreher SA, Mathew D, Kim J, Carlson JR. Translation of sensory input into behavioral output via an olfactory system. *Neuron*. 2008;59(1):110-124. doi:10.1016/j.neuron.2008.06.010
121. Kermen F, Midroit M, Kuczewski N, et al. Topographical representation of odor hedonics in the olfactory bulb. *Nat Neurosci*. 2016;19(7):876-878. doi:10.1038/nn.4317
122. Rengarajan S, Hallem EA. Olfactory circuits and behaviors of nematodes. *Current Opinion in Neurobiology*. 2016;41:136-148. doi:10.1016/j.conb.2016.09.002
123. Wilson CD, Serrano GO, Koulakov AA, Rinberg D. A primacy code for odor identity. *Nat Commun*. 2017;8(1):1477. doi:10.1038/s41467-017-01432-4
124. Abraham NM, Spors H, Carleton A, Margrie TW, Kuner T, Schaefer AT. Maintaining Accuracy at the Expense of Speed: Stimulus Similarity Defines Odor Discrimination Time in Mice. *Neuron*. 2004;44(5):865-876. doi:10.1016/j.neuron.2004.11.017
125. Uchida N, Mainen ZF. Speed and accuracy of olfactory discrimination in the rat. *Nat Neurosci*. 2003;6(11):1224-1229. doi:10.1038/nn1142
126. Szyszka P, Gerkin RC, Galizia CG, Smith BH. High-speed odor transduction and pulse tracking by insect olfactory receptor neurons. *PNAS*. 2014;111(47):16925-16930. doi:10.1073/pnas.1412051111
127. Faber T, Joerges J, Menzel R. Associative learning modifies neural representations of odors in the insect brain. *Nat Neurosci*. 1999;2(1):74-78. doi:10.1038/4576
128. Cassenaer S, Laurent G. Hebbian STDP in mushroom bodies facilitates the synchronous flow of olfactory information in locusts. *Nature*. 2007;448(7154):709-713. doi:10.1038/nature05973
129. Gupta N, Stopfer M. Functional Analysis of a Higher Olfactory Center, the Lateral Horn. *J Neurosci*. 2012;32(24):8138-8148. doi:10.1523/JNEUROSCI.1066-12.2012
130. Yamamoto D, Koganezawa M. Genes and circuits of courtship behaviour in *Drosophila* males. *Nat Rev Neurosci*. 2013;14(10):681-692. doi:10.1038/nrn3567

131. Kurtovic A, Widmer A, Dickson BJ. A single class of olfactory neurons mediates behavioural responses to a *Drosophila* sex pheromone. *Nature*. 2007;446(7135):542-546. doi:10.1038/nature05672
132. Yamazaki D, Hiroi M, Abe T, et al. Two Parallel Pathways Assign Opposing Odor Valences during *Drosophila* Memory Formation. *Cell Rep*. 2018;22(9):2346-2358. doi:10.1016/j.celrep.2018.02.012
133. Ache BW, Young JM. Olfaction: diverse species, conserved principles. *Neuron*. 2005;48(3):417-430. doi:10.1016/j.neuron.2005.10.022
134. Zhang L, Guo M, Zhuo F, Xu H, Zheng N, Zhang L. An odorant-binding protein mediates sexually dimorphic behaviors via binding male-specific 2-heptanone in migratory locust. *J Insect Physiol*. 2019;118:103933. doi:10.1016/j.jinsphys.2019.103933
135. Keller A, Gerkin RC, Guan Y, et al. Predicting human olfactory perception from chemical features of odor molecules. *Science*. 2017;355(6327):820-826. doi:10.1126/science.aal2014
136. Fdez Galán R, Sachse S, Galizia CG, Herz AVM. Odor-driven attractor dynamics in the antennal lobe allow for simple and rapid olfactory pattern classification. *Neural Comput*. 2004;16(5):999-1012. doi:10.1162/089976604773135078
137. Mazor O, Laurent G. Transient dynamics versus fixed points in odor representations by locust antennal lobe projection neurons. *Neuron*. 2005;48(4):661-673. doi:10.1016/j.neuron.2005.09.032
138. Bathellier B, Buhl DL, Accolla R, Carleton A. Dynamic Ensemble Odor Coding in the Mammalian Olfactory Bulb: Sensory Information at Different Timescales. *Neuron*. 2008;57(4):586-598. doi:10.1016/j.neuron.2008.02.011
139. Saha D, Sun W, Li C, et al. Engaging and disengaging recurrent inhibition coincides with sensing and unsensing of a sensory stimulus. *Nat Commun*. 2017;8(1):15413. doi:10.1038/ncomms15413
140. Haddad R, Weiss T, Khan R, et al. Global Features of Neural Activity in the Olfactory System Form a Parallel Code That Predicts Olfactory Behavior and Perception. *J Neurosci*. 2010;30(27):9017-9026. doi:10.1523/JNEUROSCI.0398-10.2010
141. Kepple D, Koulakov A. Constructing an olfactory perceptual space and predicting percepts from molecular structure. *arXiv:170805774 [q-bio]*. Published online June 6, 2018. Accessed July 27, 2021. <http://arxiv.org/abs/1708.05774>
142. Chemical Name Search. Accessed July 22, 2021. <https://webbook.nist.gov/chemistry/name-ser/>

143. Chae H, Kepple DR, Bast WG, Murthy VN, Koulakov AA, Albeanu DF. Mosaic representations of odors in the input and output layers of the mouse olfactory bulb. *Nat Neurosci.* 2019;22(8):1306-1317. doi:10.1038/s41593-019-0442-z
144. Nizampatnam S, Saha D, Chandak R, Raman B. Dynamic contrast enhancement and flexible odor codes. *Nat Commun.* 2018;9(1):3062. doi:10.1038/s41467-018-05533-6
145. Brown SL, Joseph J, Stopfer M. Encoding a temporally structured stimulus with a temporally structured neural representation. *Nat Neurosci.* 2005;8(11):1568-1576. doi:10.1038/nm1559
146. Broome BM, Jayaraman V, Laurent G. Encoding and decoding of overlapping odor sequences. *Neuron.* 2006;51(4):467-482. doi:10.1016/j.neuron.2006.07.018
147. Nizampatnam S, Zhang L, Chandak R, Katta N, Raman B. Invariant Odor Recognition with ON-OFF Neural Ensembles. *bioRxiv.* Published online November 8, 2020:2020.11.07.372870. doi:10.1101/2020.11.07.372870
148. Hallem EA, Carlson JR. Coding of odors by a receptor repertoire. *Cell.* 2006;125(1):143-160. doi:10.1016/j.cell.2006.01.050
149. Bhandawat V, Olsen SR, Gouwens NW, Schlieff ML, Wilson RI. Sensory processing in the *Drosophila* antennal lobe increases reliability and separability of ensemble odor representations. *Nat Neurosci.* 2007;10(11):1474-1482. doi:10.1038/nm1976
150. Chou YH, Spletter ML, Yaksi E, Leong JCS, Wilson RI, Luo L. Diversity and wiring variability of olfactory local interneurons in the *Drosophila* antennal lobe. *Nat Neurosci.* 2010;13(4):439-449. doi:10.1038/nm.2489
151. Christensen TA, Waldrop BR, Harrow ID, Hildebrand JG. Local interneurons and information processing in the olfactory glomeruli of the moth *Manduca sexta*. *J Comp Physiol A.* 1993;173(4):385-399. doi:10.1007/BF00193512
152. Sachse S, Galizia CG. Role of inhibition for temporal and spatial odor representation in olfactory output neurons: a calcium imaging study. *J Neurophysiol.* 2002;87(2):1106-1117. doi:10.1152/jn.00325.2001
153. Conchou L, Lucas P, Meslin C, Proffit M, Staudt M, Renou M. Insect Odorscapes: From Plant Volatiles to Natural Olfactory Scenes. *Frontiers in Physiology.* 2019;10:972. doi:10.3389/fphys.2019.00972
154. Garcia J, Kimeldorf DJ, Koelling RA. Conditioned Aversion to Saccharin Resulting from Exposure to Gamma Radiation. *Science.* 1955;122(3160):157-158. doi:10.1126/science.122.3160.157
155. Giurfa M. Cognition with few neurons: higher-order learning in insects. *Trends Neurosci.* 2013;36(5):285-294. doi:10.1016/j.tins.2012.12.011

156. Hall JF. Backward conditioning in Pavlovian type studies. Reevaluation and present status. *Pavlov J Biol Sci.* 1984;19(4):163-168. doi:10.1007/BF03004514
157. Hansche WJ, Grant DA. Onset versus termination of a stimulus as the CS in eyelid conditioning. *Journal of Experimental Psychology.* 1960;59(1):19-26. doi:10.1037/h0041407
158. Giurfa M, Fabre E, Flaven-Pouchon J, et al. Olfactory conditioning of the sting extension reflex in honeybees: Memory dependence on trial number, interstimulus interval, intertrial interval, and protein synthesis. *Learn Mem.* 2009;16(12):761-765. doi:10.1101/lm.1603009
159. Baracchi D, Devaud JM, d’Ettorre P, Giurfa M. Pheromones modulate reward responsiveness and non-associative learning in honey bees. *Sci Rep.* 2017;7(1):9875. doi:10.1038/s41598-017-10113-7
160. Geva N, Guershon M, Orlova M, Ayali A. Memoirs of a locust: density-dependent behavioral change as a model for learning and memory. *Neurobiol Learn Mem.* 2010;93(2):175-182. doi:10.1016/j.nlm.2009.09.008
161. Kurahashi T, Menini A. Mechanism of odorant adaptation in the olfactory receptor cell. *Nature.* 1997;385(6618):725-729. doi:10.1038/385725a0
162. Nagel KI, Wilson RI. Biophysical mechanisms underlying olfactory receptor neuron dynamics. *Nat Neurosci.* 2011;14(2):208-216. doi:10.1038/nn.2725
163. Assisi C, Stopfer M, Bazhenov M. Excitatory Local Interneurons Enhance Tuning of Sensory Information. *PLOS Computational Biology.* 2012;8(7):e1002563. doi:10.1371/journal.pcbi.1002563
164. Kato S, Kaplan HS, Schrödel T, et al. Global Brain Dynamics Embed the Motor Command Sequence of *Caenorhabditis elegans*. *Cell.* 2015;163(3):656-669. doi:10.1016/j.cell.2015.09.034
165. Briggman KL, Abarbanel HDI, Kristan WB. Optical Imaging of Neuronal Populations During Decision-Making. *Science.* 2005;307(5711):896-901. doi:10.1126/science.1103736
166. Sadtler PT, Quick KM, Golub MD, et al. Neural constraints on learning. *Nature.* 2014;512(7515):423-426. doi:10.1038/nature13665
167. Degenhart AD, Bishop WE, Oby ER, et al. Stabilization of a brain–computer interface via the alignment of low-dimensional spaces of neural activity. *Nat Biomed Eng.* 2020;4(7):672-685. doi:10.1038/s41551-020-0542-9
168. Freund G, Walker DW. Operant conditioning in mice. *Life Sciences.* 1972;11(19, Part 1):905-914. doi:10.1016/0024-3205(72)90042-2

169. Malkki H, Donga L, De Groot S, Battaglia F, Pennartz C. Appetitive operant conditioning in mice: heritability and dissociability of training stages. *Frontiers in Behavioral Neuroscience*. 2010;4:171. doi:10.3389/fnbeh.2010.00171
170. Abramson CI, Dinges CW, Wells H. Operant Conditioning in Honey Bees (*Apis mellifera* L.): The Cap Pushing Response. *PLOS ONE*. 2016;11(9):e0162347. doi:10.1371/journal.pone.0162347
171. Saha D, Leong K, Katta N, Raman B. Multi-unit Recording Methods to Characterize Neural Activity in the Locust (*Schistocerca Americana*) Olfactory Circuits. *JoVE (Journal of Visualized Experiments)*. 2013;(71):e50139. doi:10.3791/50139
172. Saha D, Li C, Peterson S, Padovano W, Katta N, Raman B. Behavioural correlates of combinatorial versus temporal features of odour codes. *Nature Communications*. 2015;6(1). doi:10.1038/ncomms7953
173. Huston SJ, Stopfer M, Cassenaer S, Aldworth ZN, Laurent G. Neural encoding of odors during active sampling and in turbulent plumes. *Neuron*. 2015;88(2):403-418. doi:10.1016/j.neuron.2015.09.007
174. Murlis J, Elkinton JS, Cardé RT. Odor Plumes and How Insects Use Them. *Annual Review of Entomology*. 1992;37(1):505-532. doi:10.1146/annurev.en.37.010192.002445
175. van der Kooij CJ, Stavenga DG, Arikawa K, Belušič G, Kelber A. Evolution of Insect Color Vision: From Spectral Sensitivity to Visual Ecology. *Annual Review of Entomology*. 2021;66(1):435-461. doi:10.1146/annurev-ento-061720-071644
176. Song BM, Lee CH. Toward a Mechanistic Understanding of Color Vision in Insects. *Frontiers in Neural Circuits*. 2018;12:16. doi:10.3389/fncir.2018.00016
177. Wada-Katsumata A, Zurek L, Nalyanya G, Roelofs WL, Zhang A, Schal C. Gut bacteria mediate aggregation in the German cockroach. *PNAS*. Published online December 2, 2015. doi:10.1073/pnas.1504031112
178. Heisenberg M. What Do the Mushroom Bodies Do for the Insect Brain? An Introduction. *Learn Mem*. 1998;5(1):1-10.
179. Hige T. What can tiny mushrooms in fruit flies tell us about learning and memory? *Neuroscience Research*. 2018;129:8-16. doi:10.1016/j.neures.2017.05.002
180. Aso Y, Hattori D, Yu Y, et al. The neuronal architecture of the mushroom body provides a logic for associative learning. *eLife*. 2014;3. doi:10.7554/eLife.04577
181. Daly KC, Christensen TA, Lei H, Smith BH, Hildebrand JG. Learning modulates the ensemble representations for odors in primary olfactory networks. *PNAS*. 2004;101(28):10476-10481. doi:10.1073/pnas.0401902101

182. Hallem EA, Carlson JR. The Spatial Code for Odors Is Changed by Conditioning. *Neuron*. 2004;42(3):359-361. doi:10.1016/S0896-6273(04)00256-9
183. Hammer M, Menzel R. Multiple Sites of Associative Odor Learning as Revealed by Local Brain Microinjections of Octopamine in Honeybees. *Learn Mem*. 1998;5(1):146-156.
184. Günel S, Rhodin H, Morales D, Campagnolo J, Ramdya P, Fua P. DeepFly3D, a deep learning-based approach for 3D limb and appendage tracking in tethered, adult *Drosophila*. O’Leary T, Calabrese RL, Shaevitz JW, eds. *eLife*. 2019;8:e48571. doi:10.7554/eLife.48571
185. Gosztolai A, Günel S, Abrate MP, et al. LiftPose3D, a deep learning-based approach for transforming 2D to 3D pose in laboratory animals. *bioRxiv*. Published online September 20, 2020:2020.09.18.292680. doi:10.1101/2020.09.18.292680
186. Karashchuk P, Rupp KL, Dickinson ES, et al. Anipose: a toolkit for robust markerless 3D pose estimation. *bioRxiv*. Published online May 29, 2020:2020.05.26.117325. doi:10.1101/2020.05.26.117325
187. Vaart K van der, Sinhuber M, Reynolds AM, Ouellette NT. Mechanical spectroscopy of insect swarms. *Science Advances*. 2019;5(7):eaaw9305. doi:10.1126/sciadv.aaw9305
188. Berman GJ, Choi DM, Bialek W, Shaevitz JW. Mapping the stereotyped behaviour of freely moving fruit flies. *J R Soc Interface*. 2014;11(99). doi:10.1098/rsif.2014.0672
189. Capelli L, Sironi S, Rosso RD. Electronic Noses for Environmental Monitoring Applications. *Sensors (Basel)*. 2014;14(11):19979-20007. doi:10.3390/s141119979
190. Furton KG, Myers LJ. The scientific foundation and efficacy of the use of canines as chemical detectors for explosives. *Talanta*. 2001;54(3):487-500. doi:10.1016/s0039-9140(00)00546-4
191. Taylor-mccabe KJ, Wingo RM, Haarmann TK. Honey bees (*Apis mellifera*) as explosives detectors: exploring proboscis extension reflex conditioned response to trinitrotolulene (TNT). *Apidologie*. Published online January 1, 2008. Accessed December 7, 2021. <https://www.osti.gov/biblio/964982-honey-bees-apis-mellifera-explosives-detectors-exploring-proboscis-extension-reflex-conditioned-response-trinitrotolulene-tnt>
192. Dunn M, Degenhardt L. The use of drug detection dogs in Sydney, Australia. *Drug Alcohol Rev*. 2009;28(6):658-662. doi:10.1111/j.1465-3362.2009.00065.x
193. Raman B, Meier DC, Evju JK, Semancik S. Designing and optimizing microsensor arrays for recognizing chemical hazards in complex environments. *Sensors and Actuators B: Chemical*. 2009;137(2):617-629. doi:10.1016/j.snb.2008.11.053
194. Nizampatnam S. Neural Dynamics, Adaptive Computations, and Sensory Invariance in an Olfactory System. :179.

195. Knaden M, Strutz A, Ahsan J, Sachse S, Hansson BS. Spatial Representation of Odorant Valence in an Insect Brain. *Cell Reports*. 2012;1(4):392-399. doi:10.1016/j.celrep.2012.03.002
196. Olsen SR, Bhandawat V, Wilson RI. Divisive Normalization in Olfactory Population Codes. *Neuron*. 2010;66(2):287-299. doi:10.1016/j.neuron.2010.04.009
197. Si G, Kanwal JK, Hu Y, et al. Structured Odorant Response Patterns across a Complete Olfactory Receptor Neuron Population. *Neuron*. 2019;101(5):950-962.e7. doi:10.1016/j.neuron.2018.12.030
198. Stensmyr MC, Giordano E, Balloi A, Angioy AM, Hansson BS. Novel natural ligands for *Drosophila* olfactory receptor neurones. *J Exp Biol*. 2003;206(Pt 4):715-724. doi:10.1242/jeb.00143
199. Simpson SJ, Despland E, Hägele BF, Dodgson T. Gregarious behavior in desert locusts is evoked by touching their back legs. *PNAS*. 2001;98(7):3895-3897. doi:10.1073/pnas.071527998
200. Matheson T, Rogers SM, Krapp HG. Plasticity in the visual system is correlated with a change in lifestyle of solitary and gregarious locusts. *J Neurophysiol*. 2004;91(1):1-12. doi:10.1152/jn.00795.2003